

STUDIES OF THE DECOMPOSITION OF ALCOHOLS
ON METAL OXIDE CATALYSTS

BY



CHANCHAL KUMAR GHOSH

A THESIS SUBMITTED TO THE DEPARTMENT OF CHEMISTRY IN PARTIAL
FULFILLMENT OF THE REQUIREMENTS FOR THE
DEGREE OF MASTER OF SCIENCE

Lakehead University
THUNDER BAY, ONTARIO, CANADA

July, 1982

ProQuest Number: 10611670

All rights reserved

INFORMATION TO ALL USERS

The quality of this reproduction is dependent upon the quality of the copy submitted.

In the unlikely event that the author did not send a complete manuscript and there are missing pages, these will be noted. Also, if material had to be removed, a note will indicate the deletion.



ProQuest 10611670

Published by ProQuest LLC (2017). Copyright of the Dissertation is held by the Author.

All rights reserved.

This work is protected against unauthorized copying under Title 17, United States Code
Microform Edition © ProQuest LLC.

ProQuest LLC.
789 East Eisenhower Parkway
P.O. Box 1346
Ann Arbor, MI 48106 - 1346

ACKNOWLEDGEMENTS

The work in preparation for this thesis was carried out from September, 1980 to July, 1982 at Lakehead University, Thunder Bay, Ontario, Canada. The author wishes to express his sincere gratitude to his research supervisor, Dr. I.M. Hoodless, for this farsighted guidance, invaluable suggestions and constant encouragement throughout this work.

In addition, the author would like to acknowledge the expert assistance provided by the technical staff of the Faculty of Science.

Financial support for this work was provided by Lakehead University; this assistance is gratefully acknowledged.

The author would also like to thank Mrs. J. Parnell for typing this thesis.

TABLE OF CONTENTS

ACKNOWLEDGEMENTS.....	i
TABLE OF CONTENTS.....	ii
ABSTRACT.....	v
1. INTRODUCTION.....	1
1.1 General.....	1
1.2 Theories of Catalyst Selectivity.....	2
1.3 Deactivation of Catalyst.....	7
1.4 Investigation of Reaction Mechanisms by Kinetic Methods.....	10
1.5 Mechanism of 2-Propanol Decomposition on Oxide Catalysts.....	13
1.6 The Aim of the Present Work.....	19
2. EXPERIMENTAL.....	21
2.1 Preparation of Samples.....	21
2.2 Characterisation of Samples.....	22
2.2.1 Surface area measurements.....	22
2.2.2 X-ray diffraction.....	23
2.2.3 Thermo-gravimetric analysis.....	25
2.3 The Catalysis Experiment.....	28
2.3.1 The pulse method.....	28
2.3.2 The catalyst vessel.....	30
2.3.3 Product trapping.....	31
2.3.4 Analysis.....	31
2.3.5 Catalyst Conditioning and Reactivation.....	34
2.3.6 Isotope effect measurements.....	34
2.3.7 Poisoning experiments.....	35
2.4 Conductivity Measurements.....	39

TABLE OF CONTENTS continued...

3.	RESULTS.....	39
3.1	Characterisation of Samples.....	39
3.1.1	X-ray diffraction.....	39
3.1.2	Surface Areas.....	43
3.1.3	Dehydroxylation.....	46
3.2	Catalytic Decomposition of 2-propanol....	51
3.2.1	Kinetics of reaction.....	51
3.2.2	Catalyst reactivation.....	54
3.3	Stabilized Catalysts.....	56
3.3.1	Effect of changes in flow rates on reactivity.....	56
3.3.2	Effect of pulse size on catalyst reactivity.....	56
3.3.3	Effect of temperature changes on the reaction rates.....	58
3.4	Fresh or Reactivated Catalysts.....	61
3.4.1	Fresh catalysts.....	61
3.4.2	Reactivated catalysts.....	61
3.5	Studies of Catalyst Poisoning on Fresh or Reactivated Catalysts.....	62
3.5.1	Self-poisoning.....	62
3.5.2	The effects of other potential poisons.....	63
3.6	Isotope Effects.....	79
3.6.1	Stabilized catalysts.....	79
3.6.2	Reactivated catalysts.....	83
3.7	Conductivity Studies.....	89
3.7.1	Measurements on samples in an inert atmosphere....	89
3.7.2	Conductivity studies of catalyst poisoning and catalyst reactivation.....	91

TABLE OF CONTENTS continued...

4.	DISCUSSION.....	100
4.1	Changes in the Solid State Properties of Nickel Oxide Brought About by the Incorporation of Alumina.....	100
4.1(a)	Dehydroxylation.....	100
4.1(b)	Changes in catalytic activity and selectivity.....	108
4.2	The Dehydrogenation Reaction.....	114
4.2.1	Kinetics of dehydrogenation on stabilized catalysts.....	114
4.2.2	Self-poisoning on unstabilized catalysts.....	115
4.2.3	Effects of added poison.....	135
4.2.4	Isotope effects.....	136
4.2.5	The Dehydrogenation mechanism.....	137
4.2.6	Activation energies and catalyst selectivity.....	142
4.3	The Dehydration Reaction.....	146
4.3.1	Kinetics and activation energies..	146
4.3.2	Effect of added poisons on dehydration reaction.....	154
4.3.3	Kinetic isotope effects.....	156
4.3.4	Dehydration reaction mechanism....	160
4.4	Conclusion.....	164
4.5	Suggestions for Further Work.....	166
5.	REFERENCES.....	168
6.	APPENDICES.....	177

ABSTRACT

The catalytic decomposition of 2-propanol has been investigated by a micropulse reactor technique in the temperature range from 461 to 547 K on nickel oxide and alumina doped nickel oxide. Nickel oxide is active for the dehydrogenation of 2-propanol, yielding acetone, but the introduction of Al^{3+} ions leads to the development of some dehydration activity; nickel aluminate is purely a dehydrating catalyst. X-ray diffraction data indicate the formation of the nickel aluminate at the higher dopant concentrations. The variations in catalyst activity and selectivity as a function of catalyst compositions have been roughly divided into three regions: region I, in which there is a significant change in activity and selectivity with very small concentrations of Al^{3+} ions; region II, in which the activity and selectivity remains virtually constant with changes in composition; region III, in which there is a marked increase in activity and dehydration selectivity with increasing concentrations of Al^{3+} ions. The behavior in region I is believed to be associated with electronic changes in nickel oxide brought about by the substitutional incorporation of Al^{3+} ion, while the behaviour

in region III is ascribed to increasing amounts of nickel aluminate in the surface zones of the samples.

Self-poisoning in the dehydrogenation reaction has been observed and an equation accounting for the self-poisoning kinetics has been proposed. It is suggested that in the dehydrogenation reaction each alcohol molecule uses one active site on the catalyst, while self-poisoning causes elimination of three sites per deactivating event. Strong chemisorption of acetone on the surface is considered to be responsible for the self-poisoning of the dehydrogenation reaction. The conclusions are supported by conductivity studies of the catalysts under reaction conditions.

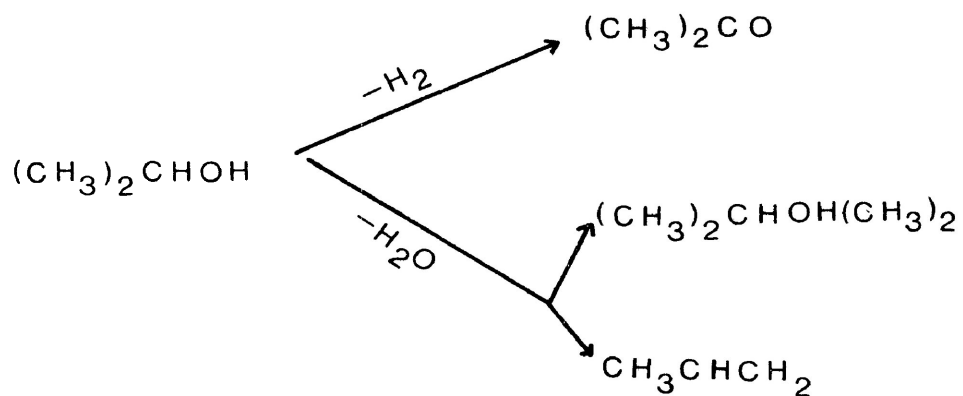
A characteristic feature of the dehydration reaction is the deviation from linearity in the Arrhenius plots at higher reaction temperatures. Isotope effect measurements show that this is not due to a diffusion-controlled reaction. The deviation is believed to be associated with the decomposition of hydroxyl groups on the catalyst surface and investigations of the thermal dehydroxylation of mixed nickel-aluminium hydroxides support this proposal.

Mechanisms for both the dehydrogenation and the dehydration reaction have been proposed. The dehydration reaction is poisoned by both weak and strong basic additives at lower temperatures but only by strong bases at higher temperatures. An E-2-type mechanism is proposed for the lower temperature reaction and with increasing temperature there is a trend towards an E-1-type mechanism. The dehydrogenation reaction is poisoned by additives containing lone pairs of electrons, indicating electron acceptor sites on the catalyst surface are the active sites.

1. INTRODUCTION

1.1 General

The decomposition of 2-propanol has been widely used as a model reaction for studying theories of catalyst selection particularly for metal oxide catalysts. The predominant modes of decomposition are dehydrogenation to give acetone and dehydration to give di-isopropyl ether or, more frequently, propene.



Despite the many investigations of 2-propanol decomposition on oxides there is still considerable controversy

over the mechanism and the detailed involvement of the catalyst in the reaction. The present thesis reports on a further study of 2-propanol on nickel(II) oxide and nickel oxide-alumina catalysts.

1.2 Theories of Catalyst Selectivity

In many of the earlier theories of catalyst selectivity, attempts were made to determine a correlation between the properties of the solid catalyst and the nature of the reaction to be catalysed. The geometric factor in catalysis was emphasized by Balandin (1) in his "multiplet theory of catalysis". The theory considers both an energy correspondence and a structural correspondence between the reacting molecules and the lattice dimensions of the catalyst. On the assumption that alcohol adsorption involves two-point attachment to the surface, the theory predicts that an increase in the crystal lattice distance would increase the dehydration activity of a catalyst while a decrease in lattice distance would enhance dehydrogenation activity (2).

A second theory, usually referred to as the electronic factor, considers electron transfer between

the reactant molecule and the solid catalyst. With semiconductors, catalyst selectivity would be related to the type of conductivity and the position of the Fermi energy level (3-6). Hauffe (3), on the assumption that the rate-limiting step in the dehydrogenation of alcohols is the migration of positive holes, predicted that dehydrogenation would be favoured by P-type semiconductors while dehydration would be the preferred reaction on n-type semiconductors. Wolkestein, considering different modes of adsorption of the alcohol came to the opposite conclusion (6). It may be noted that zinc oxide, an n-type semiconductor, and nickel oxide, a p-type semiconductor, are both highly selective catalysts for the dehydrogenation of alcohols (2).

Another approach, proposed by Roginskii (7,8), classified the majority of catalytic reactions into two types - oxidation-reduction (electronic) and acid-base (ionic). Dehydrogenation reactions fall into the electronic category and should be catalysed by solids possessing free or easily excited electrons, e.g. metals and semiconductors. The mechanism of dehydrogenation reaction is interpreted as involving the transfer of electrons from the catalyst to the reacting substance or vice versa (2).

Dehydration reactions come under the ionic category and should be affected by the nature of surface acidic or basic sites. The transfer of protons or the production of a heteropolar donor-acceptor pair would be a preliminary step in the reaction (2).

From data, available prior to 1969, of 2-propanol decomposition on oxides, Krylov (2) examined the above theories by correlation analysis. Although there was considerable dispersion in the data points, he found that the catalytic activity for dehydrogenation was a function of the catalysts lattice parameter, type of conductivity, work function and width of the forbidden energy gap. For dehydration there existed a dependence of catalytic activity upon the electronegativity difference between the oxide ion and cation. The correlation analysis is not conclusive and, in particular, the high dehydrogenation selectivity of alkaline earth oxides (9) for 2-propanol decomposition is unexpected in terms of their conduction characteristics. An alternative correlation between surface oxygen mobility and dehydrogenation activity has been proposed (9,10).

In recent years the development of sophisticated

techniques, such as Auger electron spectroscopy (AES), electron spectroscopy for chemical analysis (ESCA), and low-energy electron diffraction (LEED), has permitted more detailed study of the catalyst surfaces and modern theories of catalyst selectivity tend to consider the individual atomic sites rather than the collective solid-state properties of the catalyst. In particular, more emphasis is placed on the co-ordination unsaturation of the surface sites. Typical of these approaches are the applications of crystal and ligand field theory to adsorption behaviour of transition metal oxides (11,12) and the relationship of the coordination unsaturation of surface Cr^{+3} ions to the catalytic activity of chromium oxide (13). As such the theories tend to be specific to a particular catalyst type rather than the more general concepts discussed earlier.

One interesting aspect of the surface site approach is the change in the purpose of deliberately doping metal oxide catalysts. Previously the intention of the doping was to bring about changes in the Fermi energy level of the catalyst and to attempt to correlate this with activity changes (14). The more recent studies

are concerned with the behaviour of isolated dopant ions at low-levels of doping and cooperative behaviour between dopant ions at higher levels of doping (15,16). This type of oxide solid solution study has been reviewed by Vickerman (17), where variation of activity of solid solutions with increasing transition metal ion concentration is discussed. The general activity pattern for most of the catalyst systems indicate high activity at high dopant dilution, a fall in activity with increasing transition metal ion to a minimum in the 10 - 15 percent concentration region, then an increase in activity again at higher dopant levels.

The trend towards consideration of surface coordinate unsaturation is reminiscent of an earlier concept of "active sites" proposed by Taylor (18), i.e. not all of the surface sites are equally active. Thus, in describing the surface of the catalyst it is important to consider the purity of the sample, the method of preparation and pretreatment of the catalyst. With oxide catalysts it has frequently been observed that their catalytic activity and selectivity can be affected by the preparation temperature (19). While this, in part, may be the result

of physical changes, e.g. changes in surface area and pore structure, there is a good deal of evidence to indicate chemical factors as well (20,21). Many oxide catalysts are prepared by dehydroxylation of the metal hydroxides and it has been shown that the complete removal of hydroxyl from the surface can only be achieved at high temperatures (22,23). Infra red studies indicate that surface hydroxyls are present on the oxide catalysts under the usual reaction conditions and these may act as catalytic reaction sites (24).

1.3 Deactivation of Catalyst

In dealing with catalyst selectivity, the need to establish the detailed chemical nature of the catalyst surface has been indicated in section 1.2. However, frequently during the course of reaction, the activity of the catalyst diminishes. The cause of catalyst deactivation may be grouped loosely into:

- a) reduction of active area by sintering or migration;
- b) fouling;
- c) poisoning.

Sintering is essentially an irreversible physical process leading to a reduction of effective catalytic area. It may consist of growth of metal crystallites on a support or of a decrease in area of a non-supported catalyst (25). Fouling is generally used to describe a physical blockage such as the deposit of dust or fine powder or carbonaceous deposits. In the latter case the activity can usually be restored by removal of the coke by burning (25). Deactivation of catalysts by sintering and fouling are essentially physical changes. However, deactivation by poisoning (26) is associated with the chemical nature of the catalyst surface and will be discussed in detail.

Poisoning may be brought about by the reacting system itself (self-poisoning) or by some additives or impurities. In self-poisoning, chemical transformations of the reactants or products lead to stable surface species that can not be desorbed or displaced by the reactant.

A number of studies of catalyst self-deactivation have been concerned with catalyst coking during hydrocarbon cracking reactions. Several mechanisms have been proposed to explain the kinetics of the deactivation process. The general rate equation applicable to poisoning by reactions

parallel or consecutive to the main reaction, has the form

$$r = r_0 \psi \quad 1.1$$

where r and r_0 are the rates of the poisoned and unpoisoned reactions and ψ is the deactivation term. Froment and Bischoff (27) have postulated a relationship between ψ and the coke (or poison) content of the catalyst and this type of approach has been used by several other workers (28,29). An alternative approach, used by Wojciechowski (30) and Khang and Levenspiel (31), is to relate ψ to the reaction time. Numerous modifications of the above treatments have been made; Hegedus and Peterson (32) have extended the parallel and series mechanism to include both occurring simultaneously but at different rates, while Levenspiel (33) and Wolf and Petersen (26) have analyzed self-poisoning reactions in the same way as normal catalytic mechanisms to obtain reaction orders for poisoning. The kinetics of catalyst deactivation have been recently summarised by Corella et al (34) and by Froment (35).

The effect of added poisons may be reversible or irreversible, depending on the nature and strength of interaction between the poison and the active sites. Selective

poisoning has been explained by Kemball (36) as the phenomena in which a poison causes a catalyst to improve its selectivity. Pines and Hagg (37) and later Beřank et al (38) used selective poisons to suppress the secondary isomerization of olefins in the dehydration of alcohols on alumina. When poisoning is carried out with the aim to improve the catalyst selectivity toward a desired product, then the only requirement is that the active sites responsible for the undesired reaction path be among the adsorption sites for the poisoning additive. If, however, the aim of the poisoning experiment is the analysis of the number of active sites, then it is necessary that the poison specifically and solely interacts with the active sites. This is referred to as specific poisoning (39).

The phenomena of catalyst deactivation can lead to problems in the elucidation of reaction mechanisms by kinetic studies. This aspect is considered in the next section.

1.4 Investigations of Reaction Mechanisms by Kinetic Method

Kinetic data are usually used to develop rate equations which can be applied in the formulation of a

reaction mechanism and in the determination of optimum conditions for reaction. The major methods used in the study of the reaction kinetics are the 'static' method, the 'flow' method and the 'pulse' method.

The 'static' reactor system is one in which the reactants are introduced into a constant volume reactor at the start of an experiment and then the system is closed (40,41). The rate is followed by changes in concentration or pressure. The most important condition is that the reaction must proceed isothermally.

The 'flow' method operates essentially under steady-state conditions. In this system a mixture of reactants, often diluted by a carrier gas, is passed continuously, at a known rate of flow, through a reaction vessel containing the catalyst (42). The reaction products and unreacted starting materials are continuously removed from the system for analysis. Reaction rates and activities are frequently determined after the establishment of a steady-state condition. This condition is usually achieved by passing the reactant gas or gases over the catalyst for a period of time, sometimes at temperatures

higher than those to be used in reaction study. Reaching a steady-state activity, however, creates one of the inherent problems of this method, namely an adequate description of the chemical and physical nature of the catalyst after conditioning. The surface may be very different to the original situation. For instance, Balandin et al (43,44) have shown that during alcohol decompositions on transition metal oxides, the conditioning period caused reduction and in some cases carbonization of many catalysts.

A modification of the conventional flow method is the pulse reaction technique. It is this method which is used in the present work and so will be discussed in rather more detail. The pulse technique is one in which small amounts of reactants are injected into a carrier gas stream before the gas enters a reactor packed with a small amount of catalyst. In contrast to the 'flow' method the catalyst is not continuously exposed to the reactants.

The basic operating principles of the pulse reactor technique have been discussed by Galeski and Hightower (45) and by Kokes et al (46). The method has

been mainly used as a quantitative tool in comparing series of catalysts or in determining product distributions. In applying the pulse technique to investigations of reaction kinetics, the results can be significantly different from those obtained by the continuous flow method. The two methods give similar results for first-order kinetics (47-49) but caution is required in comparing the results for non-first order reactions (50). Hattori and Murakami (51-54) and Merrill and coworkers (55,56) have examined the effects of pulse shape, pulse width and adsorption strengths of both reactants and products on the observed kinetics obtained by the pulse technique. The general conclusion is that as the pulse width increases the kinetics approach those observed in a continuous flow reactor. One advantage of the pulse technique is that it permits investigations of changes in selectivity in the catalyst prestabilization stages.

1.5 Mechanisms of 2-Propanol Decomposition on Oxide Catalysts

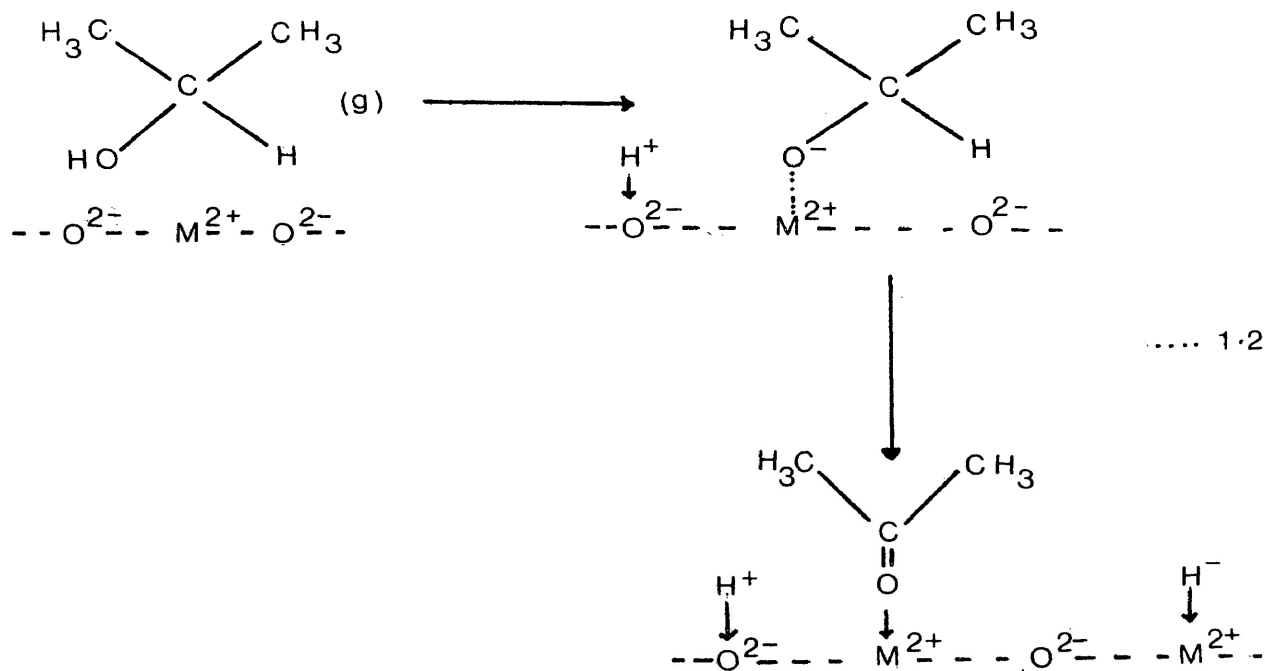
a) Dehydrogenation

The observed kinetics of the dehydrogenation reaction indicate that the rate limiting step is either the

surface reaction of the adsorbed alcohol (9) or the desorption of the product, acetone (57,58). Measurements of the kinetic isotope effect on a number of oxide catalysts (59,60) would appear to rule out desorption of acetone as the rate determining step although acetone is known to inhibit the dehydrogenation reaction (61).

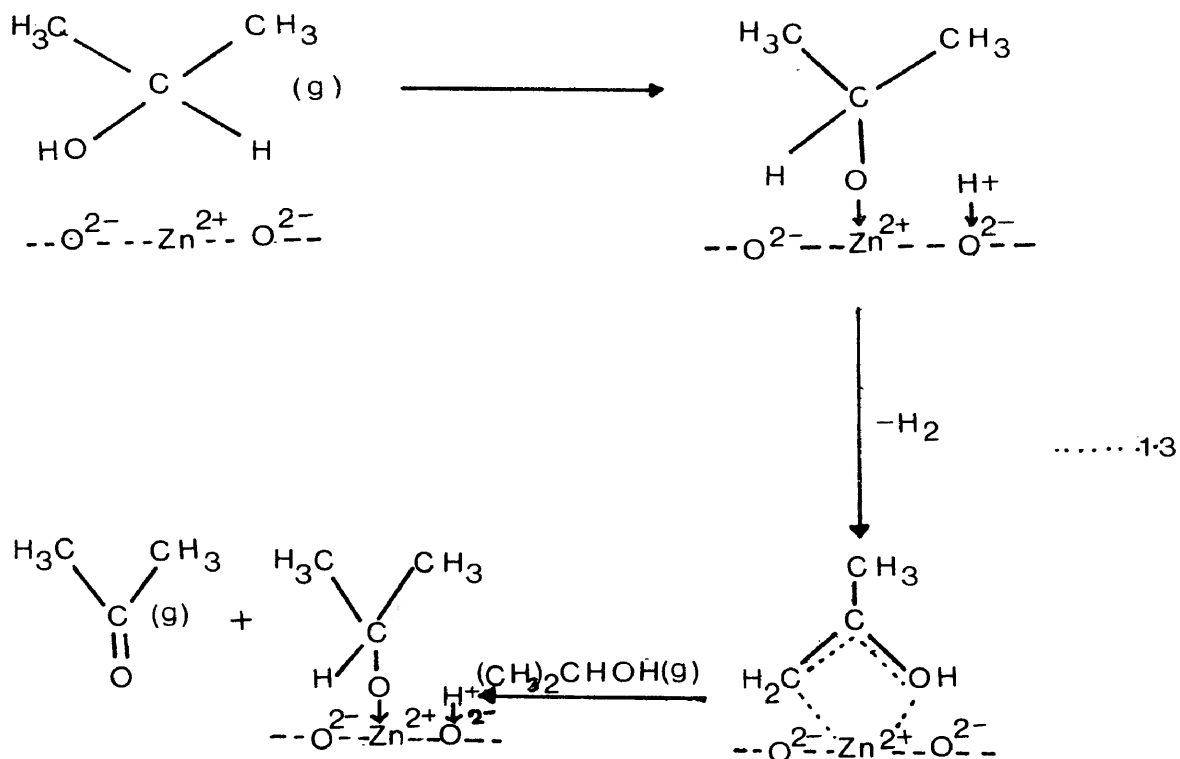
Essentially two general types of mechanisms have been proposed for the reaction of the adsorbed alcohol. One mechanism involves hydrogen atom transfer to the oxide ions of the catalyst as proposed by Krylov (57) and also by Pepe and Stone (62) but it should be noted that desorption of acetone has been assumed to be the rate-limiting process in Krylov's mechanism.

The other mechanisms all involve the transfer of the hydroxyl proton from the alcohol to a basic oxide site with the subsequent elimination of a hydride ion from the α -carbon atom. In this mechanism, the rupture of the C_{α} -H bond is considered to be a rate limiting step and this is supported by the kinetic isotope effect measurements. The mechanism proposed by Szabó and coworkers (20) is shown below as an illustration of the hydride ion transfer process.



Similar mechanisms have been suggested by Nondek et al (59), Kibby and Hall (63) and also by Eucken (64,65) and Wicke (66) although the latter involves a cyclic transition state without formation of alkoxide. Recently Tamaru et al (67) have proposed a mechanism along the same lines but involving displacement of the product acetone by another

molecule of alcohol.

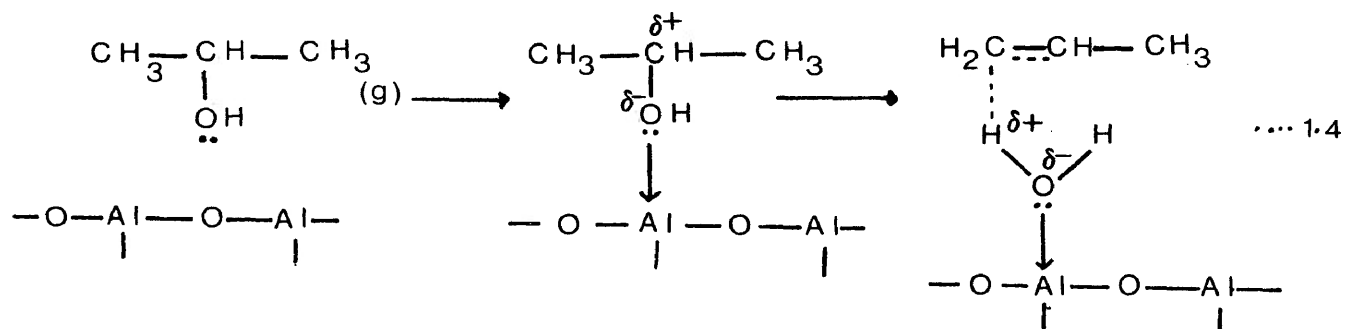


b) Dehydration

The dehydration reaction is commonly believed to proceed via a cyclic transition state but still some disagreement exists as to the surface sites used in the process. Kinetic isotope effect measurements indicate

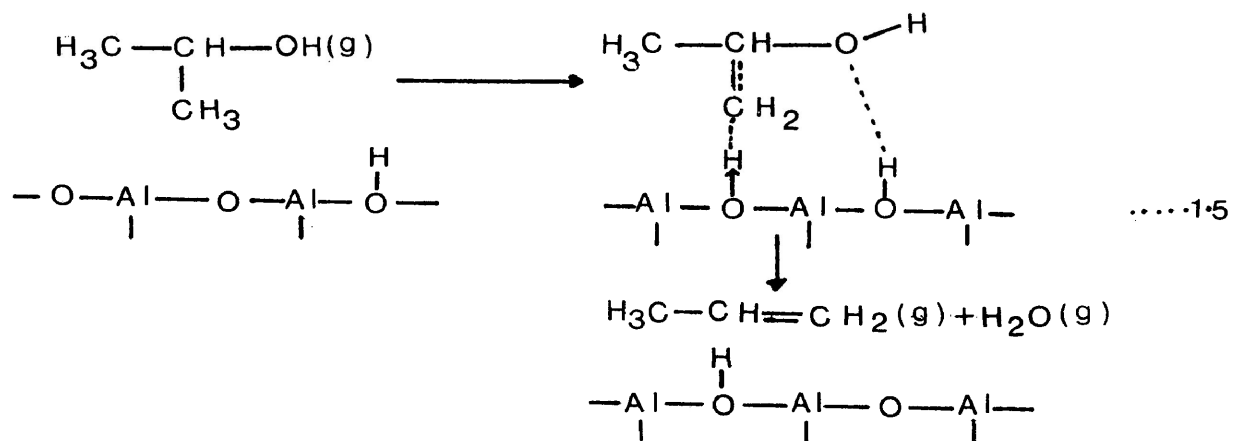
that water desorption cannot be rate limiting (60,68-70) and that an E2 type mechanism is probably involved in the production of propene. However, with increase either in the reaction temperature or in the acidity of the catalyst there is a gradual transition from E2 to an E1 (Carbonium ion) mechanism (68).

Krylov (71), Pines and Haag (72) and Jain and Pillai (73) favour adsorption of the alcohol through the oxygen of the alcoholic hydroxyl group on Lewis acid sites on the catalyst, for example:



Other mechanisms involving a covalently bonded adsorption complex in the form of surface alkoxide bonded to Lewis acid sites have been proposed by Senderens (74), Ipatieff (75) and later by Smirnova et al (76). In these mechanisms it is suggested that olefin is formed by dissociation of the surface alkoxide compound.

Knozinger and coworkers (24,68-70,77-78), who have extensively investigated the dehydration of alcohols on alumina catalysts, argue against both the involvement of Lewis acid sites and the formation of a surface alkoxide in the reaction. The results of catalyst poisoning studies using pyridine (79) and tetracyanoethylene (80) would appear to exclude Lewis acid sites as active centres and to indicate the participation of basic sites in the dehydration process. The general reaction mechanism proposed by Knozinger et al (81) and by Deo et al (82) is one in which the alcohol molecule interacts with a surface hydroxide and an oxide ion, viz.



The extent to which the mechanism proposed for reaction on alumina is applicable to other metal oxide catalysts, particularly those with different structures and electronic properties, is still not clear.

1.6 The Aim of the Present Work

The decomposition of 2-propanol has been chosen as the reaction for investigation of the catalyst selectivity of nickel oxide and a series of nickel oxide-alumina preparations. Previous studies (53,83) have shown nickel oxide to be a dehydrogenation catalyst while nickel oxide-alumina solid solutions are known to form nickel aluminate (84-86) which, on the basis of other investigations (87), would be expected to be a dehydrating catalyst. One objective of the present work was to study the changes in catalyst selectivity with increasing concentrations of nickel aluminate and to examine possible enhancements in catalyst activity due to solid-phase interfacial effects (synergetic effects) (88).

A second objective in this study was to investigate the significance of surface dehydroxylation in the

catalyst activity of the oxide. Recent work in this laboratory (89) has indicated that surface hydroxides require high temperatures, well in excess of normal catalytic temperatures, for their decomposition. In the dehydration reaction it is likely that surface hydroxides are formed and these could well influence the mechanism of the reaction and the activity of the catalyst.

2. EXPERIMENTAL

2.1 Preparation of Samples

The catalysts used were nickel(II) oxide and a series of alumina-doped nickel(II) oxide.

Hydroxides of nickel and nickel-aluminium mixtures were prepared by precipitation with ammonia (ACS Reagent Grade) from solutions of nitrate salts (Nickel(II) nitrate, Baker Analyzed' Reagent; Aluminium nitrate, B.D.H. Laboratory Chemical Group) at a pH of 8.5. The compositions of the mixtures of nickel and aluminium nitrate solutions were adjusted so that a series of hydrous oxides were obtained which on decomposition gave mixed oxides containing 0.10, 0.50, 2.56, 5.26, 14.29, 25.0 and 50 mol percent of aluminium oxide in nickel(II) oxide.

The hydroxides were washed free of nitrate with distilled water and dried in air at 373 K. The hydroxides were then thermally decomposed at 873 K in a muffle furnace for twenty-four hours. The samples were pelletised and then sintered at 1073 K for twenty-four hours after which the pellets were finely powdered to give particles of diameter less than 0.063 mm which were used as the catalyst samples.

2.2 Characterisation of Samples

The catalyst samples were characterised by surface area measurement, x-ray powder diffraction and thermogravimetric analysis.

2.2.1 Surface Area Measurements

The surface area determinations involve the measurement of the amount of gas necessary to form a monomolecular layer on a solid surface. From the number of molecules adsorbed and the area occupied by each molecule, the surface area of the solid can be determined. The following general BET equation was used (90).

$$\frac{P}{V(P_0 - P)} = \frac{1}{V_m C} + \frac{(C-1)P}{V_m C P_0} \quad \dots 2.1$$

where V is the volume of gas adsorbed per gram of material at a measured pressure P , V_m is the monolayer volume, P_0 is the saturation pressure of the adsorbate gas at liquid nitrogen temperature (93 K) and C is a constant which depends upon the heats of adsorption and liquifaction of the gas.

A plot of $P/V(P_0 - P)$ against P/P_0 gives a straight line of slope $(C-1)/V_m C$ and intercept $1/V_m C$ valid for relative pressures, P/P_0 , between 0.05 and 0.35 (91).

In this present measurement krypton was used as the adsorbate and a diagram of the apparatus is shown in Figure 2.1. The general procedure was as follows. Approximately 20 mg of the sample in the case of NiO and 10 mg in the cases of the doped samples was accurately weighed into the sample holder which was then positioned on the apparatus and evacuated to a pressure of 10^{-4} torr (1.33×10^{-3} Pa) overnight at 373 K. Krypton was admitted to volume V_a (Figure 2.1) and the pressure in this space was measured on the McLeod gauge. The gas was then expanded into the sample container which was immersed in liquid nitrogen. After equilibrium was established, (usually thirty minutes) the pressure was again measured and the volume of krypton adsorbed was calculated in the usual way (92) utilizing the computer programme 'KRBET'.

2.2.2 X-ray diffraction

The catalyst samples were analyzed by an x-ray

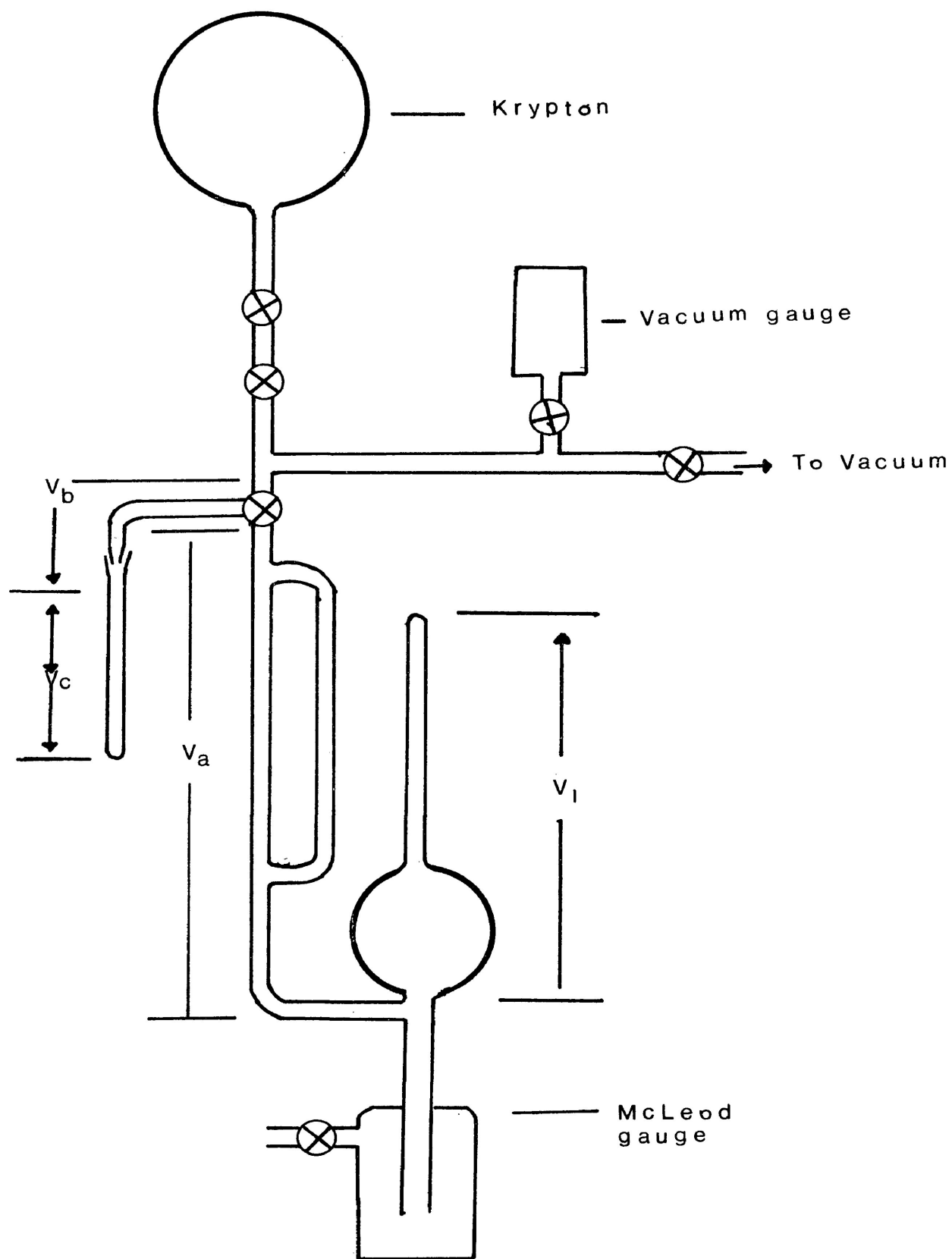


Figure 2.1: Krypton BET apparatus; $V_a = 13.6 \text{ cm}^3$, $V_b = 1.855 \text{ cm}^3$,
 $V_c = 0.865 \text{ cm}^3$, $V_I = 47.37 \text{ cm}^3$.

powder diffraction technique. The finely ground powders were sealed in capillary tubes and diffraction patterns obtained using a Philipps x-ray Generator, operating at 40 kV and 20 mA, using a nickel-filtered, copper K_{α} radiation source, equipped with a 114.83 mm Debye-Scherrer camera. The diffracted x-rays were recorded on strips of photographic film to give the familiar powder photographs of lines of varying intensities. By measurement of the lines, since the radius of the camera and the wave length (λ) of the x-rays are known, the interplanar spacings (d°) were determined and the samples identified by comparison with standards in the usual fashion (93)..

2.2.3 Thermo-gravimetric analysis

Thermobalance

A Stanton-Redcroft thermobalance, model HT-SF, was used in thermal analysis experiments. The balance had an automatic weight-loading assembly to extend the weight range in steps of 20 mg to a 200 mg maximum. A vertical sample support column was connected to the back pan of the balance as shown in the schematic diagram, Figure 2.2. A servo-driven capacity-follower device was used to transmit beam movement to the recording mechanism, while the beam

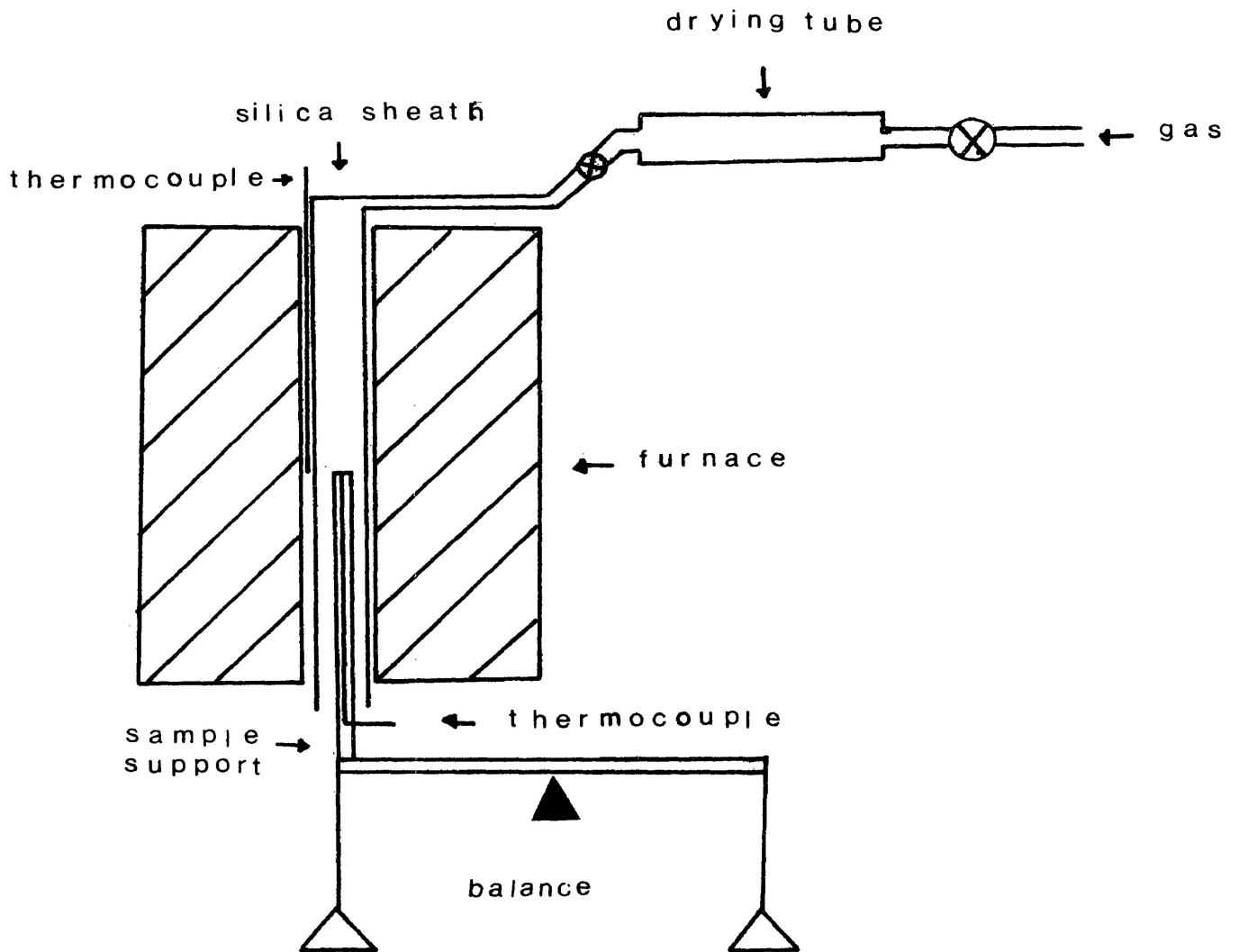


Figure 2.2: Schematic of the thermobalance assembly

was controlled by a conventional air damping arrangement. Sample temperatures were monitored on a Leeds and Northrup recorder with a platinum/platinum-rhodium (13%) thermocouple positioned within the sample support, Figure 2.2. A correction was applied for the thermocouple cold junction at room temperature. The recorder was calibrated using a Honeywell portable potentiometer over the range 0 to 10 mv. The accuracy of the sample temperature measuring arrangement was therefore limited by the accuracy in reading the recorder chart which amounted to $\pm 1^{\circ}\text{C}$ over the temperature region of interest.

Samples were heated by a 37.5 mm bore platinum/rhodium wound furnace which was mounted vertically and could be raised or lowered around the sample support. A silica sheath allowed a flowing gas, in this case nitrogen, to surround the sample continuously. The furnace temperature was controlled by a platinum/platinum-rhodium (13%) thermocouple located between the furnace wall and silica sheath. The furnace could be operated isothermally at a pre-selected temperature with a proportional controller, or in a dynamic mode in which case the furnace temperature was increased linearly at a rate of $7^{\circ}\text{C min}^{-1}$. Nitrogen was passed through a drying column, 35 mm diameter by 0.40 m

in length consisting of self-indicating silica gel and calcium sulphate, before entering the furnace.

Dynamic thermogravimetric technique

A small capacity platinum crucible, 10 mm diameter by 5 mm in height, was used to hold approximately 30 mg samples. The procedure employed was to balance the specimen on the sample support in the furnace at room temperature in a flowing nitrogen atmosphere ($230 \text{ cm}^3 \text{ min}^{-1}$ (NTP)) to achieve a straight base line, and to flush the furnace assembly. The thermobalance was then programmed to reach 873 K. Buoyancy corrections were determined using dead-burned alumina.

2.3 Catalysis Experiment

2.3.1 Pulse method

The catalytic decomposition of 2-propanol was investigated by a micropulse reactor technique on NiO and $\text{Al}_2\text{O}_3/\text{NiO}$ samples. The pulse method utilizes a fixed bed reactor with a continuously flowing carrier gas stream. A block diagram of the apparatus is shown in Figure 2.3.

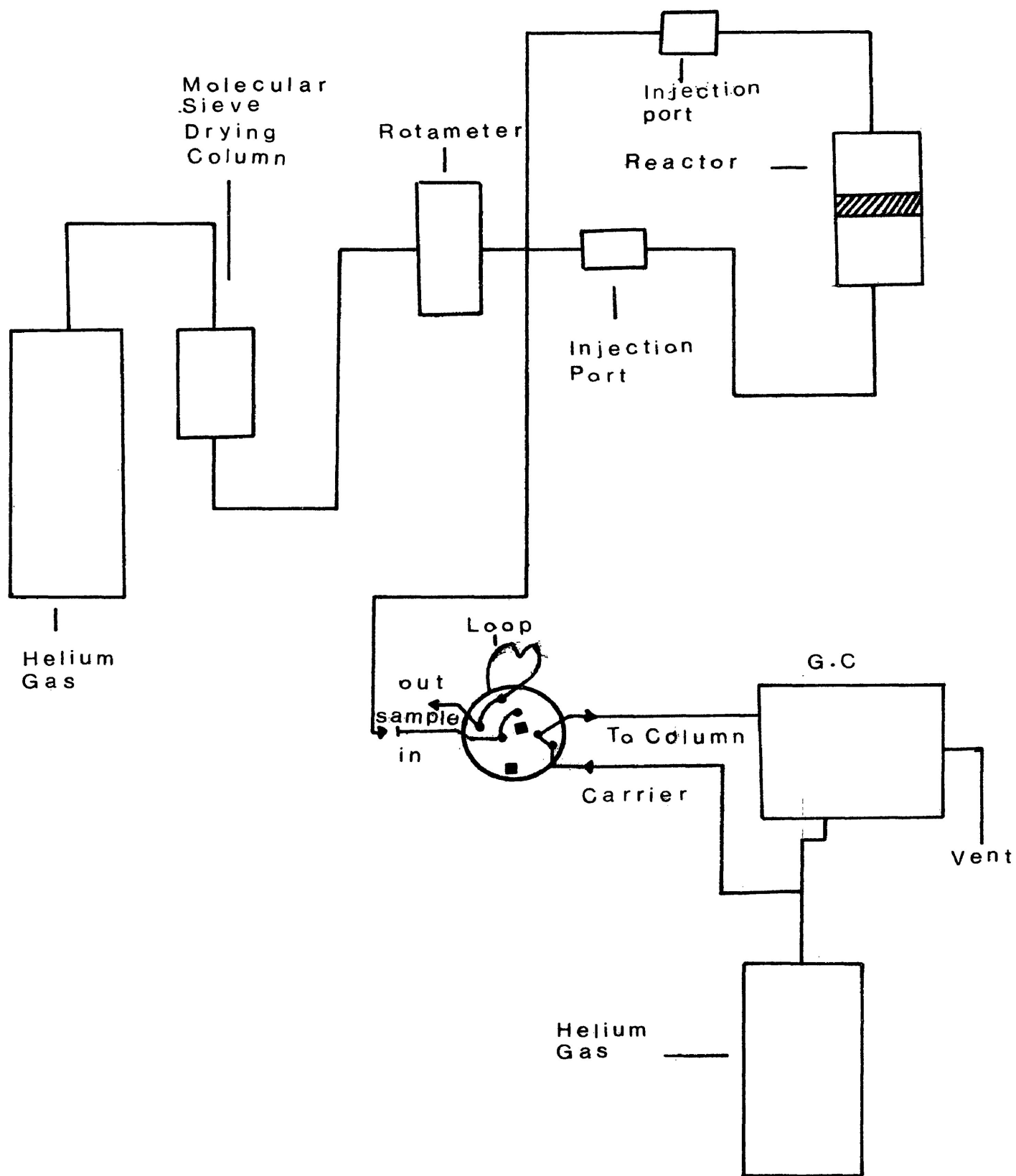


Figure 2.3: Block diagram of the apparatus for catalysis measurements.

High purity (99.99%) helium was used as the carrier gas. The gas was initially passed through a molecular seive drying column, which also acted as a pressure stabilizer, and trace amounts of oxygen were removed by oxisorb (Meser Greiesheim). Flow rates were maintained using 'Matheson Rotameters' filled with 'Matheson Millimite' fine-control needle valves. The flow rates were measured with a soap bubble burette. Pulses of alcohol (0.2-5 nm³) were injected with a Hamilton micro syringe into a pre-heated helium carrier gas stream and passed over the catalyst. The catalyst bed temperatures were monitored by a chromel/alumel thermocouple. The reaction products and unreacted alcohol emerging from the reactor were collected in a trap, cooled with liquid nitrogen, before being admitted to a gas chromatograph for analysis.

2.3.2 Catalyst vessel

The catalyst vessel was a 10 mm diameter pyrex-glass tube containing the catalyst sample mounted on a sintered glass disc sealed across the tube. Catalyst samples in the range 0.05-0.32 g were used. Blank run experiments, in which 2-propanol was passed through the reactor, indicated no reaction occurred in the absence of a catalyst for the

temperature range under investigation, i.e. below 573 K.

2.3.3 Product trapping

A trapping time of twelve minutes was employed in the experiments. Maximum recovery of products and alcohol was observed with the minimum time of twelve minute trapping for a $40 \text{ cm}^3 \text{ min}^{-1}$ gas flow rate. A typical plot for the recovery versus trapping time is shown in Figure 2.4. Furthermore, the collection time was adjusted in inverse proportion to the flow rate, thereby ensuring that conversion was determined on the basis of the same volume of gas having passed through the trap.

2.3.4 Analysis

The gas stream containing reaction products was analyzed using a dual column 'Hewlett Packard Research chromatograph Model 5750' with flame ionization and thermal conductivity detectors. Quantitative analyses of 2-propanol and products were carried out using a 1.83 m column of 10% carbowax 20 M (80-100 mesh).

Prior to each injection of alcohol, the column oven

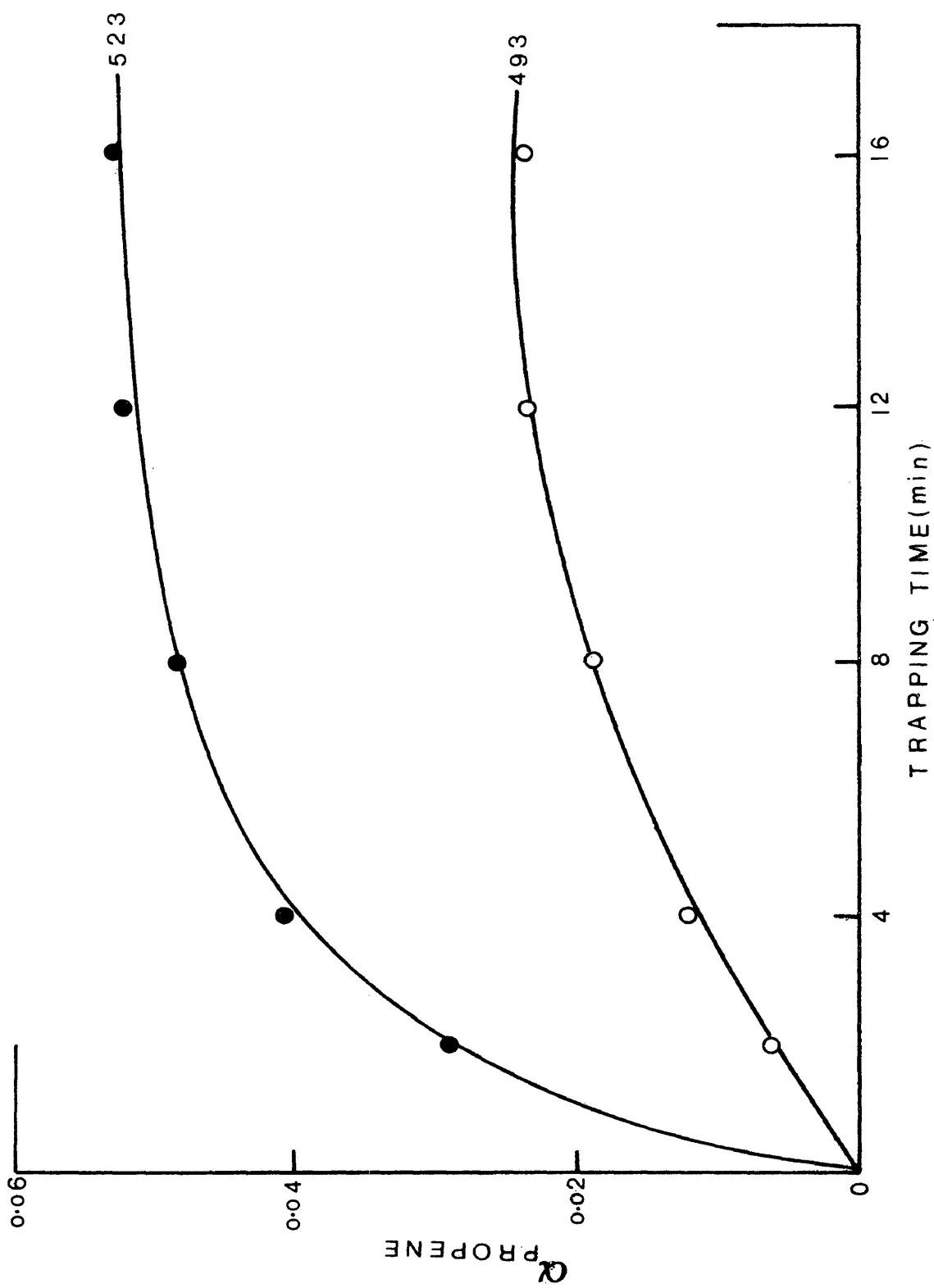


Figure 2.4: Plot of fractional dehydration, α , versus trapping time (2nm^3 inj. size). Reaction temperatures (K) are indicated in Figure.

was maintained at 323 K. When the sample was flushed on to the column from the trap, the oven temperature was increased by linear-temperature programming at $6^{\circ}\text{C min}^{-1}$ to a maximum of 413 K. The column oven was then recycled to 323 K. With the chromatograph programmed in this manner the gas stream could be sampled every thirty minutes. A helium flow of $40\text{ cm}^3\text{ min}^{-1}$ was passed through the column. The thermal conductivity detector was maintained at 473 K. with a current of 245 mA passing through the detector filaments. The detector amplifiers were adjusted where necessary to enable the peaks of the individual components to remain on the recorder scale.

The retention times of the reaction components were measured and identified by comparison with the standards. Peak areas of the individual components were used in quantitative estimations and these areas were determined from the printouts by a potentiometric recorder with integrator (Type, Fisher Recordall series 5000). Detectors were calibrated by injecting known amounts of the components into the column and measuring peak areas. Typical results are shown in Table 2.1.

Table 2.1
Calibration of Detectors

Substance	mol	Area of Peak (Arbitrary units)
2-Propanol	2.61×10^{-5}	3960
Acetone	2.70×10^{-5}	3960
Propene	4.093×10^{-6}	520

2.3.5 Catalyst conditioning and reactivation

Prior to any 2-propanol pulses the catalyst samples were conditioned in the reactor by heating at 623 K for one hour in the helium carrier gas stream. Since, as will be reported later, deactivation of catalyst samples was observed with the successive pulses of alcohol, the samples of nickel oxide could be reactivated by heating in the reactor at 623 K for one hour while the doped samples could be reactivated by heating at 623 K for two hours.

2.3.6 Isotope effect measurements

The general procedure to study the isotope effect was that at a particular reaction temperature, the catalyst would be subjected to approximately fifteen pulses of

alcohol; typically pulses 1-3 would be 2-propanol, pulses 4-6, a deuterio-alcohol, pulses 7-9, 2-propanol and so on. The reactants were spectranalyzed 2-propanol (Fisher Scientific Company) and the deuterio alcohols (Merk, Sharp and Dohme); 2-propanol-d₆ ((CD₃)₂CHOH) had an isotopic purity of 99 atom % D while for 2-propanol-2d₁ ((CH₃)₂CDOH) it was 98 atom % D. The purity of 2-propanol-OD ((CH₃)₂CHOD) was 98 atom % D.

2.3.7 Poisoning experiment

A number of studies was made of the effect of added poison on the activity and selectivity of the catalysts. In these experiments, the catalysts at the reaction temperature were subjected to pulses of potential poisons (water, air, acetic acid, phenol, acetone, benzene, aniline and n-butyl amine) and the added poisons were allowed to pass over the catalysts, prior to the injection of the alcohols approximately thirty minutes after the pretreatment pulse.

2.4 Conductivity Measurements

Electrical conductivity of the catalyst samples was measured in a flow system and also under vacuum.

One conductivity cell, constructed in pyrex, was of the flow-through type, Figure 2.5. Powder samples were compressed under pressure into a pellet form which was then clamped under slight pressure between platinum electrodes. The temperature of the sample was determined by an iron-constantan thermocouple in contact with the lower electrode. The sample was maintained in a constant flow of helium ($40 \text{ cm}^3 \text{ min}^{-1}$) and the reactant gases were injected at the injection port with a Hamilton micro syringe. The electrical conductivity was measured on a Wayne-Kerr B641 universal bridge operating at 1592 Hz.

A second conductivity cell which permitted measurement to be made in a vacuum was also constructed and the diagram of the apparatus is shown in Figure 2.6. In this arrangement the electrodes were platinum and the temperature of the sample was determined by an iron-constantan thermocouple which was in contact with the lower electrode. The conductivity was measured with a Wayne-Kerr B641 universal bridge operating at 1592 Hz. The general procedure was that the system was evacuated to approximately 1.5×10^{-2} torr (1.96 Pa) and then 2-propanol was admitted to the system. The measurements were therefore made under essentially static (as opposed to the flow-type cell) conditions and with a constant alcohol pressure in the gas phase.

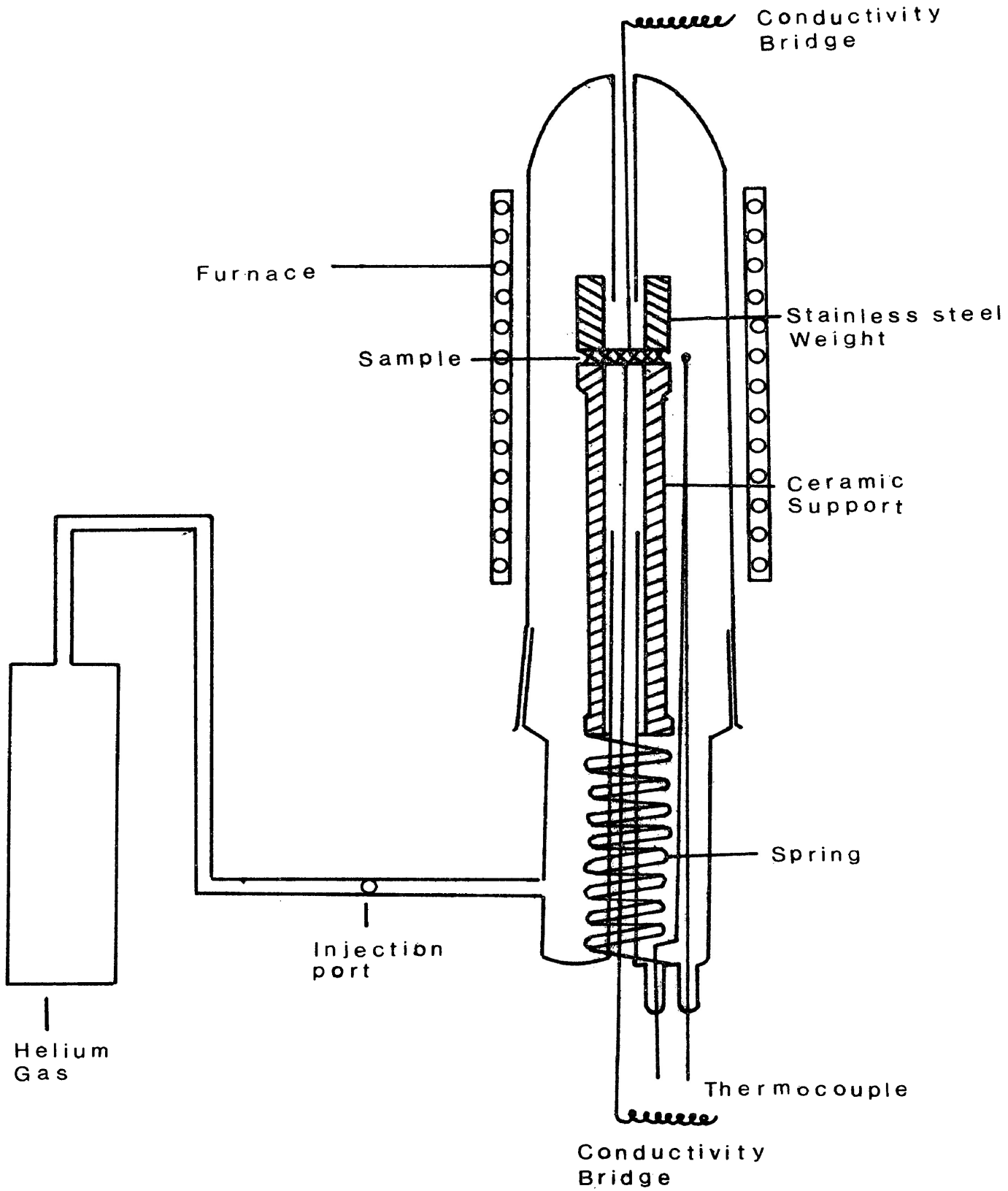


Figure 2.5: Conductivity cell used for flow conditions

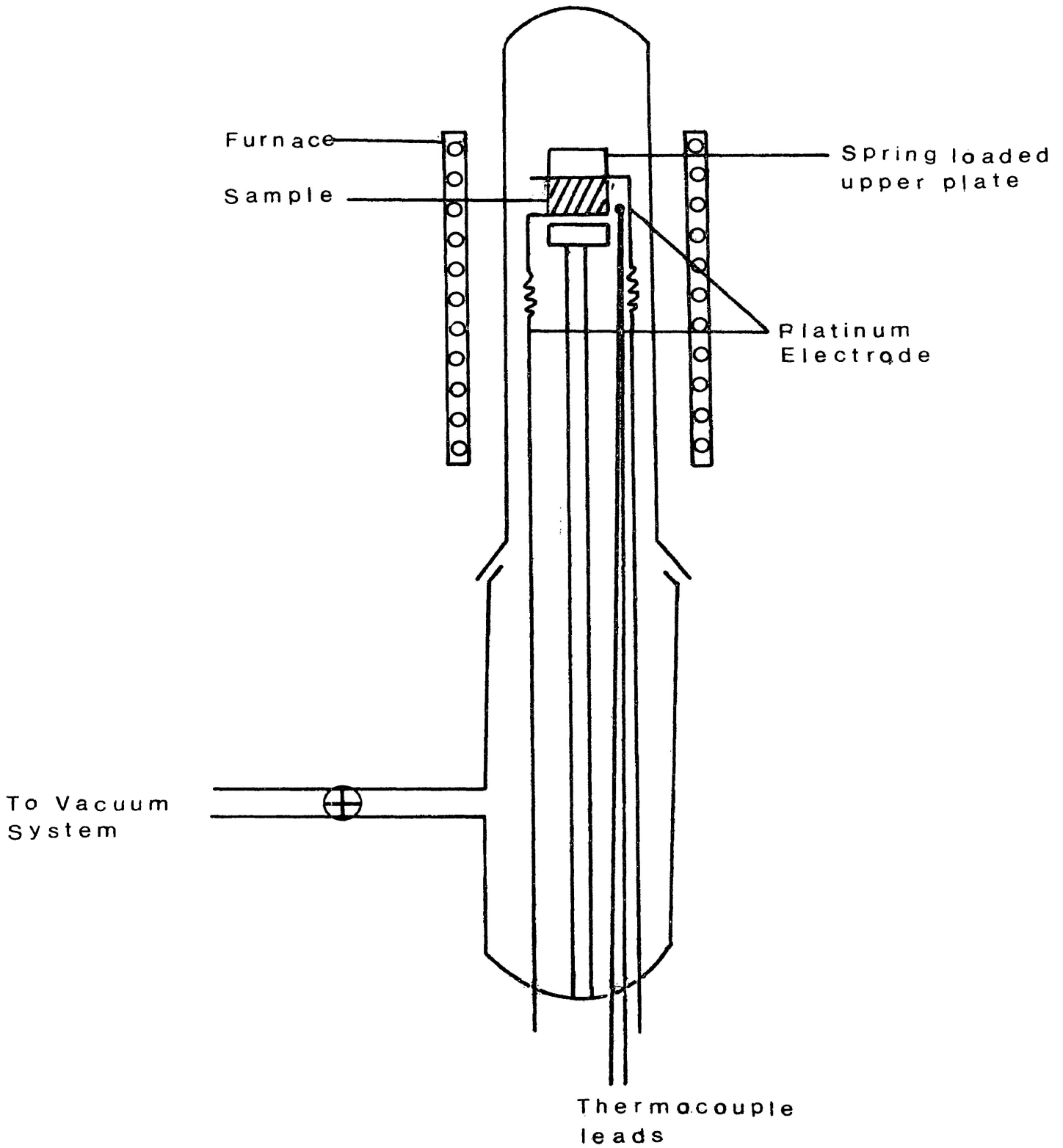


Figure 2.6: Conductivity cell used for static system

3. RESULTS

3.1 Characterisation of Samples

3.1.1 X-ray diffraction

X-ray powder patterns of the catalysts before reaction are shown in Tables 3.1 and 3.2.

Samples containing from 0 to 2.56 mol percent Al_2O_3 exhibit essentially the diffraction pattern of NiO although the observation of a very weak line at 4.68 Å in 0.5 and 2.56 mol percent specimens does not rule out the possibility of the existence of NiAl_2O_4 as a minor phase. The presence of NiAl_2O_4 is clearly shown in samples containing more than 2.56 mol percent Al_2O_3 and it appears to be the only phase present in the sample containing 50 mol percent Al_2O_3 . As shown in Table 3.3 the diffraction pattern is unchanged after the samples have been used as catalysts.

Table 3.1

X-ray powder diffraction pattern of samples containing from 0 to 2.56 mol percent Al_2O_3

(s = strong; v = very; w = weak)

		NiO/ Al_2O_3 Catalysts					
Mol % Al_2O_3		0	0.10	0.50	2.56		
NiO (94)							
d Å	I/I ₁	d Å	Intensity	d Å	Intensity	d Å	Intensity
2.41	91	2.405	s	2.42	s	4.68	vW
2.088	100	2.075	vs	2.08	vs	2.405	s
1.476	57	1.475	s	1.475	s	2.075	vs
1.259	16	1.260	ms	1.26	ms	1.475	s
1.206	13	1.204	w	1.206	w	1.257	ms
1.044	8			1.204	w	1.203	w
0.9582	7						
0.9338	21						
0.8527	17						
0.8040	7						

Table 3.2 X-ray powder diffraction pattern of samples containing from 5.26 to 50 mol percent Al_2O_3 .
(s = strong; v = very; w = weak)

		NiO/ Al_2O_3 Catalysts						
Mol % Al_2O_3		14.29	25.0	50	NiAl_2O_4 (95)			
d Å	Intensity	d Å	Intensity	d Å	Intensity	d Å	I/I_1	
4.65	w	4.65	w	4.65	ms	4.65	w	20
2.84	vW	2.848	vW	2.84	w	2.846	w	20
2.405	s	2.41	vs	2.425	vs	2.42	vs	100
2.075	vs	2.08	vs	2.08	ms			
2.005	w	2.01	ms	2.01	s	2.005	s	65
1.63	vW	1.638	vW	1.64	vW			
1.542	w	1.545	w	1.545	w	1.54	w	30
1.475	s	1.475	s	1.475	w			
1.420	w	1.424	ms	1.425	s	1.42	ms	60
1.258	ms	1.26	ms	1.26	vW			
				1.23	vW			
1.202	ms	1.205	ms	1.205	vW			
						1.360	<1	<1
						1.273	<1	<1
						1.227	10	10
						1.213	<1	<1
						1.161	8	8
						1.047	12	12
						0.921	8	8
						0.8998	8	8

Table 3.3 X-ray powder diffraction pattern of some used catalysts

(s = strong; v = very; w = weak)

NiO/Al ₂ O ₃ Catalysts						
Mol % Al ₂ O ₃	0		2.56		5.26	
	d Å	Intensity	d Å	Intensity	d Å	Intensity
			4.68	vw	4.66	vw
					2.84	vw
	2.405	s	2.406	s	2.405	s
	2.076	vs	2.078	vs	2.08	vs
					2.007	vw
					1.625	vw
					1.541	w
	1.475	s	1.475	s	1.480	s
					1.424	w
	1.256	ms	1.258	ms	1.26	ms
	1.204	w	1.203	w	1.208	w

3.1.2 Surface areas

Gas adsorption data obtained from the BET apparatus were analysed with the aid of the APL programme 'KRBET' (Appendix I). Typical plots of $P/V(P_0 - P)$ versus P/P_0 are shown in Figures 3.1 and 3.2. The results are summarized in Table 3.4. The area occupied by one atom of krypton on a solid surface was taken as 19.5 \AA^2 (92).

Surface areas measured after reaction were found not to change appreciably.

Table 3.4 Surface areas

		NiO/Al ₂ O ₃ Catalysts						
Mol % Al ₂ O ₃	0	0.10	0.50	2.56	15.26	14.29	25.0	50
Surface area (m ² g ⁻¹)								
unused	3.02	62.43	36.45	42.00	31.70	41.60	73.65	76.72
used	2.98			41.60	30.20			

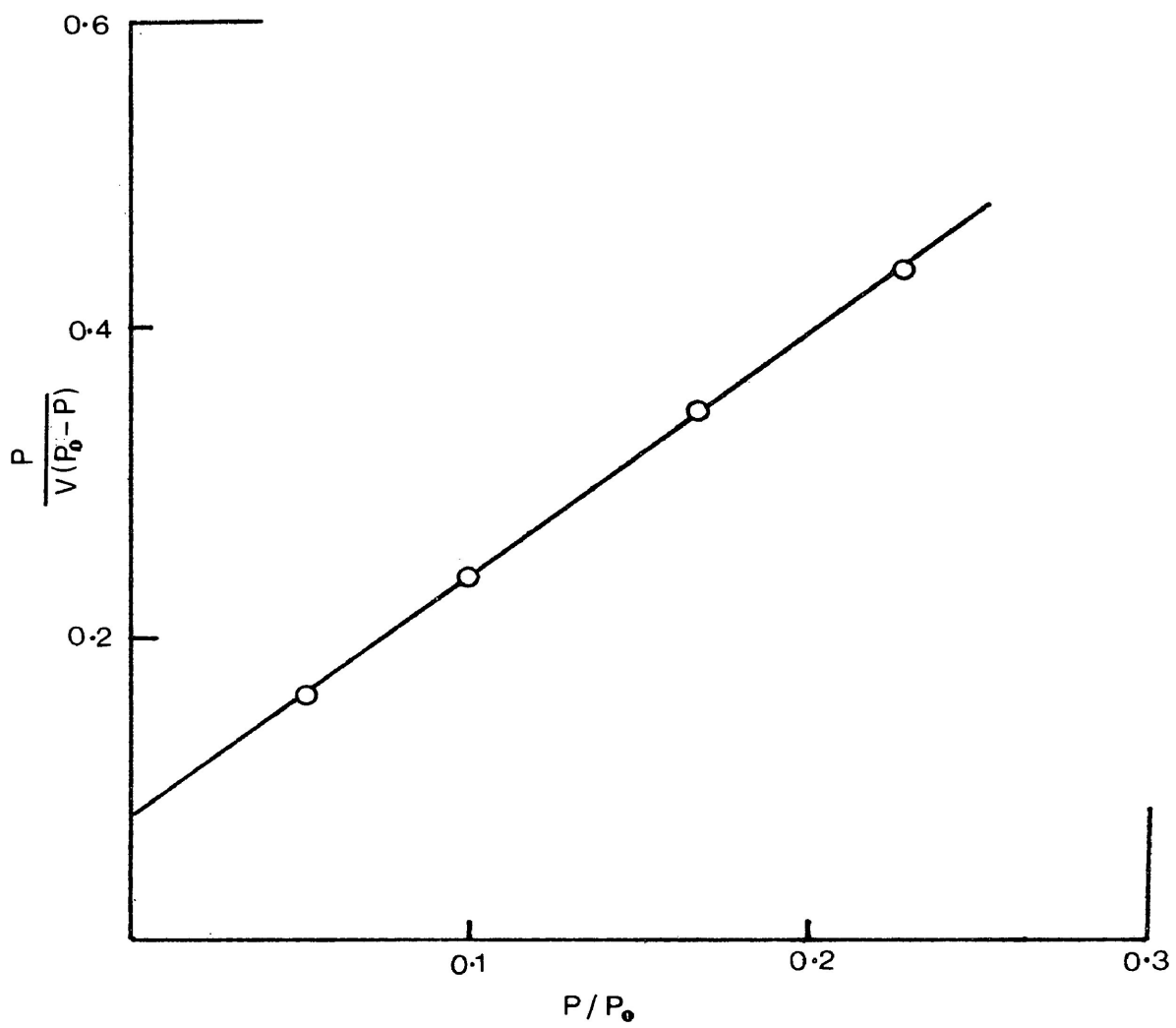


Figure 3.1: Surface area plot for NiO

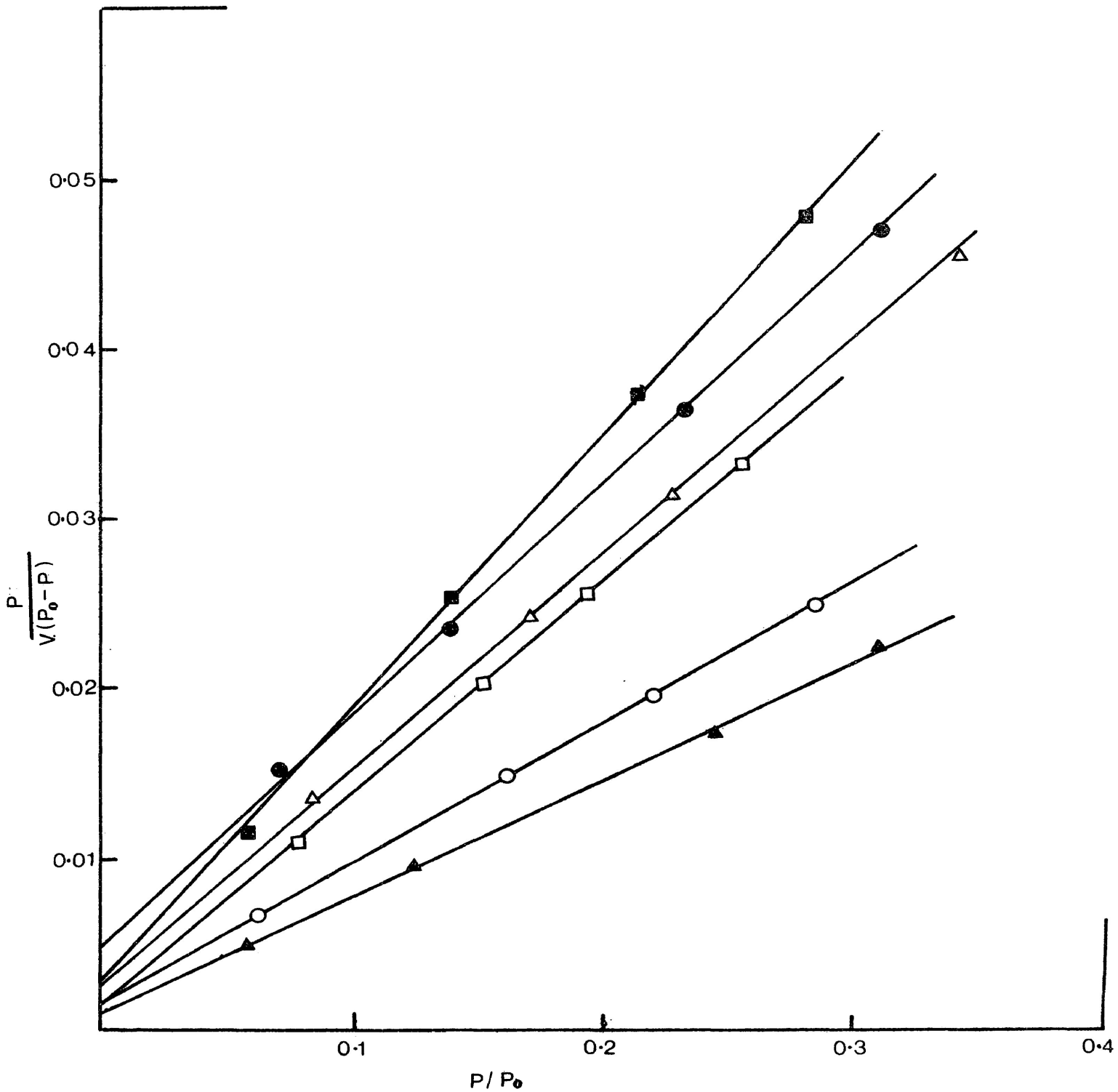


Figure 3.2: Surface area plots for doped sample; ○, 0.1 mol % Al_2O_3 ; ●, 0.5 mol % Al_2O_3 ; □, 2.56 mol % Al_2O_3 ; ■, 5.26 mol % Al_2O_3 ; △, 14.29 mol % Al_2O_3 ; ▲, 50 mol % Al_2O_3 .

3.1.3 Dehydroxylation

The thermal decomposition of pure Ni(OH)_2 and doped Ni(OH)_2 was monitored thermogravimetrically in a nitrogen atmosphere using a heating rate of 7°C min^{-1} . The results are presented as weight loss versus temperature in Figures 3.3 and 3.4. An initial period of rapid weight loss is observed which is followed by a period of deceleration and slow approach to constant weight loss values.

Treatment of data was made by the method of Coats and Redfern (96) who used a kinetic expression of the form:

$$\frac{d\alpha}{dt} = k(1-\alpha)^n \quad \dots 3,1$$

where α is the fraction decomposed; k is the rate constant at temperature T and n is the order of the reaction. The method requires a plot of

$$\log \frac{1-(1-\alpha)^{1-n}}{(1-n)T^2} \quad \text{versus } 1/T.$$

For the correct value of n , a linear plot of slope $-E/2.3 R$ is obtained where E is the activation energy. In the present

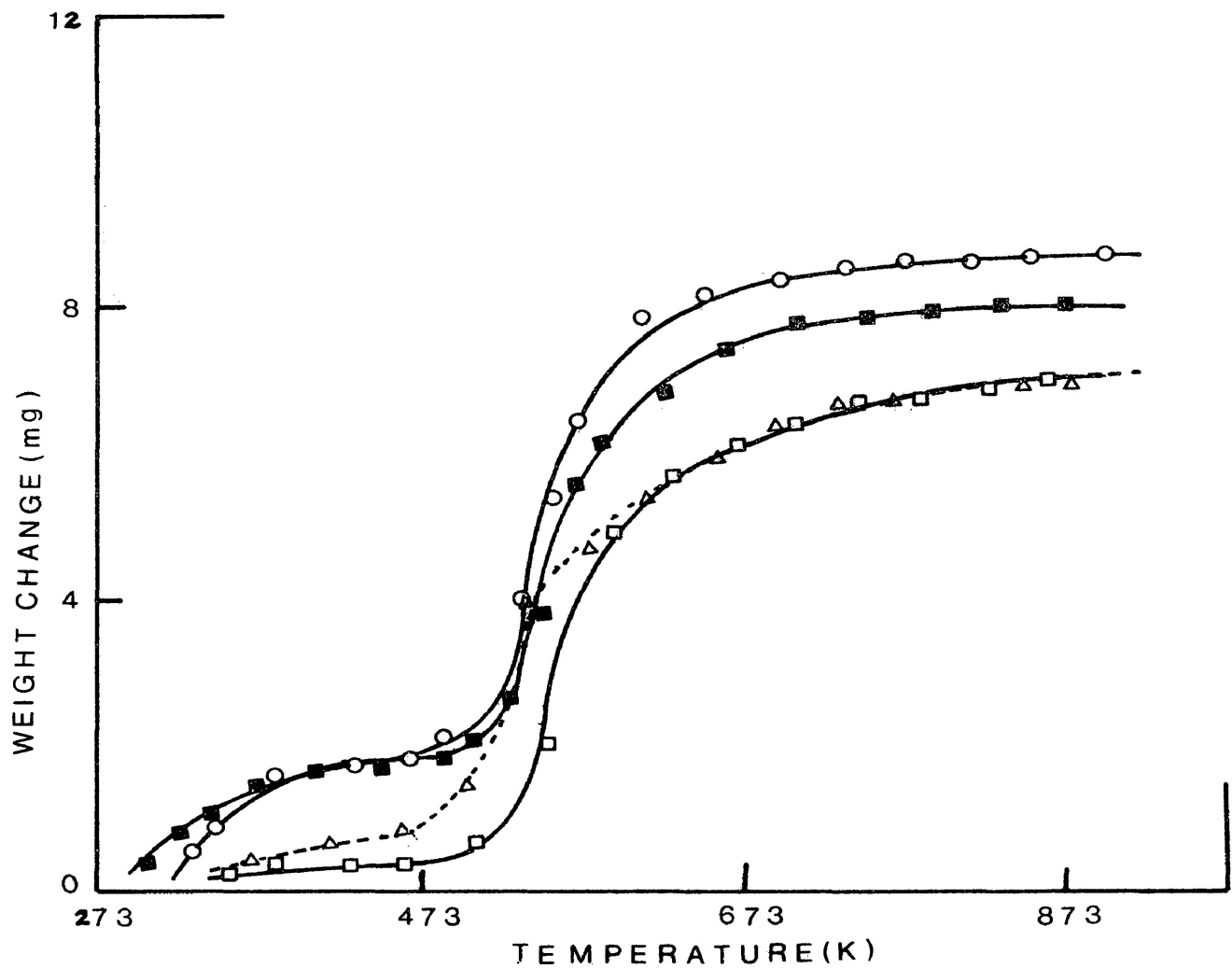


Figure 3.3: Thermogravimetric curves for decomposition of hydroxides;
O, NiO; ■, 0.1 mol % Al₂O₃; Δ, 0.5 mol % Al₂O₃;
□, 2.56 mol % Al₂O₃.

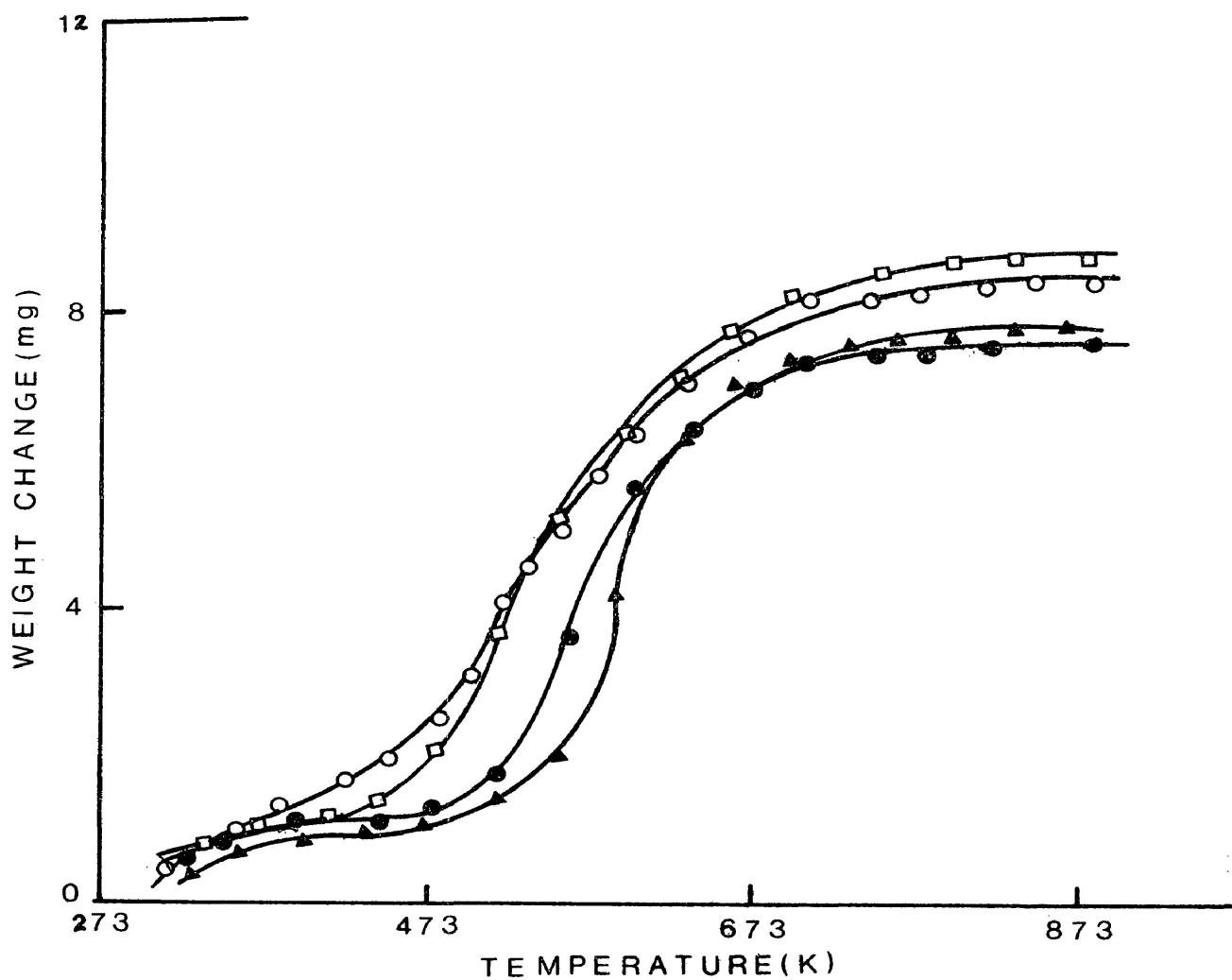


Figure 3.4: Thermogravimetric curves for decomposition of hydroxides;
●, 5.26 mol % Al₂O₃; ▲, 14.29 mol % Al₂O₃; ○, 25 mol % Al₂O₃;
□, 50 mol % Al₂O₃.

investigation the activation energies for the decomposition of pure and doped hydroxides are determined from the plots of

$$-\log \left[\frac{1 - (1 - \alpha)^{1-n}}{T^2(1-n)} \right] \text{ versus } 1/T \text{ for the special case of } n = 1.$$

Some typical plots are illustrated in Figure 3.5. The temperature for onset of reaction and the activation energies for decomposition are summarized in Table 3.4a. It should be noted that the activation energies are relatively unchanged if other values of n , i.e. $n = 0$, $n = 1/2$, and $n = 2/3$, are used in equation 3.1.

Table 3.4a Dehydroxylation of $\text{Ni}(\text{OH})_2$ and doped $\text{Ni}(\text{OH})_2$

Mol % Al_2O_3	Temperature for onset of reaction (K)	Activation Energy (kJ mol^{-1})
0	493	172.13
0.20	488	144.71
0.50	473	87.65
2.56	488	115.41
5.26	478	67.08
14.29	473	61.19
25.0	433	55.72
50.0	433	60.56

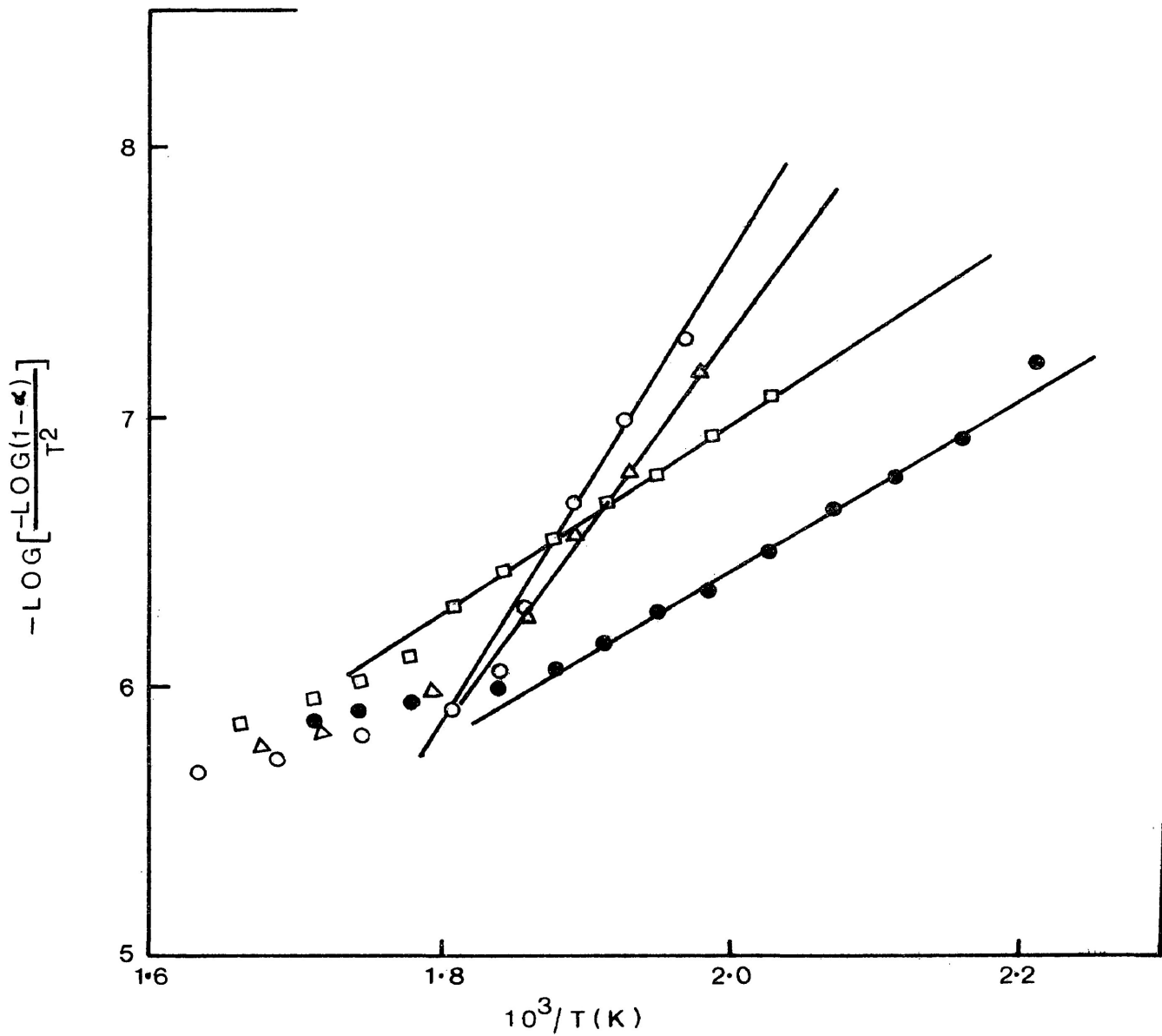


Figure 3.5: Plot of $\log \left[\frac{-\log(1-\alpha)}{T^2} \right]$ versus reciprocal temperatures;
 ○, NiO; △, 0.1 mol % Al_2O_3 ; □, 5.26 mol Al_2O_3 ;
 ●, 50 mol % Al_2O_3 .

3.2 Catalytic Decomposition of 2-Propanol

3.2.1 Kinetics of reaction

The nature of the reaction products

The decomposition of 2-propanol was investigated mainly over the temperature range 461 to 543 K on pure and doped NiO. NiO was active for the dehydrogenation of 2-propanol, yielding acetone but the introduction of alumina leads to the development of dehydration activity, yielding propene as well as acetone. The most significant feature is that the dehydrogenation activity decreases remarkably with successive pulses of alcohol for all the catalysts in the temperature range under investigation, while the dehydration activity increased slightly with successive pulses of 2-propanol. Typical plots of fractional conversion (α) versus injection number are shown in Figures 3.6 and 3.7.

The marked self-inhibition of the dehydrogenation reaction leads to problems in comparing the various catalysts since their activity is a function of the number of previous alcohol injections. The results of activity studies, particularly those for dehydrogenation, can be divided into three categories:

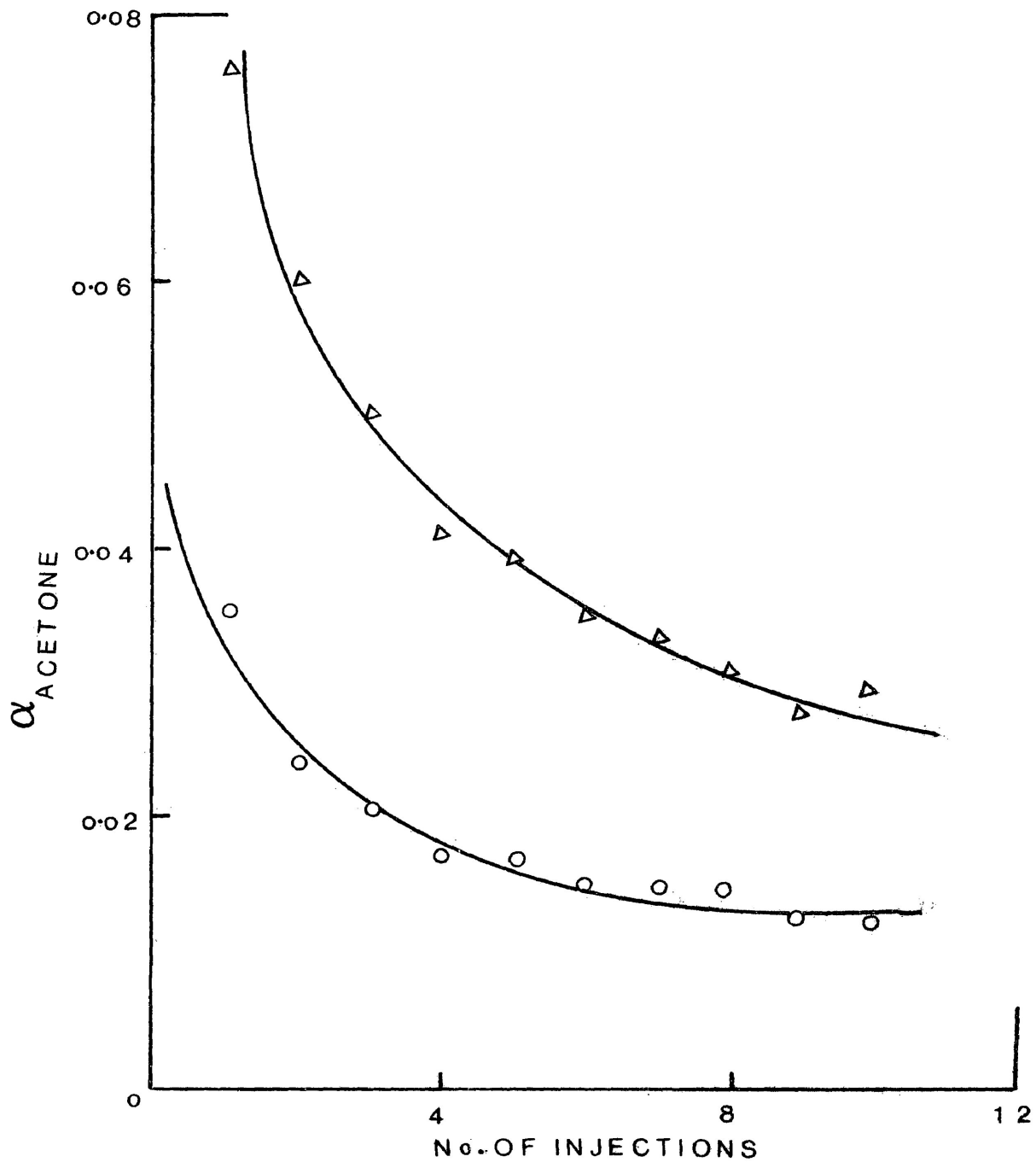


Figure 3.6: Typical plot of fractional dehydrogenation, α , versus number of injections (2nm^3 inj. size); O, 493 K; Δ , 523 K; NiO catalyst.

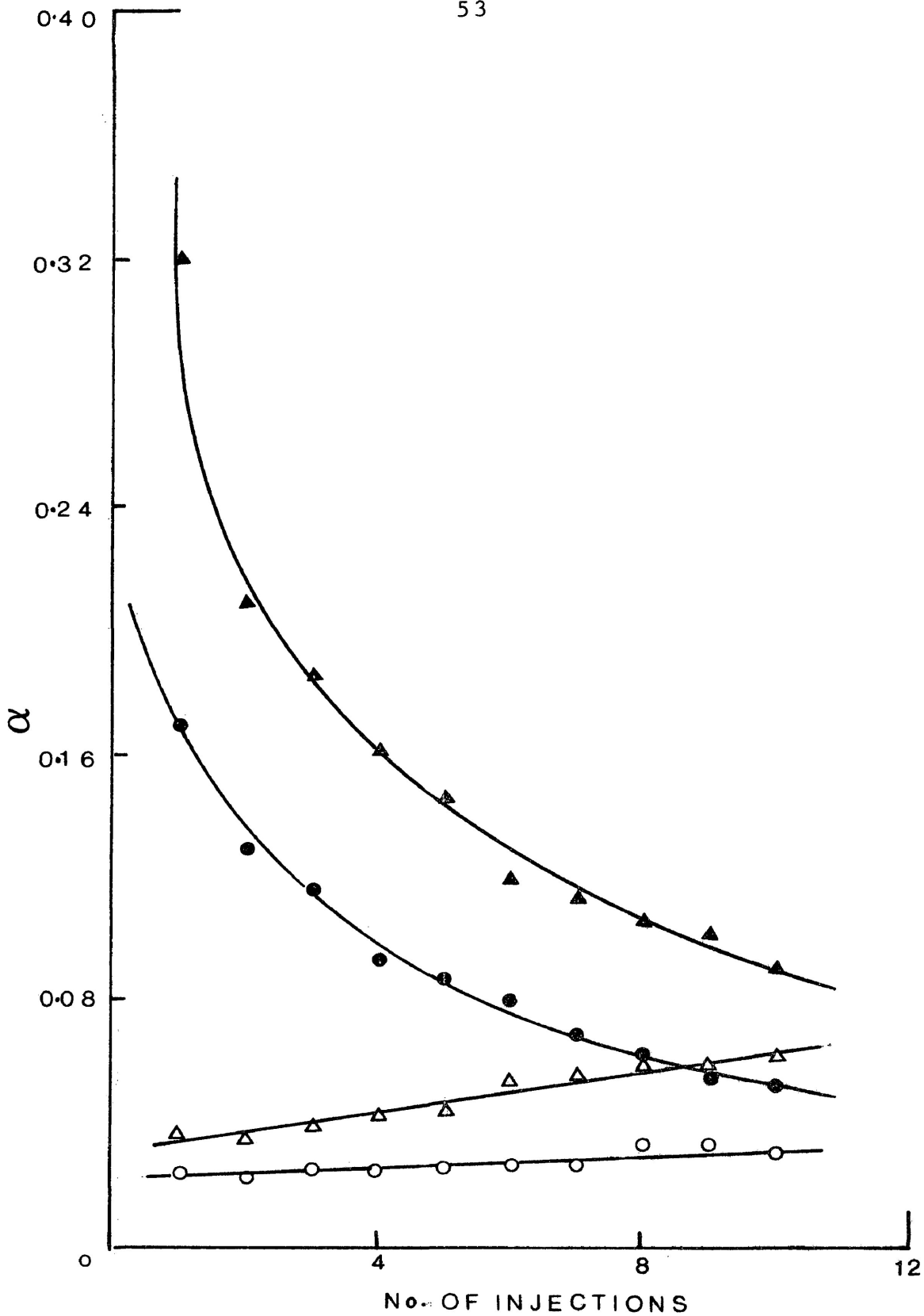


Figure 3.7: Typical plot of fractional dehydrogenation and dehydration, α , versus number of injections (2nm^3 inj. size); \circ , \bullet , 0.5 mol % Al_2O_3 ; Δ , \blacktriangle , 14.29 mol % Al_2O_3 ; open symbols for propene and solid symbols for acetone. Reaction temperature was 493 K.

- (a) Stabilized catalysts. In these cases the catalyst has been subjected to at least 100 nm³ of 2-propanol (50 injections) prior to the reported results and at this stage, the rate of decrease of the dehydrogenation activity is within experimental error.
- (b) Fresh or reactivated catalysts. In these cases only the results of the first alcohol injection on each catalyst is reported. It should be noted that even the fresh catalysts have been subjected to the pre-anneal at 623 K.
- (c) Activity changes on fresh and reactivated catalysts. In these cases the changes in dehydrogenation activity as a function of the number of alcohol injections are reported.

3.2.2. Catalyst Reactivation

As noted earlier (section 2.3.5), the catalysts can be reactivated by heating at 623 K for one hour (for NiO) or two hours (for the doped samples). Some measure of the effectiveness of the reactivation procedure is given in Table 3.5.

Table 3.5

Catalyst Reactivation

Catalyst (mol % Al ₂ O ₃)	Reaction Temperature (K)	Results on Fresh Catalyst (First injection)		Results on used catalyst after reactivation (First injection)	
		α -propene	α -acetone	α -propene	α -acetone
0	493	-	0.0353	-	0.0352
	523	-	0.0757	-	0.0749
0.50	493	0.0243	0.1681	0.0250	0.1590
	523	0.0311	0.4272	0.0320	0.4082
5.26	523	0.0329	0.3297	0.0353	0.3156
14.29	493	0.0379	0.3198	0.0374	0.2918
	523	0.0629	0.5464	0.0673	0.5193

In a number of cases, attempts have been made to trap out species being removed from the catalyst surface during the reactivation at 623 K. In these studies small amounts of acetone, carbon dioxide, water and trace amounts of 2-propanol were detected. However, it should be pointed out that compounds with very low boiling points could not be trapped out in this system and products of this type would not be detected. Thus,

for example, if methane is introduced into the carrier gas stream the trapping system does not recover even trace amounts of methane.

3.3 Stabilized Catalysts

3.3.1 Effect of changes in Flow Rate on Reactivity

The kinetics of dehydrogenation and dehydration were briefly examined on two samples of catalysts (5.26 mol % Al_2O_3) by varying the reactant-catalyst contact time as shown in Figure 3.8. The results are consistent with zero order kinetics at lower temperatures, but at higher temperatures, although the conversion decreased with increasing space velocity, the curves did not extrapolate through the origin. Rather, a finite intercept at infinite flow rate is indicated.

3.3.2 Effect of pulse size on the catalyst Reactivity

The relation between conversion (α) of 2-propanol and the apparent pulse intensity which is defined by the injected amount of alcohol was examined on the catalyst samples containing 2.56 and 5.26 mol percent Al_2O_3

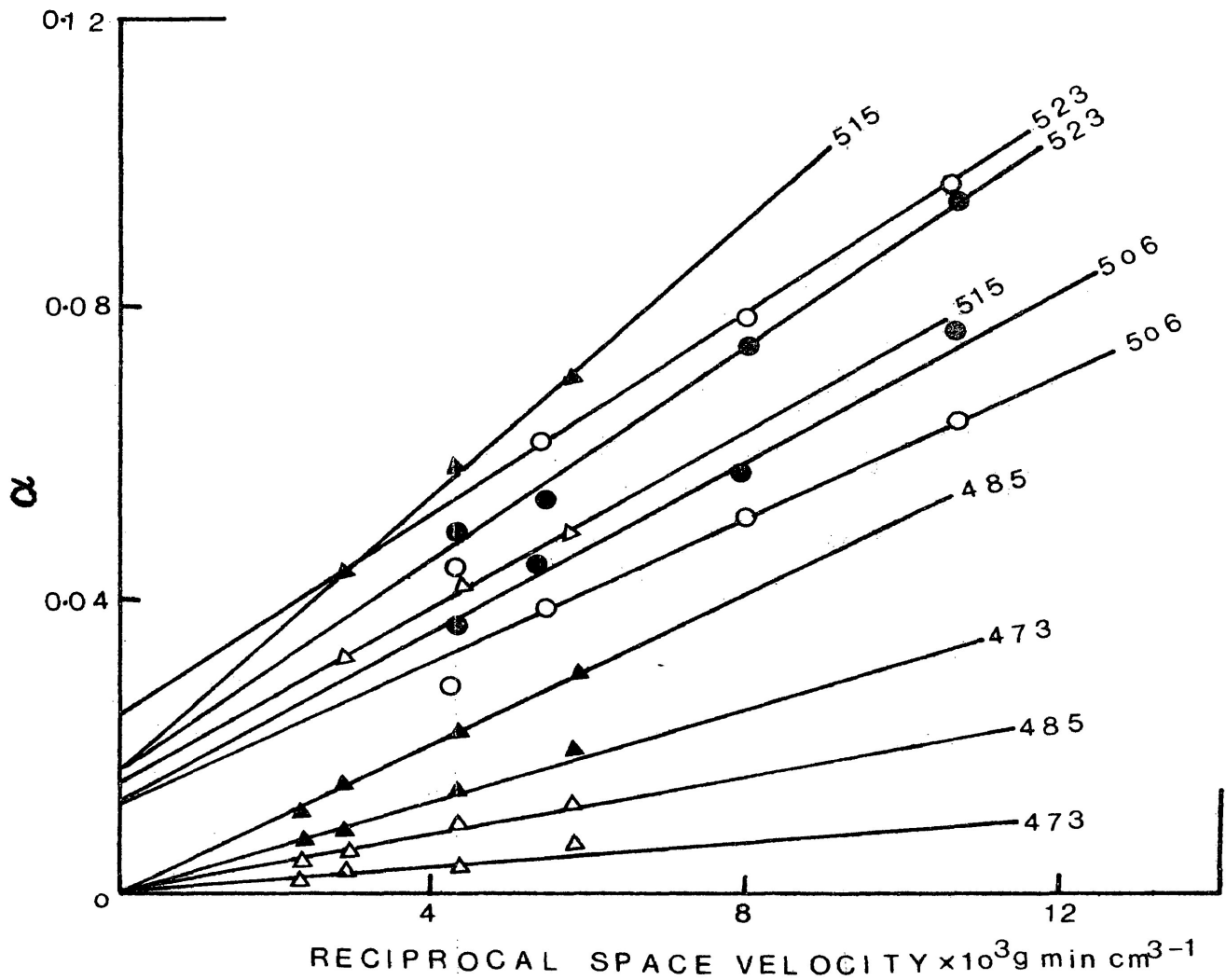


Figure 3.8: Fractional dehydrogenation and dehydration of 2-propanol (2nm^3 inj. size) on samples containing 5.26 mol % Al_2O_3 ; space velocity was varied by changes in flow rates; Δ , \blacktriangle , 0.1712 g; \circ , \bullet , 0.3203 g; open symbols for propene, solid symbols for acetone; reaction temperatures (K) are indicated in Figure.

at 493 K and 523 K. The results are shown in Figures 3.9 and 3.10. As shown in the figures, the conversion decreased with the increase in the pulse intensity or pulse width.

3.3.3 Effect of temperature changes on the Reaction Rates

The effect of temperature changes on the decomposition rates of 2-propanol over the catalysts were investigated in the range 453-543 K. The fractional conversion (α) to propene is shown in Table 3.6; α is determined on the basis of the products and reactants recovered. The results for the catalyst containing 50 mol percent Al_2O_3 are not included in Table 3.6 because of the high reactivity of this catalyst. For this sample, a lower temperature range (413-463 K) and a higher flow rate ($60 \text{ cm}^3 \text{ min}^{-1}$) were employed and under these conditions, the catalyst exhibited purely dehydration activity. These results are given in Table 3.7. As noted earlier the dehydrogenation is self-inhibiting and increases in temperature "destabilize" the catalyst activity for dehydrogenation thus making the results non-reproducible. The effect of temperature on the dehydrogenation activity

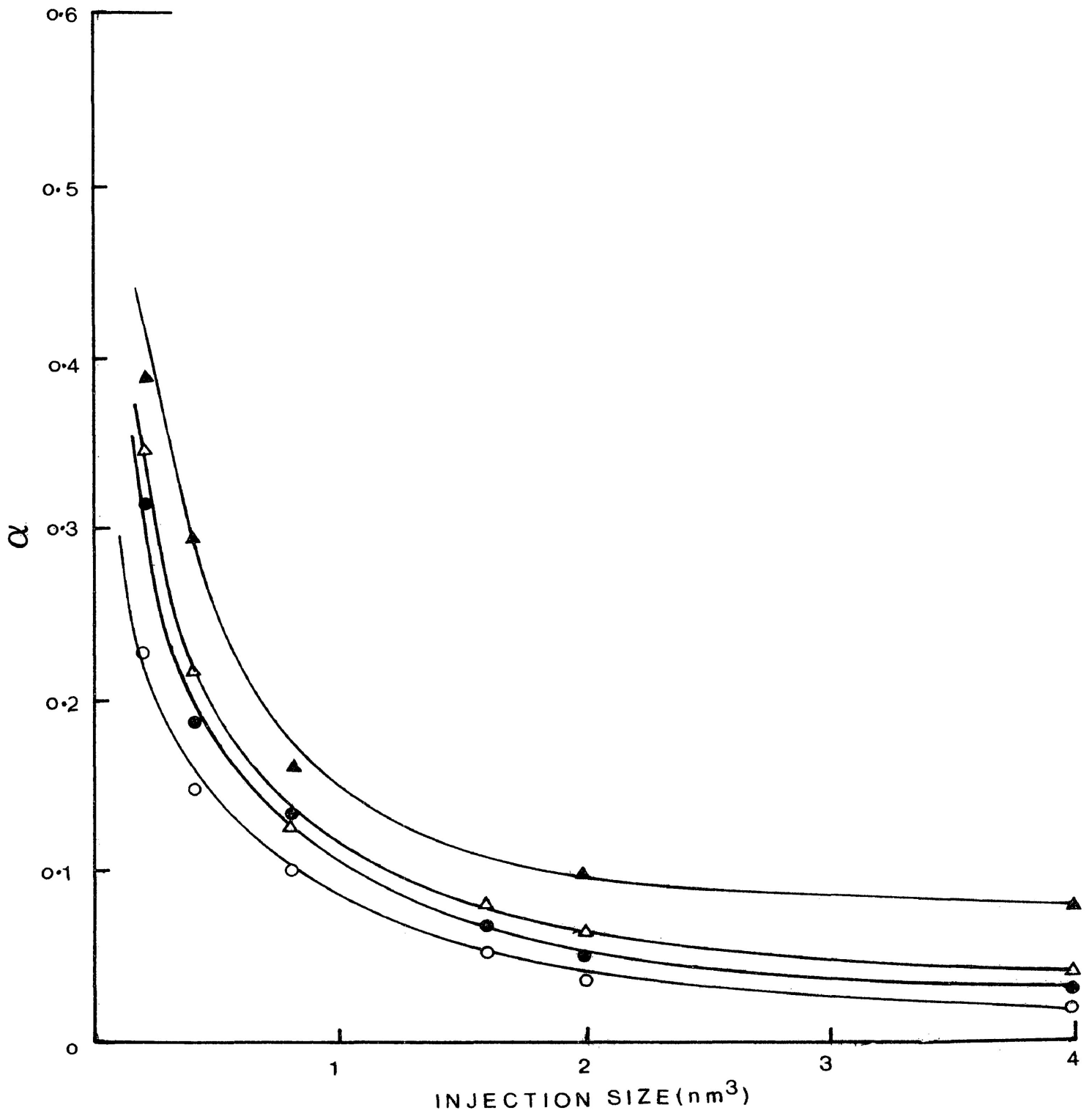


Figure 3.9: Effect of injection size on fractional conversion, α , on sample containing 2.56 mol % Al_2O_3 ; \circ, \bullet , 493 K; Δ, \blacktriangle , 523 K; open symbols for propene, solid symbols for acetone.

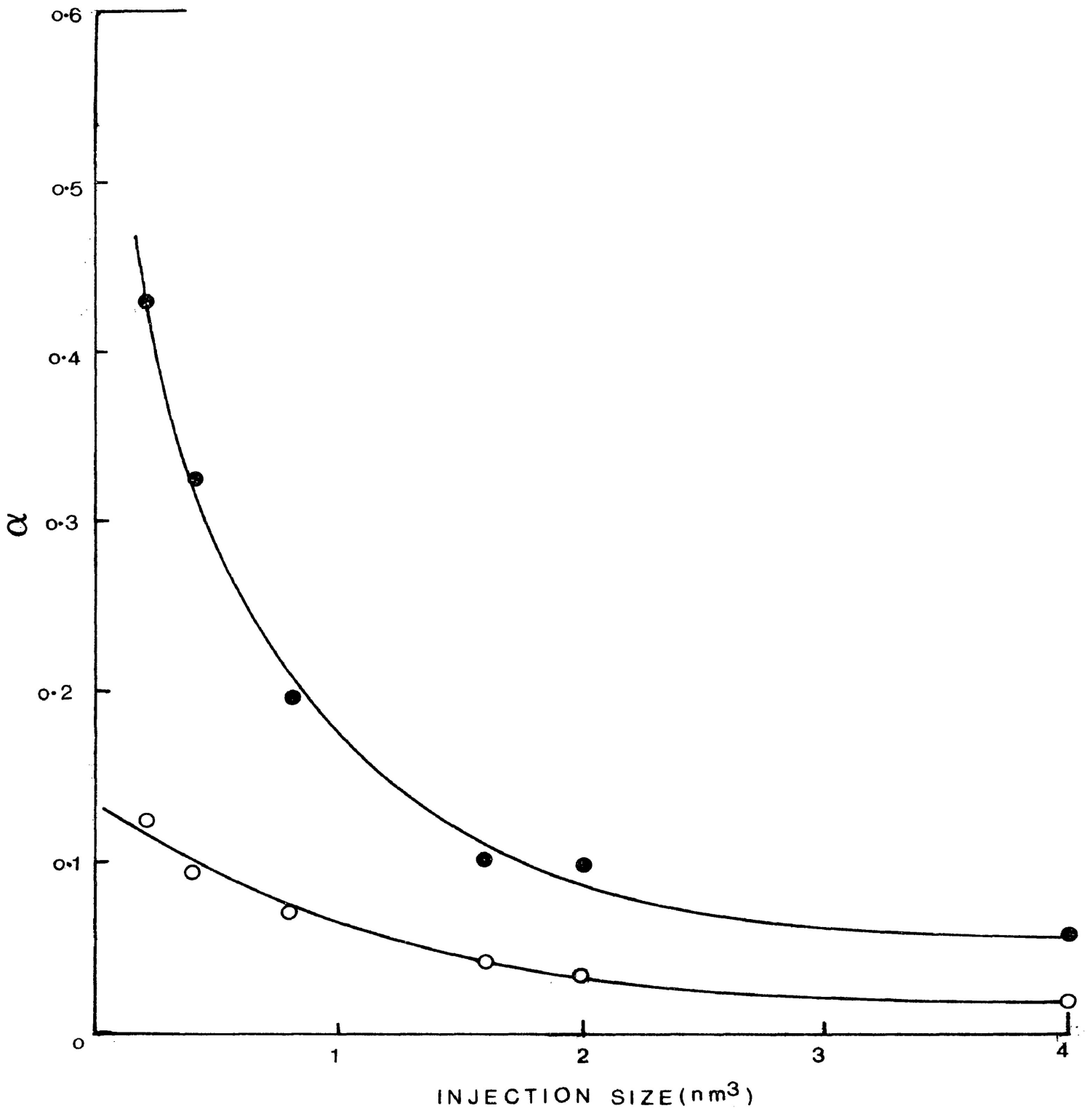


Figure 3.10: Effect of injection size on fractional conversion, α , on sample containing 5.26 mol % Al_2O_3 at 523 K; ○, propene; ●, acetone.

of fresh and reactivated catalysts is reported in a later section.

3.4 Fresh or Reactivated Catalysts

3.4.1 Fresh catalysts

In order to compare the initial activity of the different catalyst compositions, the rate of decomposition of 2-propanol at 461 K on the catalyst samples has been determined. The results are reported in Table 3.8. One significant feature of the results is that, with the doped samples, the recovery of the products and reactant, i.e. the total area on the chart print-out, is anomalously low for the first few injections. This leads to an artificially high value of conversion (α) particularly for the first injection.

3.4.2 Reactivated catalysts: Effect of temperature changes on the reactivity

The self-inhibition of the dehydrogenation reactions leads to problems in determining the temperature dependence of the rate of dehydrogenation of 2-propanol. In order to determine this temperature dependence a single pulse of 2-propanol was admitted to the catalyst at each

temperature and between each reaction temperature the catalyst was reactivated at 623 K by the standard procedure. These experiments were carried out on the samples containing 5.26 and 14.29 mol percent Al_2O_3 , and the results are reported in Table 3.9.

3.5 Studies of Catalyst Poisoning on Fresh and Reactivated Catalysts

3.5.1 Self-poisoning

Investigations of the self-poisoning in acetone formation on NiO and the doped samples were carried out at 493 K and 523 K, the catalyst being reactivated prior to the measurements at each reaction temperature. The catalysts were subjected to a series of ten injections of 2-propanol at each reaction temperature and the fractional conversion (α) to propene and acetone for each injection was determined. The results are reported in Tables 3.11 and 3.12 and some typical plots of α as a function of the number of injections are given in Figures 3.6 and 3.7.

Additional studies of other factors which could affect the self-poisoning of the dehydrogenation reaction

were made. Thus, the effects of time interval between injections (Table 3.13), pulse size (Table 3.14 and Table 3.15) and catalyst size (Table 3.16) on the self poisoning were investigated.

3.5.2 The effects of other potential poisons

A number of studies were also made of the effects of catalyst pretreatment on the dehydration and dehydrogenation activity at reaction temperatures of 493 K and 523 K. In these experiments, the catalysts, at the reaction temperature, were subjected to pulses of added poison followed by injection of 2-propanol approximately 30 minutes after the pretreatment pulse. The catalyst was reactivated before admission of each poison. Some results of these types of experiments are given in Table 3.17.

Adsorption of acetic acid, phenol, acetone, carbondioxide, aniline and n-butyl amine poisoned the dehydrogenation activity to a marked extent both at the lower and higher temperatures. However, dehydrogenation activity virtually remained unaffected by the preadsorption of benzene.

Decreases in the dehydration activity were observed with preadsorption of acetic acid, phenol, benzene, water, aniline and n-butyl amine at the lower temperature. n-Butyl amine and acetic acid acted as more powerful poisoning agents in comparison with other poisons. A slight recovery in activity was observed with successive pulses of 2-propanol. No appreciable change in activity was observed with preadsorption of benzene and phenol at higher temperatures. Carbon dioxide slightly deactivated the dehydration activity, but recovery was marked with successive injections of 2-propanol. Although acetone poisoned the dehydrogenation activity to a remarkable extent it did not appear to affect the dehydration activity at all.

Table 3.6

Fractional conversion of 2-propanol to
propene as a function of temperature

Temperature (K)	NiO/Al ₂ O ₃ catalyst						
	Mol%Al ₂ O ₃	0.10	0.50	2.56	5.26	14.29	25.0
		α Propene (Per m ² of catalyst surface)					
461		0.0017	0.0025	0.0010	0.0009	0.0024	0.0328
473		0.0033	0.0038	0.0022	0.0017	0.0057	0.0453
483		0.0053	0.0066	0.0048	0.0033	0.0092	0.0538
493		0.0078	0.0079	0.0087	0.0053	0.0122	0.0561
503		0.0103	0.0109	0.0113	0.0073	0.0159	0.0624
513		0.0126	0.0130	0.0153	0.0096	0.0185	0.0697
523		0.0136	0.0162	0.0160	0.0106	0.0208	0.0810
533		0.0155	0.0180	0.0170	0.0117	0.0225	0.0979
543		0.0172	0.0240	0.0216	0.0125	0.0244	0.1160

NOTE: Although this and the following tables quote the fractional conversion to the fourth decimal place, experimental error precludes any significance being placed on the last digit.

Table 3.7 Fractional conversion of 2-propanol to propene as a function of temperature for catalyst containing 50 mol percent Al_2O_3

Temperature (K)	α_{Propene} (Per m^2 of catalyst surface)
413	0.0024
423	0.0087
433	0.0236
443	0.0507
453	0.0767
463	0.0872

Table 3.8

Fractional conversion of 2-propanol to propene,
acetone and the fraction recovered on the fresh
catalysts for reaction at 461 K

Catalyst Mol%Al ₂ O ₃	Surface area ² of sample (m ²)	Number of injections	**α Propene	**α Acetone	Fraction Recovered
0	0.4884	1	-	0.0270	0.9863
		2	-	0.0250	1.0000
		3	-	0.0238	0.9937
		4	-	0.0210	0.9683
0.10	8.215	1	0.0167	0.2054	0.8262
		2	0.0129	0.1642	0.9184
		3	0.0128	0.1447	0.9713
		4	0.0138	0.1405	1.0000
0.50	4.33	1	0.0126	0.0905	0.9420
		2	0.0108	0.0847	1.0000
		3	0.0099	0.0629	0.9944
		4	0.0098	0.0604	0.9886
2.56	4.94	1	0.0058	0.0845	0.9458
		2	0.0059	0.0773	0.9884
		3	0.0059	0.0690	0.9912
		4	0.0058	0.0611	0.9898

continued...

Table 3.8

continued...

Catalyst Mol%Al ₂ O ₃	Surface area ² of sample (m ²)	Number of injections	**α Propene	**α Acetone	Fraction Recovered
5.26	4.62	1	0.0040	0.0712	0.8903
		2	0.0040	0.0684	0.9675
		3	0.0039	0.0618	0.9845
		4	0.0039	0.0559	1.0000
14.29	5.48	1	0.0143	0.1033	0.8285
		2	0.0122	0.0908	1.0000
		3	0.0129	0.0836	0.9993
		4	0.0131	0.0712	0.9996
25.0	5.03	1	0.1610	0.1000	0.8856
		2	0.1588	0.0720	0.9668
		3	0.1609	0.0585	1.0000
		4	0.1701	0.0560	0.9889
*50	4.02	1	0.0304	-	0.7836
		2	0.0319	-	0.9866
		3	0.0321	-	1.0000
		4	0.0332	-	0.9781

*Temperature: 423 K, Flow rate: 60.0 cm³ min⁻¹**α values are not corrected to m² of the catalyst surface

Table 3.9 Fractional conversion of 2-propanol to propene and acetone as a function of temperature when the catalyst was activated between injections

Catalyst mol%Al ₂ O ₃	Sample Weight (g)	Temperature (K)	α Propene (per m ² of catalyst surface)	α Acetone
5.26	0.1471	475	0.0020	0.0197
		483	0.0026	0.0235
		492	0.0034	0.0292
		504	0.0038	0.0332
		514	0.0048	0.0505
		527	0.0063	0.0692
		536	0.0072	0.0730
		547	0.0081	0.0895
14.29	0.1318	461	0.0025	0.0160
		473	0.0047	0.0265
		483	0.0056	0.0339
		493	0.0068	0.0404
		503	0.0077	0.0484
		513	0.0099	0.0621
		523	0.0122	0.0808
		533	0.0152	0.0965
		543	0.0191	0.1170

Table 3.11 Fractional conversion of 2-propanol to propene and acetone as a function of number of injections at 493 K.

Catalyst Mol% Al ₂ O ₃	Surface area of sample (m ²)	No. of Injections	**α _{Propene}	**α _{Acetone}
0	0.4884	1	-	0.0353
		2	-	0.0244
		3	-	0.0206
		4	-	0.0173
		5	-	0.0171
		6	-	0.0151
		7	-	0.0150
		8	-	0.0149
		9	-	0.0123
		10	-	0.0120
0.50	4.33	1	0.0243	0.1681
		2	0.0231	0.1296
		3	0.0259	0.1163
		4	0.0250	0.0937
		5	0.0262	0.0864
		6	0.0272	0.0805
		7	0.0264	0.0686
		8	0.0342	0.0620
		9	0.0346	0.0543
		10	0.0316	0.0536
2.56	6.56	1	0.0610	0.1330
		2	0.0527	0.1064
		3	0.0591	0.1015
		4	0.0538	0.0902
		5	0.0545	0.0936
		6	0.0506	0.0811
		7	0.0546	0.0779
		8	0.0518	0.0731
		9	0.0509	0.0720
		10	0.0490	0.0703

Table 3.11

continued...

Catalyst Mol% Al ₂ O ₃	Surface area of sample (m ²)	No. of Injections	**α Propene	**α Acetone
14.29	5.48	1	0.0379	0.3198
		2	0.0358	0.2095
		3	0.0398	0.1855
		4	0.0435	0.1608
		5	0.0443	0.1458
		6	0.0551	0.1185
		7	0.0562	0.1135
		8	0.0617	0.1052
		9	0.0611	0.1026
		10	0.0639	0.0917

**α-values are not corrected to m² of the catalyst surface

Table 3.12 Fractional conversion of 2-propanol to propene and acetone as a function of number of injections at 523 K

Catalyst Mol% Al ₂ O ₃	Surface area of sample (m ²)	No. of Injections	**α _{Propene}	**α _{Acetone}
0	0.4884	1	-	0.0757
		2	-	0.0604
		3	-	0.0501
		4	-	0.0411
		5	-	0.0397
		6	-	0.0357
		7	-	0.0338
		8	-	0.0310
		9	-	0.0273
		10	-	0.0290
0.50	4.33	1	0.0311	0.4272
		2	0.0362	0.2824
		3	0.0403	0.2272
		4	0.0454	0.1979
		5	0.0433	0.1694
		6	0.0494	0.1477
		7	0.0475	0.1231
		8	0.0493	0.1101
		9	0.0528	0.1052
		10	0.0537	0.1025
2.56	6.56	1	0.0797	0.2355
		2	0.0790	0.2184
		3	0.0889	0.1991
		4	0.0913	0.1743
		5	0.1008	0.1482
		6	0.0972	0.1442
		7	0.1088	0.1237
		8	0.0985	0.1302
		9	0.1036	0.1199

Table 3.12

continued...

Catalyst Mol % Al ₂ O ₃	Surface area of sample (m ²)	No. of Injections	**α Propene	**α Acetone
5.26	3.24	1	0.0329	0.3297
		2	0.0392	0.2036
		3	0.0462	0.1686
		4	0.0480	0.1424
		5	0.0547	0.1365
		6	0.0578	0.1226
		7	0.0616	0.1140
		8	0.0628	0.1035
		9	0.0646	0.1014
14.29	5.48	1	0.0629	0.5464
		2	0.0623	0.3438
		3	0.0698	0.2988
		4	0.0800	0.2577
		5	0.0813	0.2058
		6	0.0889	0.1939
		7	0.0911	0.1767
		8	0.0968	0.1629
		9	0.0952	0.1482
		10	0.1029	0.1485

**α -values are not corrected to m² of the catalyst surface

Table 3.13 Fractional conversion of 2-propanol to acetone as a function of time between injections on NiO at 523 K

Surface area of sample (m ²)	No. of Injections	* α Acetone			
		Injection interval (min)	17	30	45
0.4884	1		0.0772	0.0749	0.0734
	2		0.0552	0.0595	0.0544
	3		0.0473	0.0525	0.0442
	4		0.0453	0.0511	0.0585
	5		0.0360	0.0360	0.0404
	6		0.0356	0.0353	0.0365
	7		0.0328	0.0353	0.0357
	8		0.0273	0.0332	0.0336
	9		0.0253	0.0263	0.0305
	10		0.0278	0.0288	0.0273

* α -values are not corrected to m² of the catalyst surface

Table 3.14 Fractional conversion of 2-propanol to
Acetone as a function of pulse size on
NiO at 523 K

Surface area of sample (m ²)	No. of Injections	* α Acetone	
		Pulse size (nm ³)	
		2	4
0.4884	1	0.0749	0.0681
	2	0.0595	0.0481
	3	0.0525	0.0433
	4	0.0511	0.0387
	5	0.0360	0.0355
	6	0.0353	0.0284
	7	0.0353	0.0251
	8	0.0332	0.0256
	9	0.0263	0.0270
	10	0.0310	0.0256

* α -values are not corrected to m² of the catalyst surface

Table 3.15

Fractional conversion of 2-propanol to propene and acetone as a function of pulse size on catalyst containing 0.5 mol % Al_2O_3 at 493 K

Surface Area of Sample (m^2)	No. of Injections	Pulse width (nm^3)			
		1*	2*	α Propene	α Acetone
4.33	1	0.0335	0.2021	0.0243	0.1681
	2	0.0472	0.1456	0.0231	0.1296
	3	0.0518	0.1064	0.0259	0.1163
	4	0.0538	0.0894	0.0250	0.0937
	5	0.0520	0.0930	0.0262	0.0864
	6	0.0571	0.0814	0.0272	0.0805
	7	0.0532	0.0792	0.0264	0.0686
	8	0.0541	0.0747	0.0342	0.0620
	9	0.0547	0.0703	0.0346	0.0543
	10	0.0525	0.0658	0.0316	0.0536

* α -values are not corrected to m^2 of the catalyst surface

Table 3.16

Fractional conversion of 2-propanol to propene and acetone as a function of catalyst size on sample containing 14.29 mol percent Al_2O_3 at 523 K.

No. of Injections	Flow rate ($cm^3 \text{ min}^{-1}$)	Sample weight (g)			α Propene	α Acetone	α Propene	α Acetone	α Propene	α Acetone
		0.0989	0.1600	0.2828						
	75									
1		-			0.0791	0.3998	0.1471	0.6144		
2		0.0581	0.1980	0.0703	0.2942	0.1257	0.4665			
3		0.0608	0.1578	0.0780	0.2597	0.1217	0.4376			
4		0.0670	0.1505	0.0769	0.2454	0.1347	0.3874			
5		0.0702	0.1471	0.0781	0.2218	0.1374	0.3512			
6		0.0700	0.1274	0.0817	0.1987	0.1560	0.3569			
7		0.0746	0.1246		0.1522	0.3285				
	60									
1		0.0827	0.1267	0.1094	0.2090	0.1748	0.3254			
2		0.0815	0.1200	0.1134	0.1947	0.1681	0.3017			
3		0.0794	0.1078	0.1061	0.1771	0.1726	0.2689			
4		0.0810	0.1074	0.1113	0.1661	0.1796	0.2739			
5		0.0828	0.1046	0.1105	0.1621	0.1830	0.2603			
	40									
1		0.0880	0.1128	0.1288	0.1603	0.1995	0.2939			
2		0.0883	0.1040	0.1250	0.1570	0.1986	0.2853			
3		0.0879	0.1020	0.1272	0.1445	0.1968	0.2610			
4		0.0935	0.1090	0.1297	0.1497	0.1963	0.2586			
5		0.0850	0.0977	0.1243	0.1445	0.1984	0.2484			
	30									
1		0.0946	0.1120	0.1353	0.1688	0.2112	0.2705			
2		0.0951	0.1078	0.1331	0.1559	0.2061	0.2533			
3		0.0936	0.1020	0.1347	0.1533	0.2101	0.2567			
4		0.0881	0.0987	0.1323	0.1482	0.2034	0.2359			
5		0.0937	0.0977	-	-	0.2141	0.2388			

* α -values are not corrected to m^2 of the catalyst surface; catalyst samples were not reactivated between each flow rate.

Table 3.17 The effects of pretreatment on the dehydration and dehydrogenation activity of the catalysts

Catalyst Mol%Al ₂ O ₃	Surface area of sample (m ²)	Temp. (K)	Pretreatment Added reagent	Volume (nm ³)	*α Propene		*α Acetone	
					Before treatment	After treatment	Before treatment	After Treatment
0	0.4884	523	acetone	1.0	-	-	0.0757	0.0223
			acetic acid	1.0	-	-	0.0756	0.0052
0.50	4.33	493	acetone	1.0	0.0243	0.035	0.1681	0.1229
			acetone	1x10	-	0.0236	-	0.0300
			acetic acid	1x9	-	trace	-	trace
			phenol	1x5	-	0.0080	-	0.0291
			benzene	1x3	-	0.0148	-	0.1742
			n-butyl amine	1x10	-	0.0015	-	0.0169
523			acetic acid	1x9	0.0311	trace	0.4272	trace
			phenol	1x5	-	0.0304	-	0.0762
			carbondi-oxide	100	-	0.0289	-	0.3249
			aniline	1x4	-	0.0200	-	0.1213
			n-butyl amine	1x10	-	0.0080	-	0.0571

*α-values are not corrected to m² of the catalyst surface

3.6 Isotope Effects

3.6.1 Stabilized catalyst

Isotope effects in 2-propanol decomposition were investigated in the temperature range 486 - 547 K on a catalyst sample containing 5.26 mol percent Al_2O_3 . Substitution of deuterium for hydrogen leads to significant changes in the degree of conversion of 2-propanol. The fractional conversions for 2-propanol, 2-propanol- d_6 and 2-propanol- 2d_1 at different temperatures are shown in Figure 3.11. With 2-propanol- d_6 , the propene yield is reduced while the acetone yield is reduced with 2-propanol- 2d_1 as the reactant. The substitution of deuterium in the hydroxyl group does not appear to affect the extent of either the dehydration or the dehydrogenation reactions. Detailed results are given in Appendix II. The isotope effects, defined as the ratio of the fractional conversion of the alcohol to that of the deuterio-alcohol, as a function of temperature are summarized in Table 3.18.

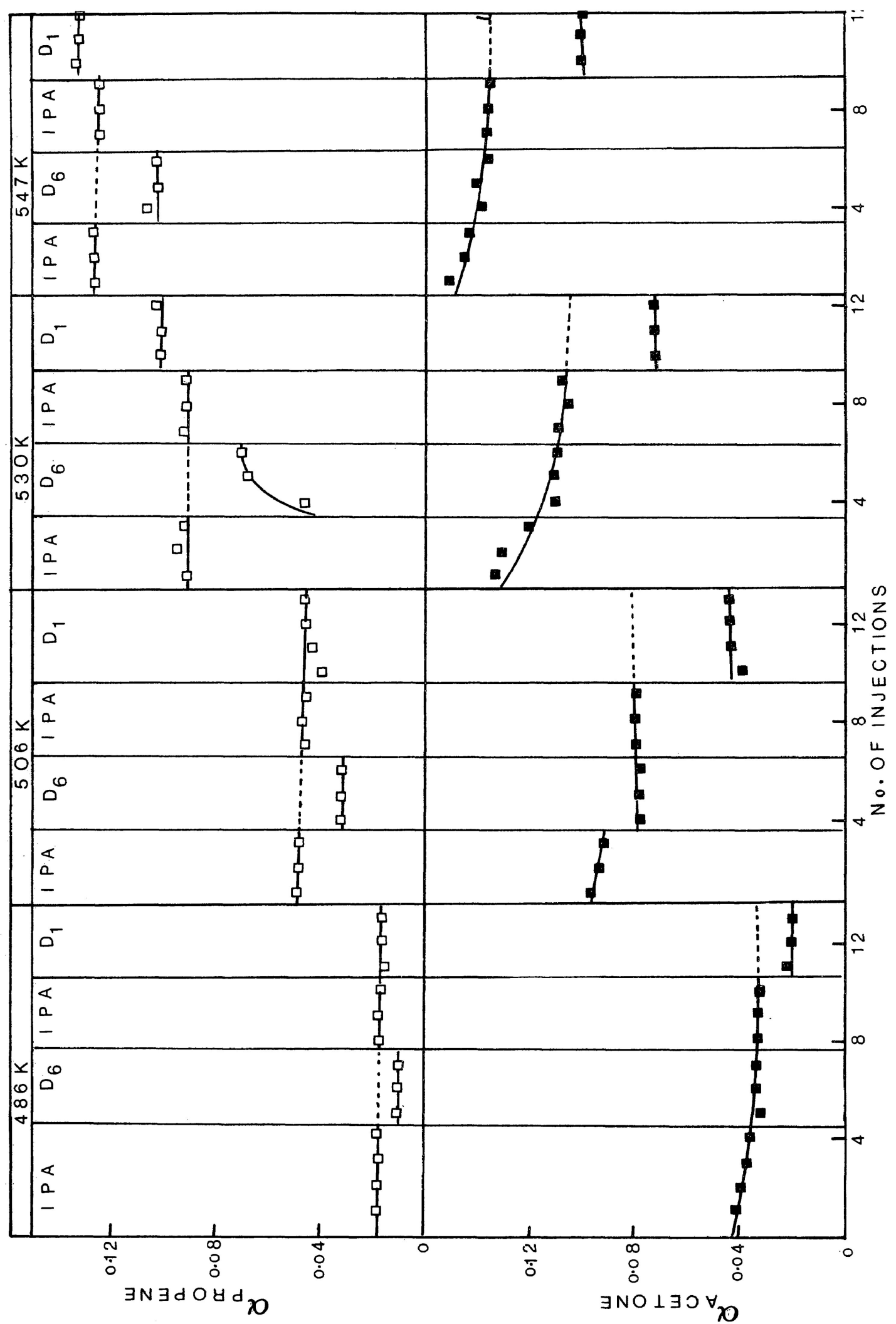


Figure 3.11: Fractional conversion of 2-propanol and deuterio-alcohols (2nm³ inj. size) on stabilized sample containing 5.25 mol % Al₂O₃; IPA, 2-propanol; D₆, 2-propanol-d₆; D₁, 2-propanol-2d₁.

Table 3.18 Isotope effects in the Dehydration and Dehydrogenation of 2-propanol on a catalyst sample containing 5.26 mol percent Al_2O_3

Temperature (K)	Isotope effect ($\alpha\text{H}/\alpha\text{D}$)			
	In propene formation		In acetone formation	
	(a)*	(b)*	(a)*	(b)*
486	1.75	1.04	0.99	1.70
506	1.48	1.03	0.99	1.68
530	1.31	0.90	0.99	1.50
547	1.21	0.95	0.98	1.35

* column (a) refers to comparison of α for 2-propanol and 2-propanol- d_6 ($(\text{CD}_3)_2\text{CHOH}$) while column (b) refers to the comparison of α for 2-propanol and 2-propanol- 2d_1 ($(\text{CH}_3)_2\text{CDOH}$).

Isotope effects were also determined on a stabilized NiO catalyst sample, in the temperature range 500 - 540 K. The fractional conversions of the alcohols and deuterio-alcohols are given in Figure 3.12. An isotope effect is not observed with 2-propanol- d_6 , but with 2-propanol- 2d_1 , the effect is clearly observed. It is to be noted that substitution of deuterium in the hydroxyl group

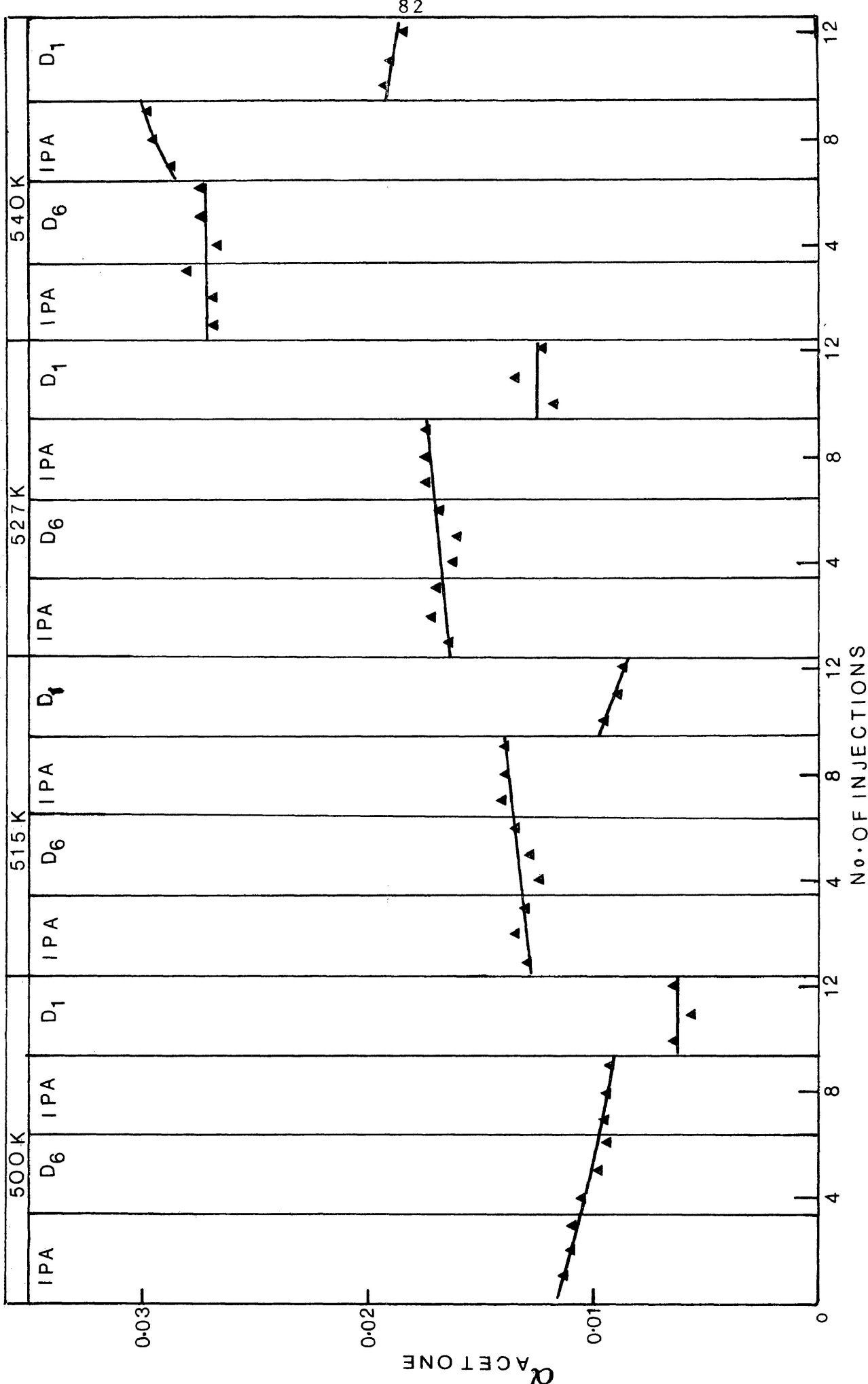


Figure 3.12: Fractional conversion of 2-propanol and deuterio-alcohols (2nm³ inj. size) on stabilized NiO; IPA, 2-propanol; D₆, 2-propanol-d₆; D₁, 2-rpropanol-2d₁.

does not show any isotope effect. The results of these measurements are summarized in Table 3.19.

Table 3.19. Isotope effects in the Dehydrogenation of 2-propanol on stabilized NiO catalyst sample

Temperature (K)	Isotope effect (α_H/α_D)	
	(a)*	(b)*
500	1.02	1.58
515	1.02	1.50
527	1.01	1.44
540	0.95	1.50

*column (a) refers to comparison of α for 2-propanol and 2-propanol- d_6 ($(CD_3)_2CHOH$) while column (b) refers to the comparison of α for 2-propanol and 2-propanol- $2d_1$ ($(CD_3)_2CDOH$)

3.6.2 Reactivated catalysts

Isotope effects were also examined on a reactivated NiO catalyst sample in the temperature range 473 - 488 K. The fractional conversions for alcohols and deuterio-alcohols

are illustrated in Figure 3.13. Although it is difficult to decide about the magnitude of isotope effect because of the deactivation of the catalyst sample with successive reactant pulses, there is no doubt that with 2-propanol-2d₁ the conversion to acetone is significantly less than with 2-propanol.

Since in the decomposition of the deuterio-alcohols any surface hydroxyl sites on the catalyst may become deuterated, the effect of deuteration of these sites on the extent of 2-propanol decomposition has been investigated. The deuterated surface was obtained by subjecting the catalyst to 15 nm³ (15 ul) of 2-propanol-d₈ ((CD₃)₂CDOD) prior to each series of deuterio-alcohol injections. The effects were studied on a catalyst sample containing 0.5 mol percent Al₂O₃ at reaction temperatures of 493 and 523 K. These results are shown in Figures 3.14 and 3.15. Comparison of the results is difficult because of changes in the catalyst activity which is complicated by the additional injections of 2-propanol-d₈. However, the average isotope effect observed is similar for both deuterated and non-deuterated surfaces as shown in Table 3.20. It should be noted that the average isotope effects are in good agreement with those observed for

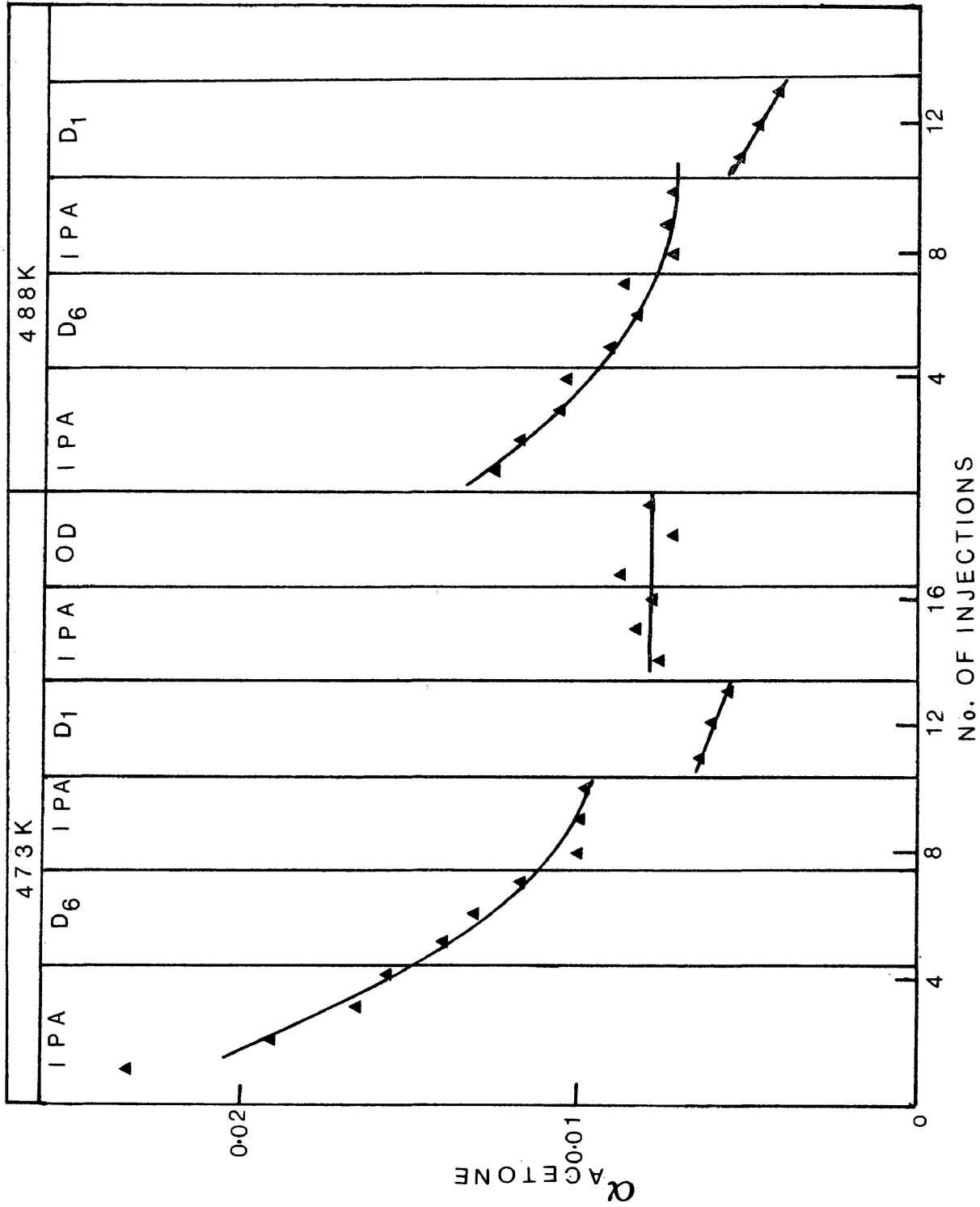


Figure 3.13: Fractional conversion of 2-propanol and deuterio-alcohols (2nm^3 inj. size) on reactivated NiO; IPA, 2-propanol; D₆, 2-propanol-d₆; D₁, 2-propanol-2d₁, OD, 2-propanol-OD.

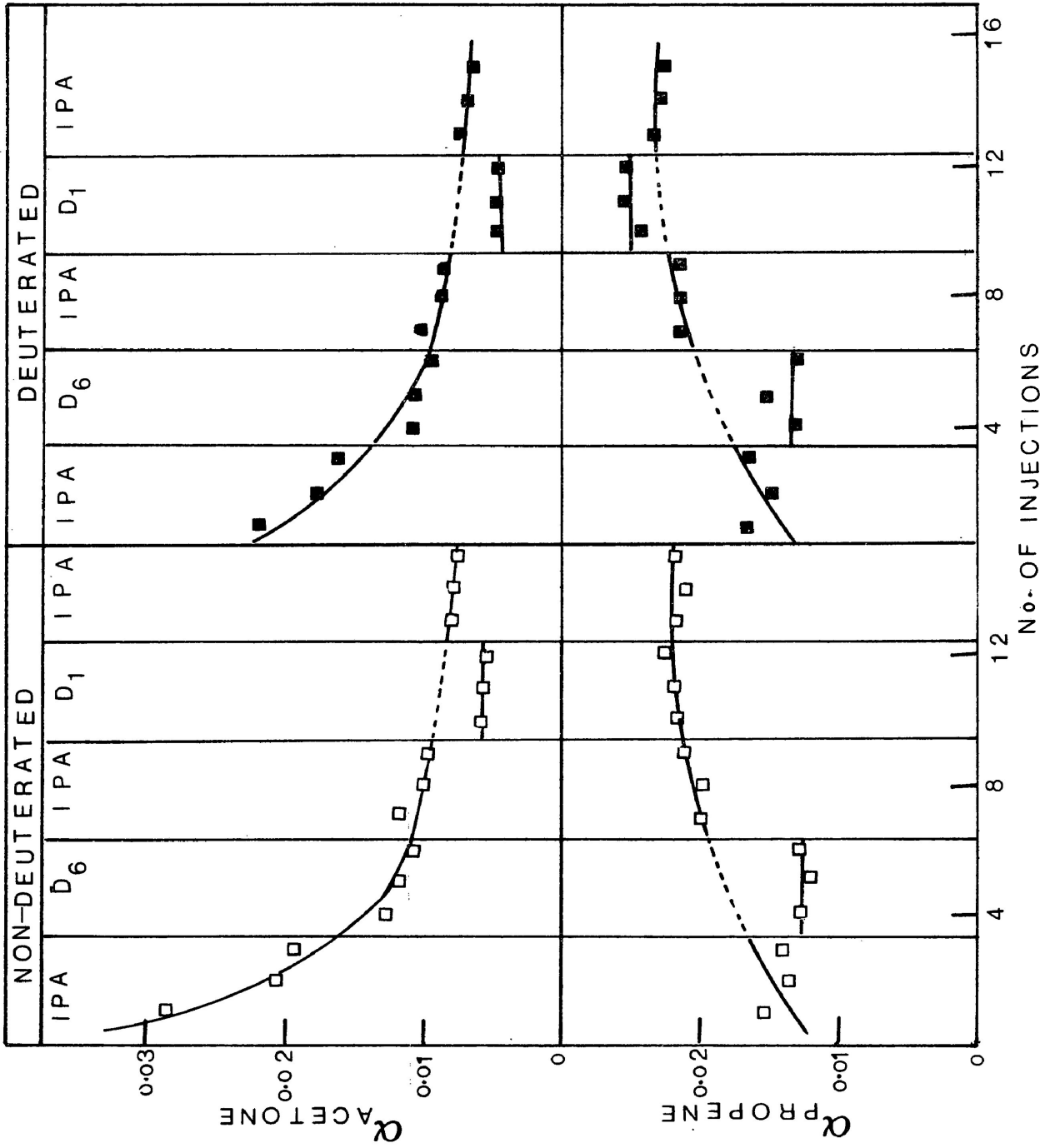


Figure 3.15: Fractional conversion of 2-propanol and deuterio-alcohols (2nm^3 inj. size) on reactivated sample containing 0.5 mol % Al_2O_3 at 523 K; IPA, 2-propanol; D_6 - 2-propanol- d_6 ; D_1 , 2-propanol- 2d_1 .

stabilized catalysts (Table 3.18), except for the propene results at 493 K, which give unusually low values.

Table 3.20 Average Isotope effects in the Dehydration and Dehydrogenation of 2-propanol on a catalyst sample containing 0.5 mol percent Al_2O_3 .

Temperature (K)	Surface	Isotope effect ($\alpha_{\text{H}}/\alpha_{\text{D}}$)			
		In Propene Formation		In Acetone Formation	
		(a)*	(b)*	(a)*	(b)*
493	non-deuterated	1.16	1.21	1.0	1.70
	deuterated	1.21	1.05	1.0	1.63
523	non-deuterated	1.45	0.95	1.0	1.57
	deuterated	1.40	0.89	1.04	1.66

* column (a) refers to comparison of α for 2-propanol and 2-propanol- d_6 ($(\text{CD}_3)_2\text{CHOH}$) while column (b) refers to the comparison of α for 2-propanol and 2-propanol- 2d_1 ($(\text{CD}_3)_2\text{CDOH}$).

3.7 Conductivity Studies

3.7.1 Measurements on Catalyst Samples in an Inert Atmosphere

Most conductivity studies were carried out under flow conditions in a system which is similar, but not identical, to that used in the catalysis investigations. A few conductivity measurements were also made under "low vacuum" conditions (approximately 1.33 Pa).

The variation in electrical conductance with temperature for catalyst samples containing 5.26 and 50 mol percent Al_2O_3 are shown in Figure 3.16. Since conductance, i.e. $1/\text{resistance}$, is measured and determination of the sample dimensions was not possible, no direct comparisons can be made in terms of the magnitude of the conductance. However, the activation energy for conduction is the same in both samples (72.1 kJ mol^{-1} for 5.26 mol percent doped sample and 72.3 kJ mol^{-1} for 50 mol percent doped sample). The value for the activation energy is similar to that reported for NiO (58) and indicates that it is electronic rather than ionic conductance which is being measured.

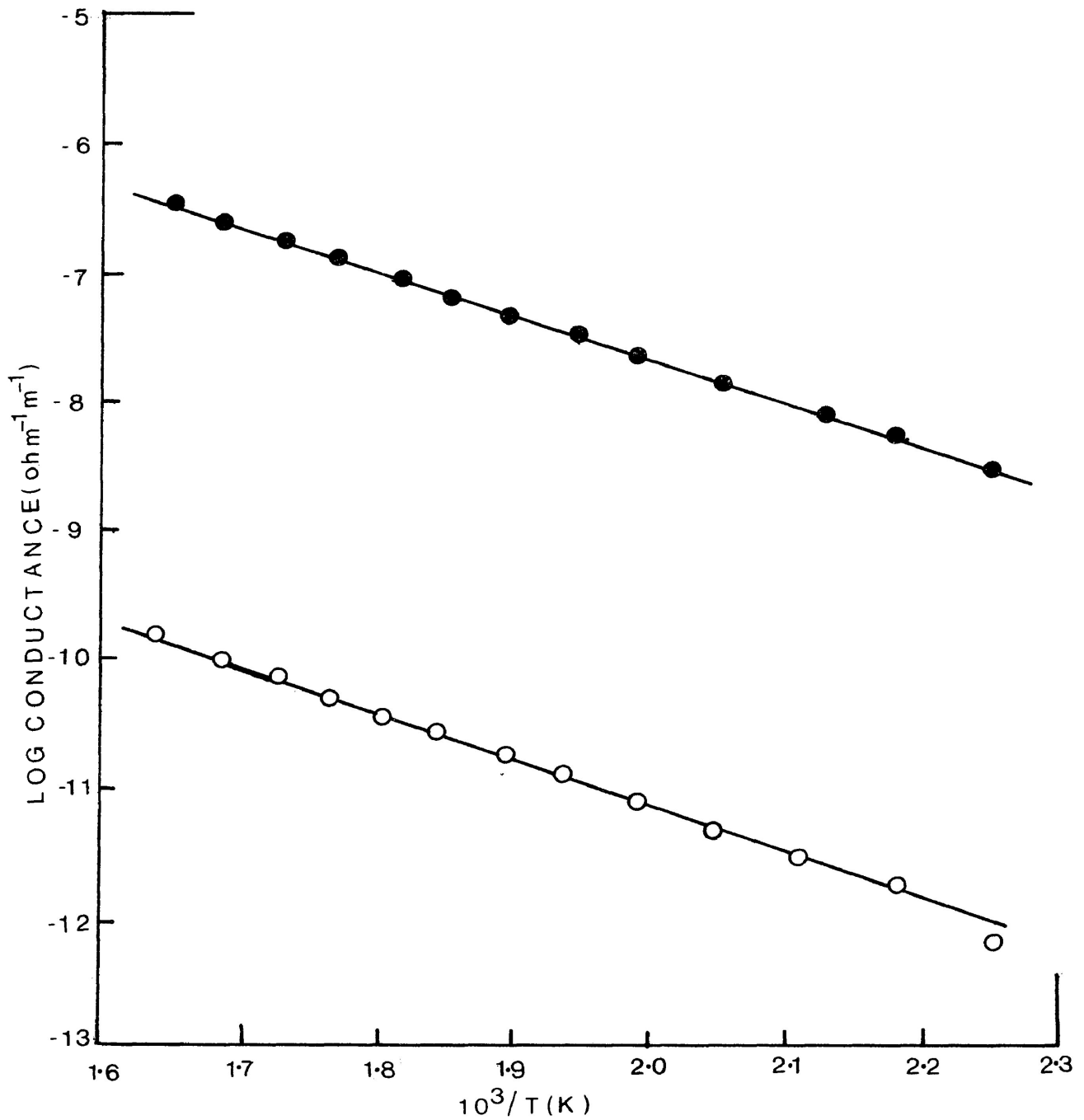


Figure 3.16: Plot of log conductance versus reciprocal temperatures (2nm³ inj. size); ●, 5.2 mol % Al₂O₃; ○, 50 mol % Al₂O₃.

3.7.2 Conductivity studies of catalyst poisoning and catalyst reactivation

a) Self-poisoning

Electrical conductivity was measured under flow conditions during the catalytic reaction of 2-propanol on NiO and doped samples at 493 and 523 K. At a particular temperature, the catalyst was subjected to a number of injections of 2-propanol and the changes in electrical conductivity with time were noted. The time interval between injections was 30 minutes. Some typical results for NiO and NiO doped with 5.26 mol percent Al_2O_3 are shown in Figures 3.17 and 3.18. Admission of 2-propanol vapour to the catalyst causes a decrease in conductivity, the individual decreases diminishing with increasing injection number. Under the flow conditions used, $40 \text{ cm}^3 \text{ min}^{-1}$, the reactant-catalyst contact time will be less than two seconds so that the changes in conductivity continue well beyond the time when 2-propanol would be expected to be present in the gas phase. Figures 3.17 and 3.18 show that after six or seven injections the conductivity changes are relatively insignificant but there is no evidence of recovery in the conductivity over the time period investigated. The observed decrease in con-

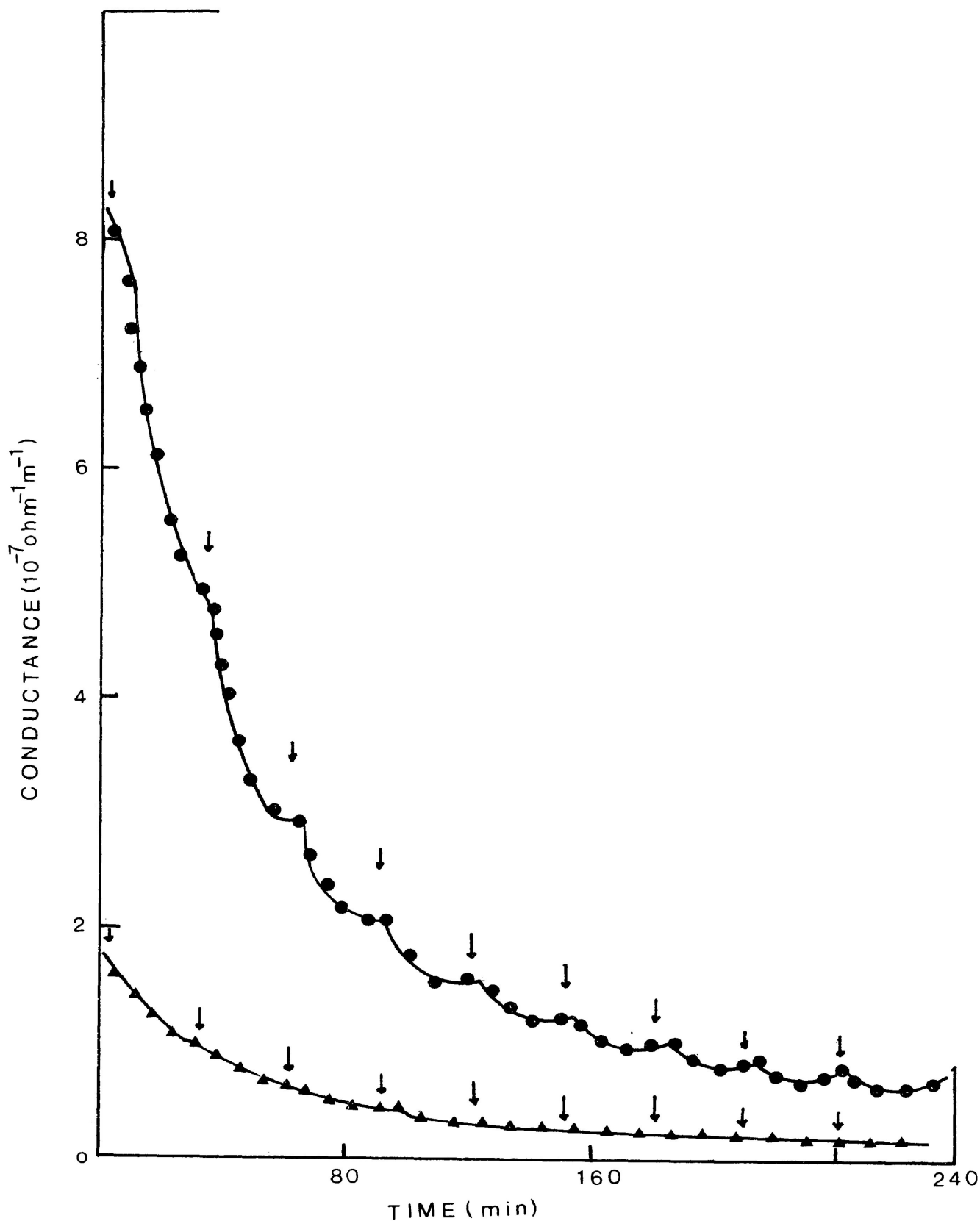


Figure 3.17: Changes in conductance with 2-propanol injections (2 nm^3 inj. size) on NiO; \blacktriangle , 493 K; \bullet , 523 K; arrows indicate time at which injections were made. Although not evident in diagram, small decreases in conductivity with 2-propanol injections occur beyond fifth injection at 493 K.

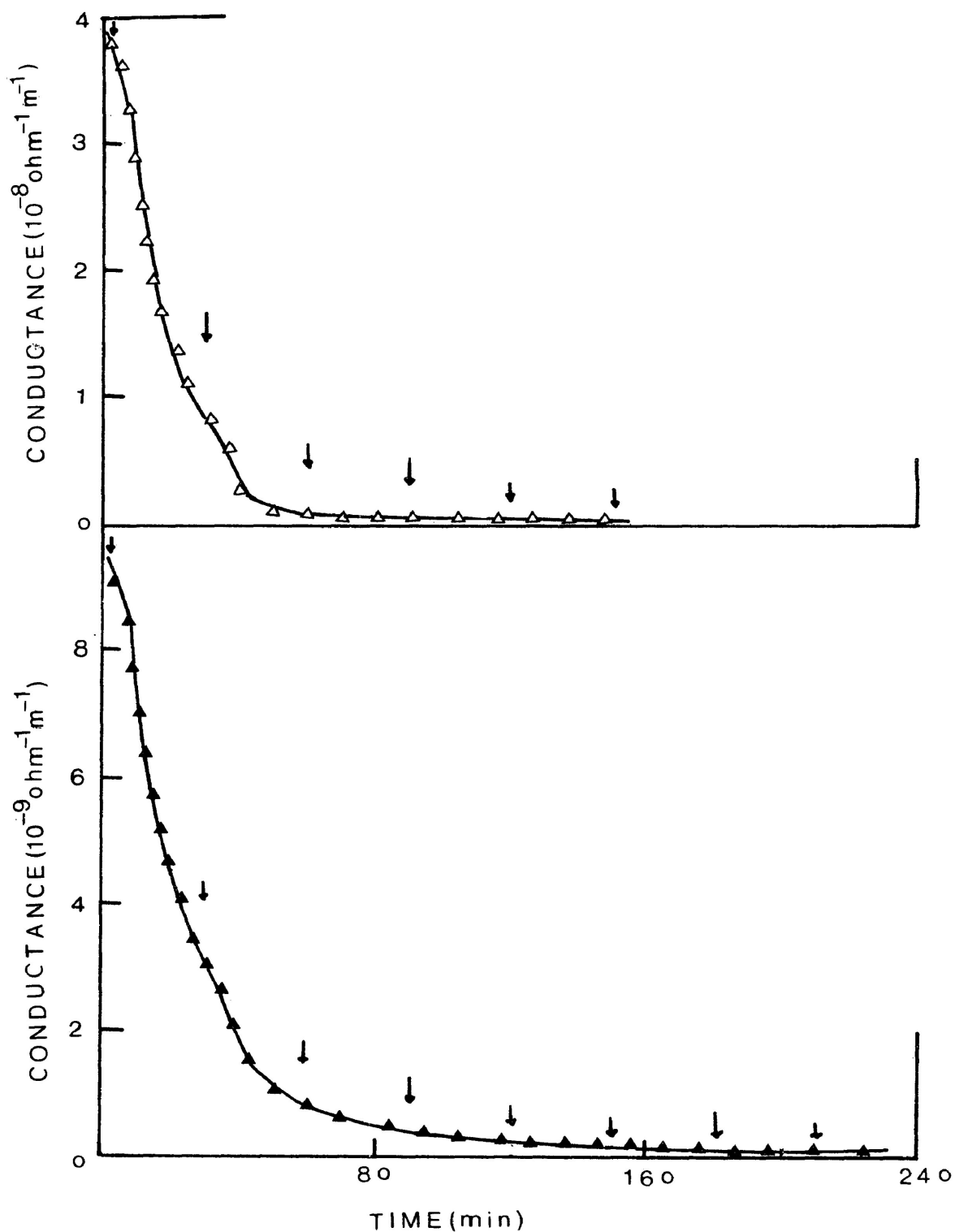


Figure 3.18: Changes in conductance with 2-propanol injections (2nm^3 inj. size) on sample containing 5.26 mol % Al_2O_3 ; \blacktriangle , 493 K; \triangle , 523 K; arrows indicate time at which inj. were made.

Although not evident in diagram small changes in conductivity with 2-propanol injections occur beyond the fourth injection.

ductivity with successive injections of 2-propanol shows a similar trend to the decrease in dehydrogenation activity of the catalyst when subjected to 2-propanol pulses, (Figures 3.6 and 3.7). It should be noted that injections of 2-propanol on to the catalyst containing 50 mol percent Al_2O_3 did not produce a decrease in the catalyst conductivity; this sample has earlier been shown to be entirely a dehydration catalyst in 2-propanol decomposition (Table 3.7).

(b) Effects of added poison

Effects of acetone, oxygen, acetic acid, carbon-dioxide, propene and water on the conductivity of the catalysts were investigated. During chemisorption of acetone the conductivity of NiO and the doped samples, with one exception, decreased. No change in conductivity was observed with acetone injection on the sample containing 50 mol percent Al_2O_3 over the temperature range 473 to 543 K. Effects of acetone on the conductivity of NiO at 523 K, both before and after the catalyst's exposure to 2-propanol are given in Figure 3.19.

The results show that 2-propanol and acetone

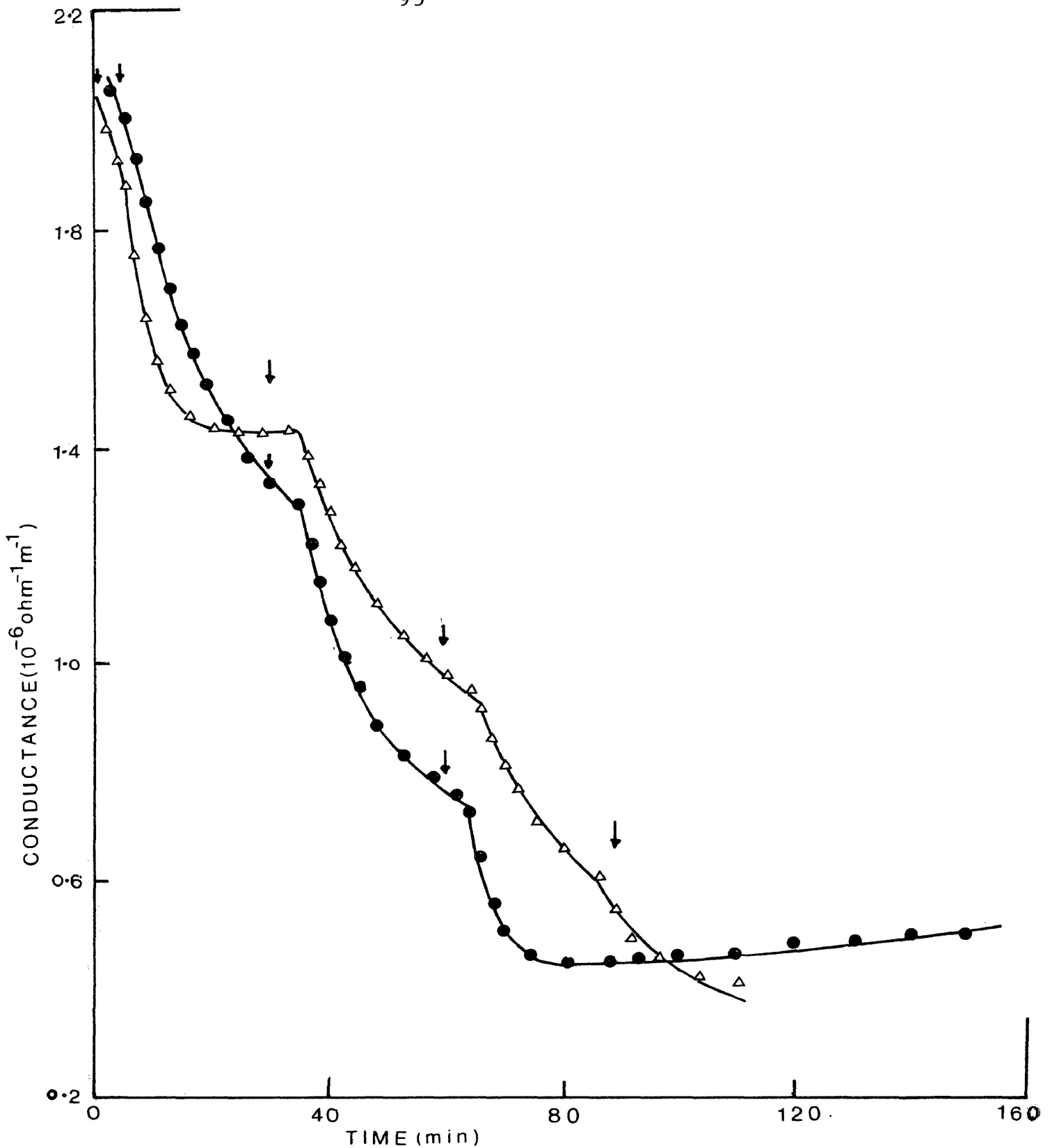


Figure 3:19: Effect of acetone injections on the conductivity of NiO at 523 K before and after 2-propanol injections; Δ , injection one was 1 nm^3 ($1 \mu\text{l}$) of acetone followed by 2 nm^3 ($2 \mu\text{l}$) injection of 2-propanol; \bullet , injection one and two was 2 nm^3 ($2 \mu\text{l}$) of 2-propanol followed by 0.5 nm^3 ($0.5 \mu\text{l}$) injection of acetone; arrows indicate time at which injections were made.

produce similar decreases in the conductivity; this suggests that the effect of 2-propanol may be due to the product from the dehydrogenation reaction on the catalyst, i.e. acetone. Bielanski et al (58) arrived at the same conclusion on their conductivity studies of this system.

The effects of other added poisons on the catalyst conductivity were generally small compared with that of acetone. Oxygen produced a slight increase in conductivity as shown in Figure 3.20 while carbon dioxide or propene injections produced slight decreases. However, injections of acetic acid or water resulted in a significant decrease in catalyst conductivity. The catalyst sample containing 50 mol percent Al_2O_3 was again unusual in that the poisons had no effect on the conductivity.

(c) Catalyst reactivation

In the present work it has been observed that significant changes in conduction occur during the reactivation of the catalyst. Figure 3.21 shows some conductivity results for a sample of NiO. The catalyst at 523 K was subjected to two pulses of 2-propanol with a consequent

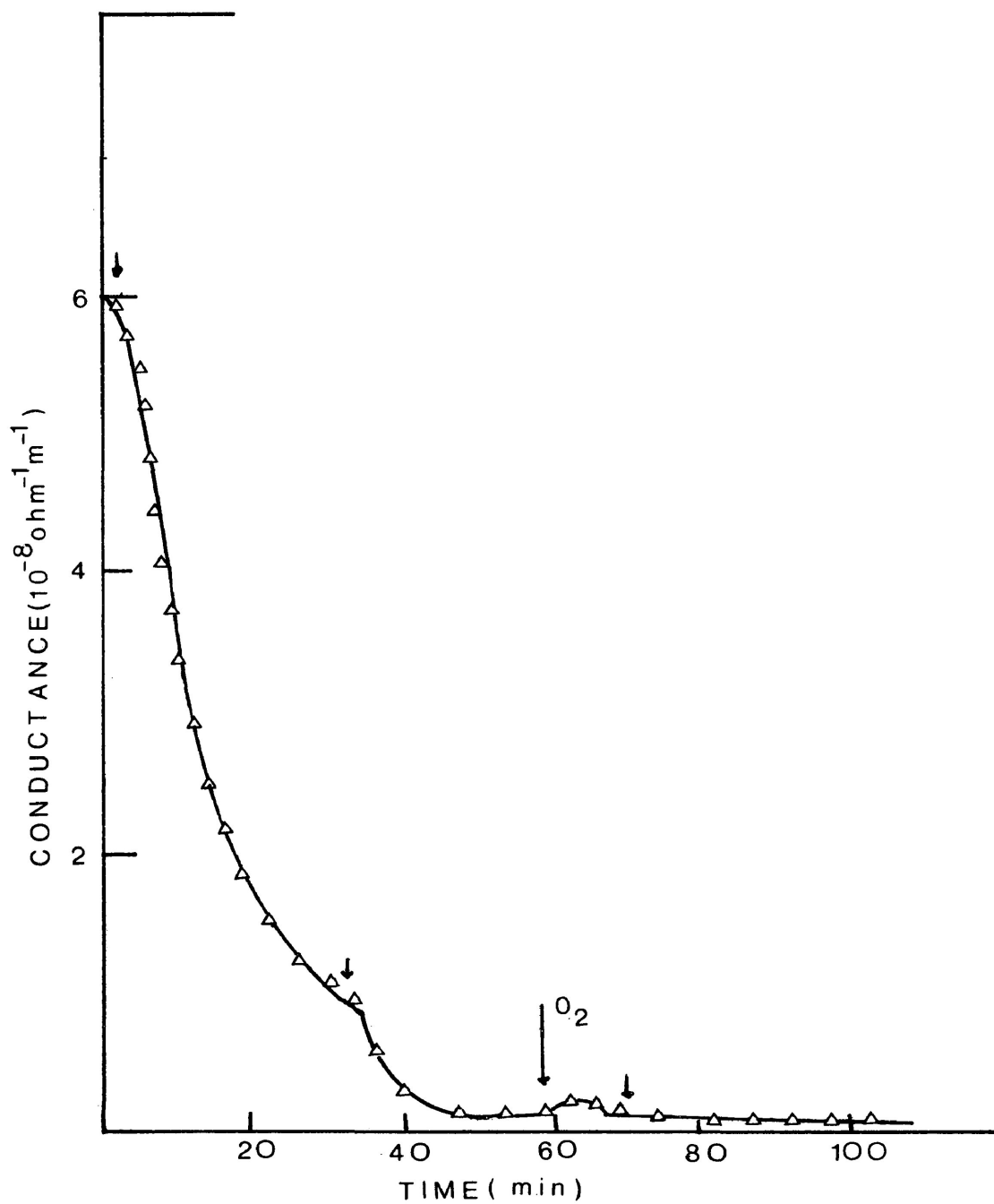


Figure 3.20: Effect of Oxygen (200 nm^3) on the conductivity after 2-propanol injections (2 nm^3 inj. size) on sample containing 5.26 mol % Al_2O_3 at 533 K; arrows indicate time at which injections were made.

decrease in conductivity; the sample was heated from 523 to 623 K and maintained at this temperature. The conductivity increases to a maximum value at approximately 613 K, then decreases and appears to stabilize at value of conductance corresponding to that originally observed for that sample.

In a second type of experiment the catalyst sample was maintained in vacuum (1.33 Pa) until the sample conductivity was constant. The catalyst was then exposed to 2-propanol vapour for approximately fifteen minutes, after which the system was evacuated. Some results for a sample containing 5.26 mol percent Al_2O_3 at reaction temperatures of 513 and 625 K are shown in Figure 3.22. At 513 K, the conductivity increased very slowly during evacuation and it took about nine hours to regain the original value but at 625 K, the initial conductivity is restored in approximately two and a half hours.

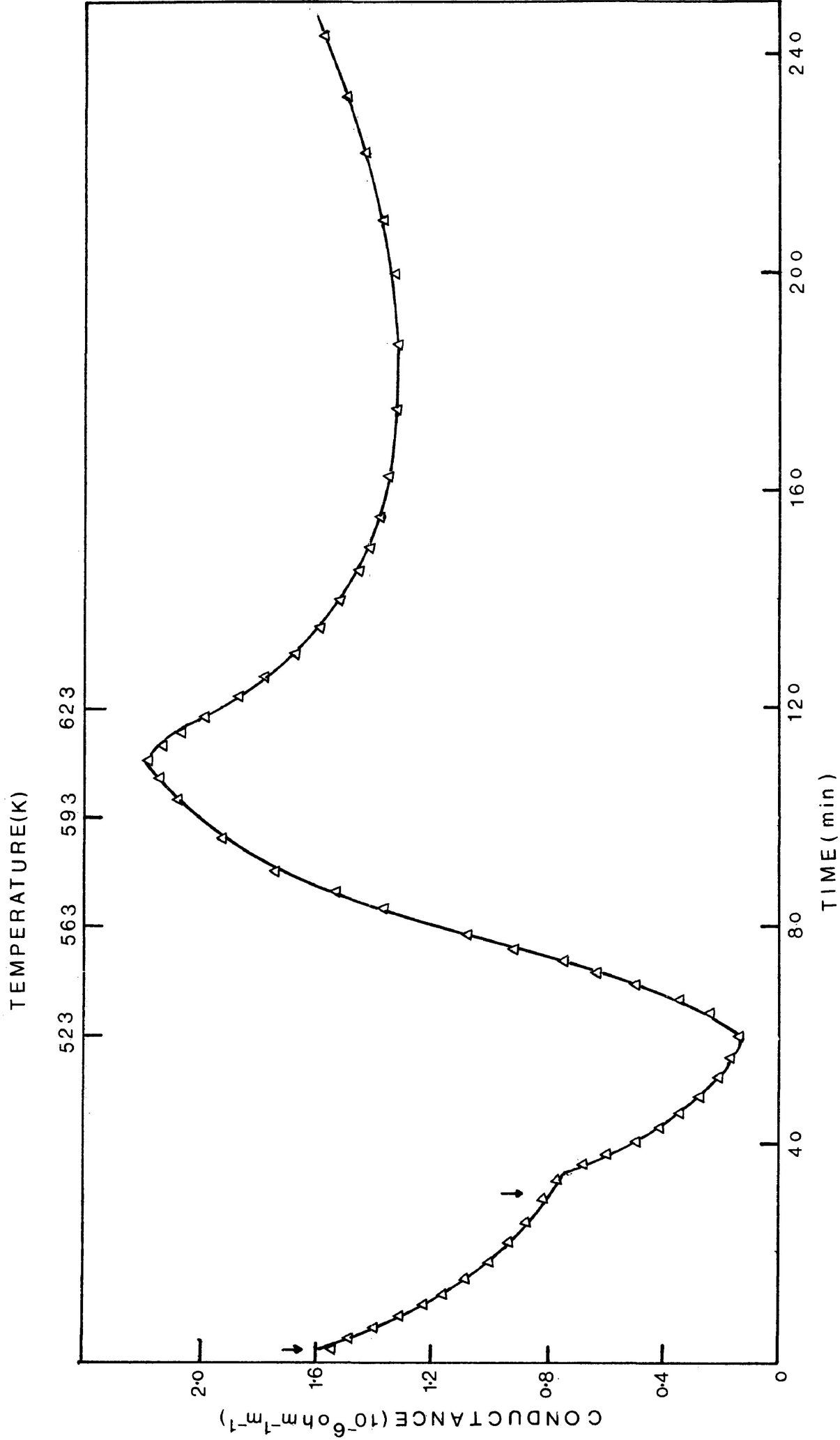


Figure 3.21: Effect of heat treatment on the conductivity of NiO after 2-propanol injections (2nm^3 inj. size)

at 523 K; arrows indicate time at which injections were made. Final sample temperature was 623 K.

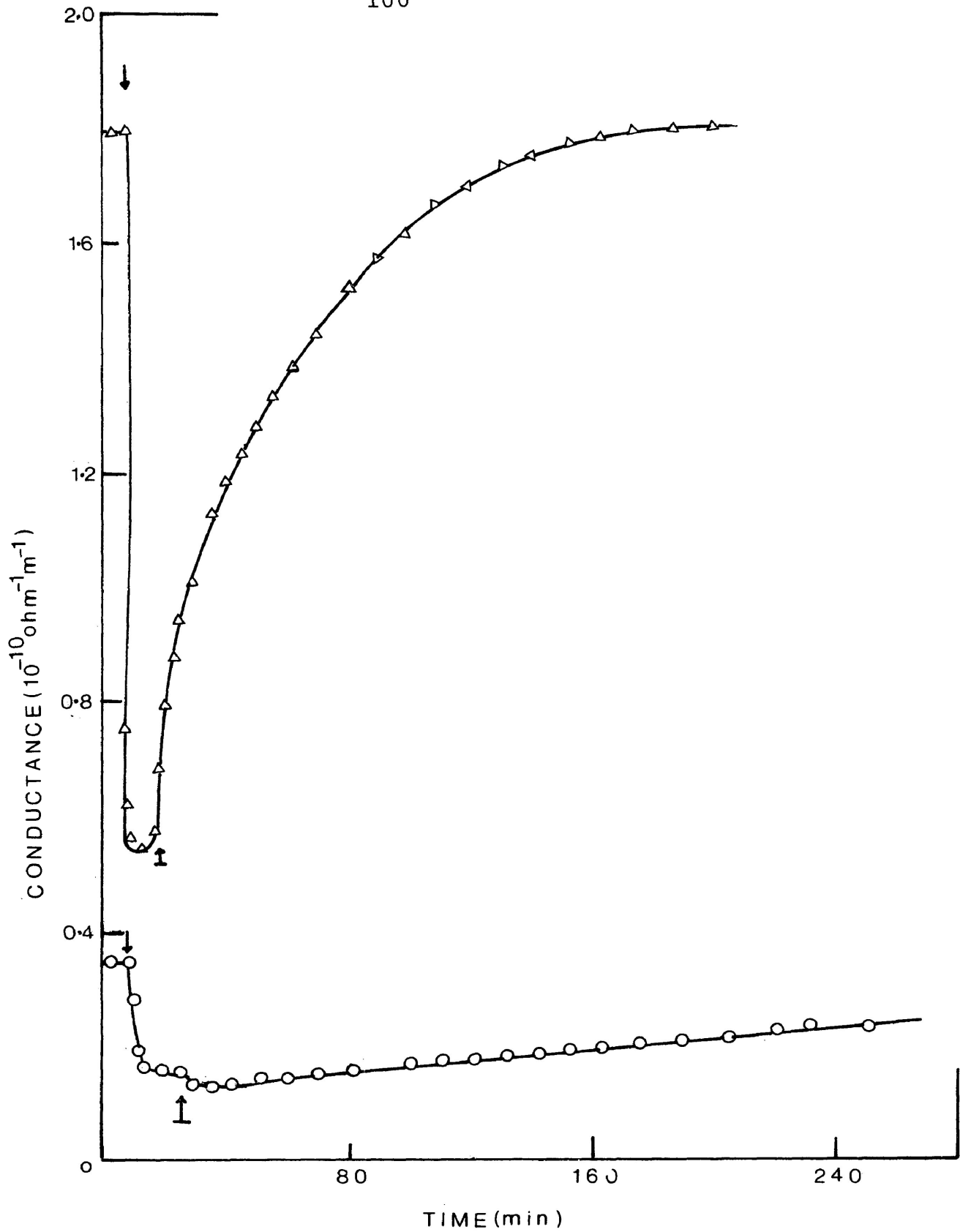


Figure 3.22: Effect of evacuation on the conductivity after 2-propanol exposure on sample containing 5.26 mol % Al_2O_3 ; O, 513 K; Δ , 615 K; Arrows indicate time at which 2-propanol was exposed. Vacuum applied at time indicated by \uparrow .

4. DISCUSSION

4.1 Changes in the Solid-State Properties of Nickel Oxide Brought About by the Incorporation of Alumina

On the basis of the present results it appears that the doping of nickel oxide by alumina leads to the following important changes:

- i) reduction in activation energy for dehydroxylation of the hydroxide (Table 3.4a),
- ii) increase in surface area of the resulting oxide (Table 3.4),
- iii) formation of a spinel-type of structure, i.e. nickel aluminate (Table 3.2),
- iv) overall decrease in catalytic activity, except for the nickel aluminate sample, and an increase in the dehydration selectivity of the catalyst with increasing amounts of Al^{3+} ion (Table 3.8).

4.1(a) Dehydroxylation

The thermal decomposition of nickel hydroxide has been the subject of several investigations. Previous studies of the isothermal dehydroxylation have reported values of the activation energy for reaction in air as

188.9 kJ mol⁻¹ (97) and 119 kJ mol⁻¹ (98) and for the reaction in vacuum as 118.5 kJ mol⁻¹ (97). In the present investigation an activation energy of 172 kJ mol⁻¹ is obtained (Table 3.4a), which compares favourably with that reported by Fahim et al (97) for the dehydroxylation reaction in air. A dynamic thermal method, as opposed to an isothermal method, has been employed in the present study and, as has been mentioned by Sharp (99), the former method of study tends to give higher activation energies due to the build-up water vapour pressure in the vicinity of the sample.

Table 3.4a indicates that the incorporation of Al³⁺ ions in the hydroxide leads to a reduction in the activation energy for the dehydroxylation reaction. El-Salaam et al (98) have observed a similar decrease in activation energy for dehydroxylation of Ni(OH)₂ doped with 0.5 mol percent Al³⁺ ions. The general trend for the present results is that the activation energy for dehydroxylation is reduced continuously with increasing Al³⁺ ions content of the sample up to a limit of 5.26 mol percent Al₂O₃. Further additions of Al³⁺ ions do not appear to affect the activation energy for dehydroxyla-

tion. It is important to note that the sample containing 2.56 mol percent Al_2O_3 shows anomalous behaviour; this anomaly will be discussed later in this section.

Two general mechanisms have been proposed for solid-state dehydroxylation reactions. The homogeneous mechanism (100) involves at least five steps in the process, for example, (i) liberation of the proton from one of the hydroxyl groups of the formula unit, (ii) liberation of other hydroxyl groups, (iii) formation of water, (iv) migration of water to the surface, and (v) liberation of water from the surface. The inhomogeneous mechanism (101) also involves at least five steps in the dehydroxylation process, viz., (i) liberation of the proton, (ii) proton diffusion to the surface, (iii) cation counter-migration to the deprotonated regions to balance the charge in that zone, (iv) water formation at the surface, and (v) liberation of water from the surface. Although the results of the present investigation do not permit identification of a mechanism, El-Salaam et al (98) have attempted to interpret their dehydroxylation results for both Li^+ doped and Al^{3+} doped $\text{Ni}(\text{OH})_2$ in terms of the inhomogeneous mechanism. The view is expressed that the dopant changes

the point defect concentrations in the host matrix and this in turn will affect proton migration and cation counter-migration. However, it is important to realize in this regard that the dopant level should be compatible with the intrinsic defect concentration and this point has been emphasised by Van Gool (102). Data on point defect concentrations in nickel hydroxide are not available but it is relevant to consider the situation for nickel oxide. Nickel oxide is a non-stoichiometric oxide of the general type $\text{Ni}_{(1-y)}\text{O}$. Measurements of the degree of non-stoichiometry, i.e. y , indicate that over the temperature range 1200 to 1800 K, y varies from approximately 10^{-4} to 10^{-3} (103-105). Thus, the intrinsic defect concentration at the temperatures used in the catalyst preparation is unlikely to exceed 0.01 mol percent. The observed continuous decrease in activation energy for the dehydroxylation reaction with dopant concentration well in excess of 0.01 mol percent leads to the suggestion that changes in point defect concentrations cannot entirely account for the decrease in activation energy. It is further noted that, if the reaction were diffusion-controlled, changes in point defect concentrations would be expected to alter the rate of diffusion but it is difficult to see why

the activation energy should be so drastically reduced unless there is a change in the reaction mechanism from that in nickel hydroxide. It is more probable that, on doping with Al^{3+} ions, a small portion of the dopant is incorporated in the lattice resulting in impurity-created point defects while the remainder is involved in the formation of a new compound with the host matrix.

X-ray powder diffraction patterns of the more highly doped nickel hydroxides provide evidence for new compound formation. The data for a sample containing 5.26 mol percent Al_2O_3 is given in Appendix III. The diffraction pattern indicates the presence of a mixed hydroxide, probably $\text{Ni}_5\text{Al}_4\text{O}_2(\text{OH})_{18}\cdot 6\text{H}_2\text{O}$, together with the hydrated nickel hydroxide ($3\text{Ni}(\text{OH})_2\cdot 2\text{H}_2\text{O}$) phase. Previous studies of thermal decomposition of the mixed hydroxide (106) have reported formation of a spinel-type oxide product. It is proposed that the reduction in activation energy for dehydroxylation of the hydroxides is associated with the thermal decomposition of the mixed hydroxide.

As shown in Table 3.4a the temperature for the

on-set of thermal decomposition decreases with increasing Al^{3+} ion concentration. The sample containing 50 mol percent Al_2O_3 should be entirely composed of the mixed hydroxide, and from its observed decomposition temperature, it is reasonable to suggest that decomposition of the mixed hydroxide occurs at a significantly lower temperature than that for nickel hydroxide. The observed decrease in both the activation energy for dehydroxylation and the on-set temperature for decomposition is considered to be due to the increasing amounts of the mixed hydroxide present which more readily decomposes. The proposal can also partially account for the observed significant increase in surface area of the doped oxides. For the decomposition of solids, the overall reaction can be considered to involve two processes, viz. (1) nucleation of the product, and (2) growth of the product phase. If the mixed hydroxide is present in small amounts, the decomposition at the lower temperatures could provide the nucleation sites for the dehydroxylation of nickel hydroxide. The net effect of the presence of the mixed hydroxide would be to enhance the nucleation rate but, because of the lower temperatures involved, growth of the product nuclei would be reduced; a smaller product particle

size would be obtained which would result in a larger surface area. The situation would be similar to the "time-temperature-transformations" in steels (107). However, other factors such as occluded water in the hydroxide and initial particle size of the hydroxide, could also affect the surface area of the resulting oxide.

The formation of spinel compound (NiAl_2O_4) is evident from X-ray diffraction pattern (Table 3.2) in the sample containing 50 mol percent Al_2O_3 . The NiAl_2O_4 structure is one in which approximately 20 percent of the Ni^{2+} ions occupy tetrahedral sites and the remainder are in octahedral sites, while approximately 40 percent of the Al^{3+} ions occupy tetrahedral sites with the remainder in octahedral sites (108). Moreover, the relative amount of nickel ions in tetrahedral and octahedral sites depends somewhat on the condition of preparation (109). The diffraction patterns of the samples containing from 5.26 to 25.0 mol percent Al_2O_3 also indicate the presence of nickel aluminate phase along with the nickel oxide phase. With the samples containing less Al_2O_3 it would be difficult to detect the aluminate phase by X-ray powder diffraction. The previously reported

results on the phase composition in the NiO-Al₂O₃ system are contradictory both with respect to the crystallinity of the aluminate and also to the extent of solubility of the NiAl₂O₄ phase in NiO (110-113). Within the limits of accuracy of the present work, the appearance of the NiAl₂O₄ phase is not accompanied by a distortion in the NiO lattice and it would be reasonable to assume that the aluminate has only limited solubility in the nickel oxide.

It has been mentioned earlier that the sample containing 2.56 mol percent Al₂O₃ is somewhat unusual with respect to the activation energy for dehydroxylation reaction. Several samples of this composition have been used to confirm this observation. The reasons for this anomalous behaviour are not clear. From the thermogram as shown in Figure 3.3 it appears that there is very little loosely bonded or unbound water present in sample containing 2.56 mol percent Al₂O₃ in comparison with the other doped samples and the weight change in the temperature range 373-473 K is insignificant. It is possible that the absence of this loosely bonded water could retard the rate of product nucleation leading to a

higher activation energy for dehydroxylation.

4.1(b) Changes in catalytic activity and selectivity

The total activity, defined as fraction of alcohol decomposed per square metre of the catalyst surface, and the selectivity for dehydration and dehydrogenation on fresh catalyst samples (considering only the first injection) at 461 K are shown in Figures 4.1 and 4.2 respectively. Total activity decreases significantly with the introduction of Al^{3+} ions and continues up to about 2.56 mol percent Al_2O_3 ; it then shows only minor changes up to a composition of 14.29 mol percent Al_2O_3 , beyond which a sharp rise in activity is observed. In terms of selectivity, nickel oxide is purely a dehydrogenation catalyst and nickel aluminate is a dehydrating catalyst. Incorporation of very small amounts of Al_2O_3 (0.1 mol percent) produces some dehydration capacity. The selectivity for dehydration is about 7% at this composition. The selectivity remains more or less constant up to a composition of 14.29 mol percent Al_2O_3 , beyond which there is a marked increase in the dehydration activity. The variation of catalyst activity and selectivity as a function of catalyst composition can be roughly divided into three regions:

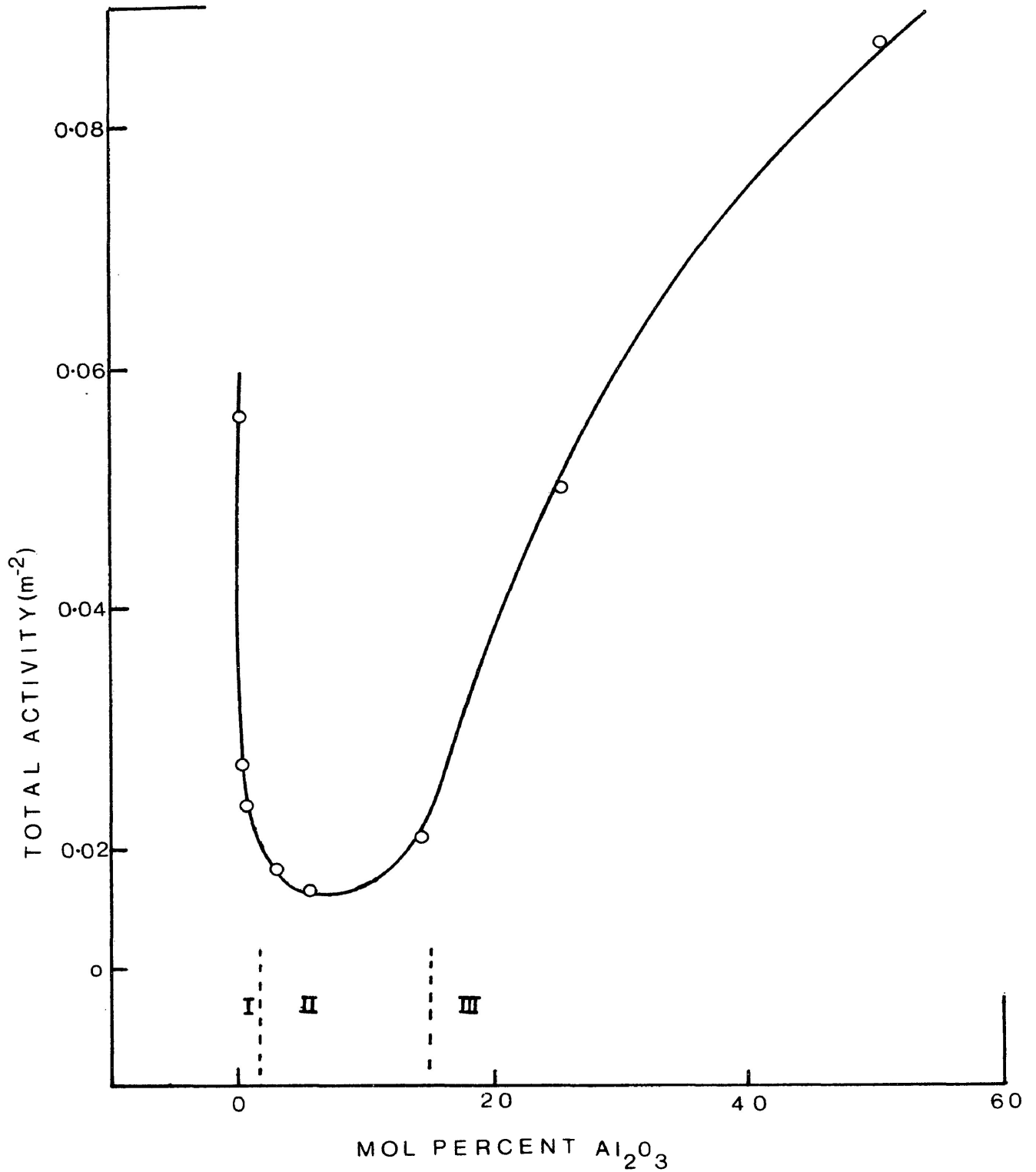


Figure 4.1: Total activity of the catalysts for 2-propanol decomposition as a function of catalyst composition at 461 K; three regions are indicated in Figure.

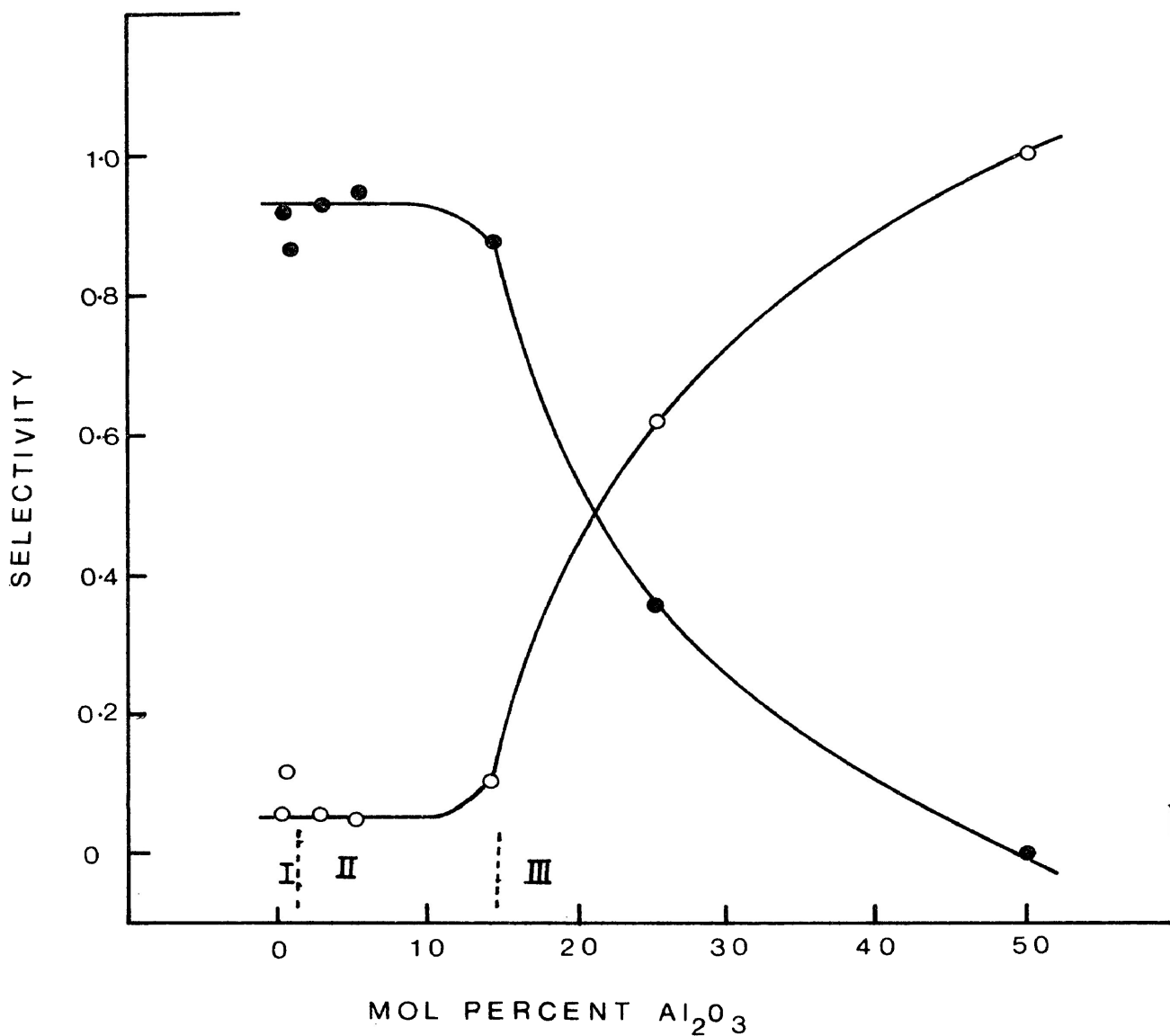
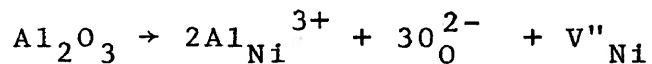


Figure 4.2: Selectivity of the catalysts for 2-propanol decomposition as a function of catalyst composition at 461 K; O, dehydration; ●, dehydrogenation; three regions are indicated in Figure.

region I, in which there is a significant change in activity and selectivity with very small concentrations of Al^{3+} ions; region II, in which the activity and selectivity remains virtually constant with changes in composition; region III, in which there is a marked increase in activity and dehydration selectivity with increasing concentrations of Al^{3+} ions.

On the basis of the discussions presented in section 4.1(a) it would be expected that region I is associated with changes in point defect concentrations. Al^{3+} ions could be substitutionally incorporated in nickel oxide by the following defect reactions:

(a) the Al^{3+} ions could replace Ni^{2+} ions,



(b) the Al^{3+} ions could replace Ni^{3+} ions.

Since NiO is known to be a p-type semiconductor, an increase in the cation vacancy concentration would be expected by (a) while (b) would produce a decrease in the positive hole concentration. Comparison of the ionic sizes of Ni^{2+} , Ni^{3+} and Al^{3+} ions would indicate (b) is the more likely process. Conductivity measurements on NiO, shown

in Figure 3.17, indicate that in the 2-propanol dehydrogenation reaction, the interaction of the alcohol or the reaction products with the catalyst surface leads to a decrease in conductivity. Thus it appears that positive holes are involved in the dehydrogenation mechanism. Incorporation of Al^{3+} ions by reaction (b) would produce a decrease in positive hole concentration and hence a decrease in the dehydrogenation activity as is observed.

The catalyst activity and selectivity in region II suggests that there is relatively little change in surface composition with increasing Al^{3+} ion concentration in this region. The scheme for dehydroxylation reaction discussed previously is compatible with this observation. If the mixed hydroxide decomposes initially to give nickel aluminate and the aluminate particles act as nuclei for nickel hydroxide dehydroxylation, the resulting particles will be as shown in Figure 4.3.

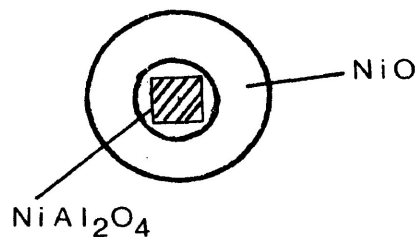


Figure 4.3

As a result the surface will be essentially NiO containing a limited amount of Al^{3+} ions as described for region I. Relatively little change in catalyst activity would be expected in this region unless synergetic effects of the type described by Kuriacose et al (88) are significant. The present observations show no evidence of the synergetic effects of the matrix.

With further increase in the amount of mixed hydroxide a composition will be reached where there is insufficient nickel hydroxide present for the resulting nickel oxide to 'cover' the entire surface of the nickel aluminate. The sample containing 50 mol percent Al_2O_3 indicates that the aluminate has a high catalytic activity and is a dehydrating catalyst. Thus, the behaviour in region III can be associated with the increasing amounts of nickel aluminate in the surface zones.

The present results are in contrast to those obtained in studies of the effects of Cr^{3+} ions in $\alpha\text{-Al}_2\text{O}_3$ (15) and Cr^{3+} ions in MgAl_2O_4 (16) on the decomposition of 2-propanol. However, in these systems, formation of additional compounds is unlikely and the changes in selectivity originate from the substitution of Cr^{3+} ions for Al^{3+} ions.

4.2 The Dehydrogenation Reaction

4.2.1 Kinetics of dehydrogenation on stabilized catalysts

The plots of conversion against reciprocal space velocity (Figure 3.8) are consistent with zero order kinetics. However, in the plot, a finite intercept at infinite flow rate ($1/F=0$) is observed for the higher temperatures. This type of behaviour has also been reported by Bett and Hall (114) for the dehydration of 2-butanol over hydroxyapatite catalysts. The observed kinetics can be explained by a model proposed by Hattori and Murakami (54) for a pulse reaction coupled with an irreversibly adsorbed reactant. According to their analysis the approximate equation for a small value of contact time can be written as:

$$\alpha = \left(1 - \frac{q_s V}{2\Omega}\right) \frac{k q_s \theta}{C_o} + \frac{q_s V}{\Omega} \quad \dots 4.1$$

where α = fractional conversion,

C_o = maximum concentration of inlet pulse
(mol/cm³ of bed),

q_s = site density (mol/cm³ of bed),
 V = volume of catalyst bed,
 θ = contact time,
 k = surface reaction rate constant,
 Ω = amount of inlet pulse.

The finite intercept in the plots is due to the second term in equation 4.1, which represents the conversion due to reaction after the pulse has left the catalyst bed and, as such, is independent of flow rate. At lower temperatures, the curves pass through the origin. If the catalyst surface is energetically heterogeneous, then increasing the temperature could increase the site density which could account for the finite intercept at higher temperatures. Additionally, if the irreversible adsorption process is activated, increasing temperature could enhance this reaction.

4.2.2 Self-poisoning of unstabilized catalyst

Self-poisoning in the dehydrogenation reaction on nickel oxide and the doped samples has been mentioned earlier (sections 3.2.1 and 3.5.1). Apart from the catalyst

sample containing 2.56 mol percent Al_2O_3 , the data for self-poisoning have been found to fit an empirical relationship of the form:

$$\alpha = A/\sqrt{n} \quad \dots 4.2$$

where n is the injection number and A , for a given set of conditions, i.e. injection size, flow rate, catalyst mass, temperature, etc., is a constant. Plots of α for dehydrogenation versus $1/\sqrt{n}$ are shown in Figure 4.4. It has been reported in section 3.7.2 that the conductivity of nickel oxide and the doped samples decreases with 2-propanol injections. Linearity in the plots of limiting conductivity after each injection versus $1/\sqrt{n}$ is also obtained. Some typical plots for nickel oxide are shown in Figure 4.5.

In order to determine the physical significance of A and n in equation 4.2, a number of studies of the effects of (1) time interval between injections, (2) pulse size, (3) reactant-catalyst contact time, on the self-poisoning behaviour have been carried out. The variation in self-poisoning with time interval between injections is shown in Figure 4.6. Apart from the first injections which

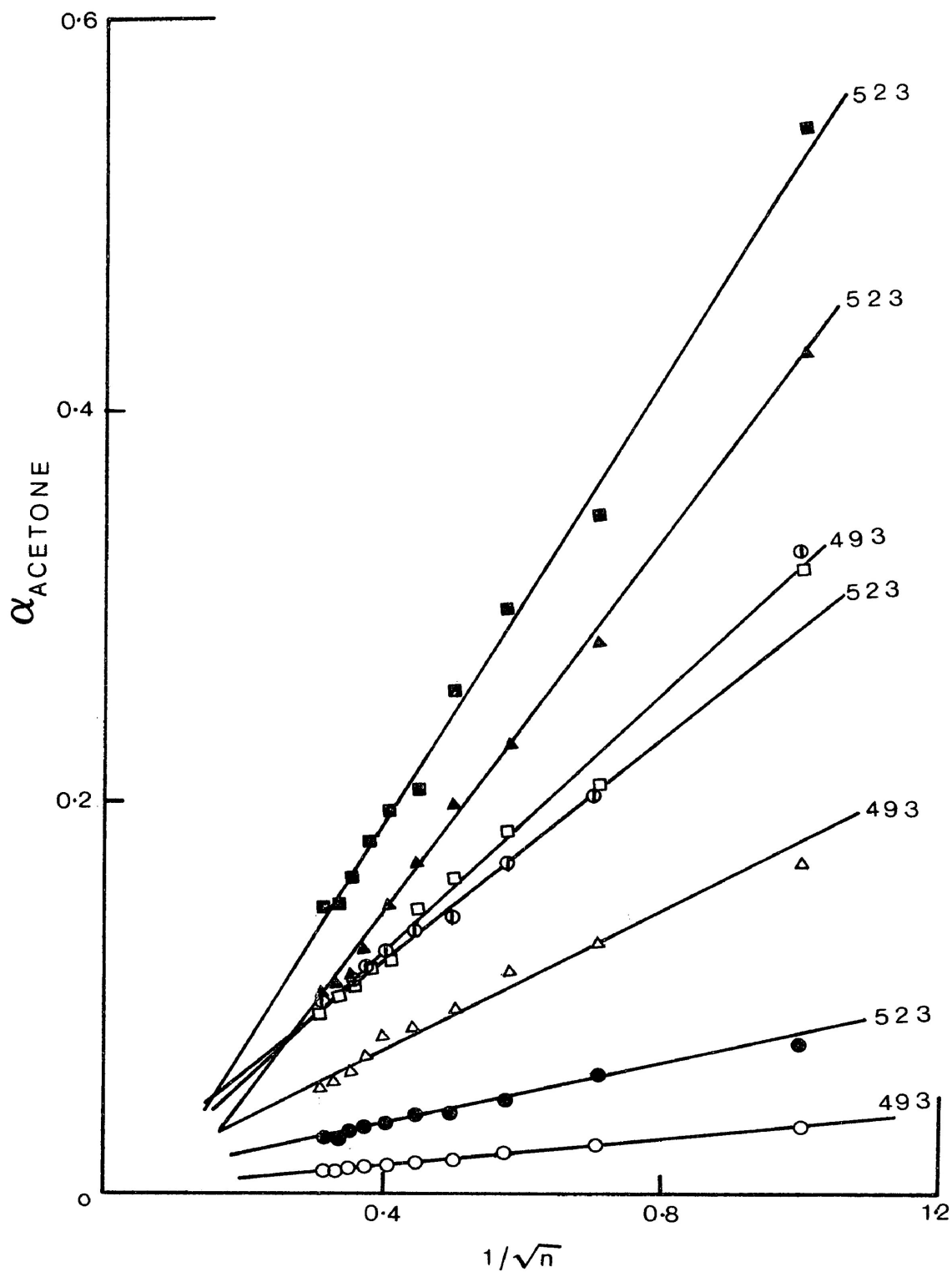


Figure 4.4: Plot of fractional dehydrogenation, α , versus $1/\sqrt{n}$ (2nm^3 inj. size); \circ , \bullet , NiO; Δ , \blacktriangle , 0.5 mol % Al_2O_3 , \odot , 5.26 mol % Al_2O_3 ; \square , \blacksquare , 14.29 mol % Al_2O_3 . Reaction temperatures (K) are indicated in Figure.

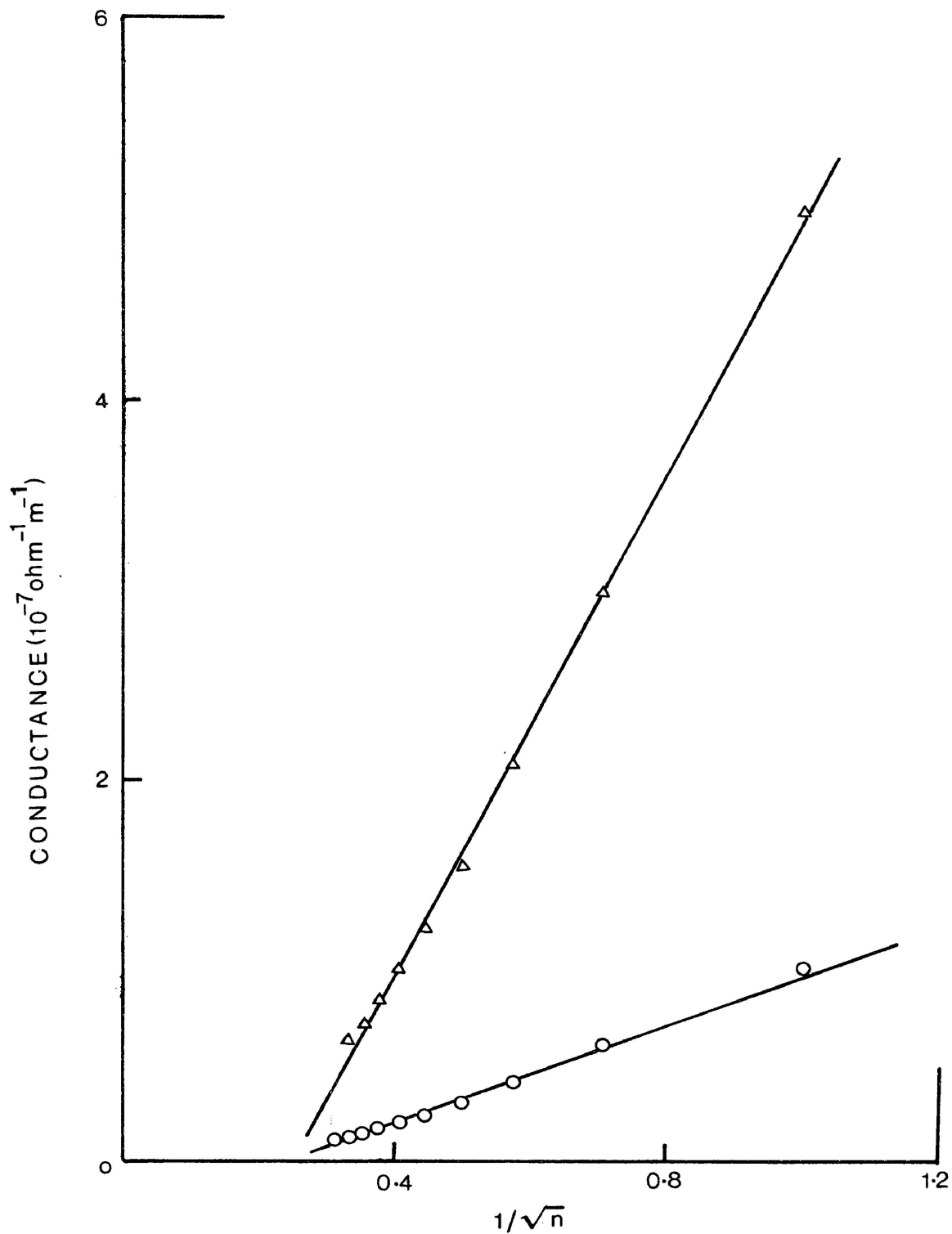


Figure 4.5: Plot of limiting conductivity of NiO after each 2-propanol injection (2nm^3 inj. size) versus $1/\sqrt{n}$; O, 493 K; Δ , 523 K.

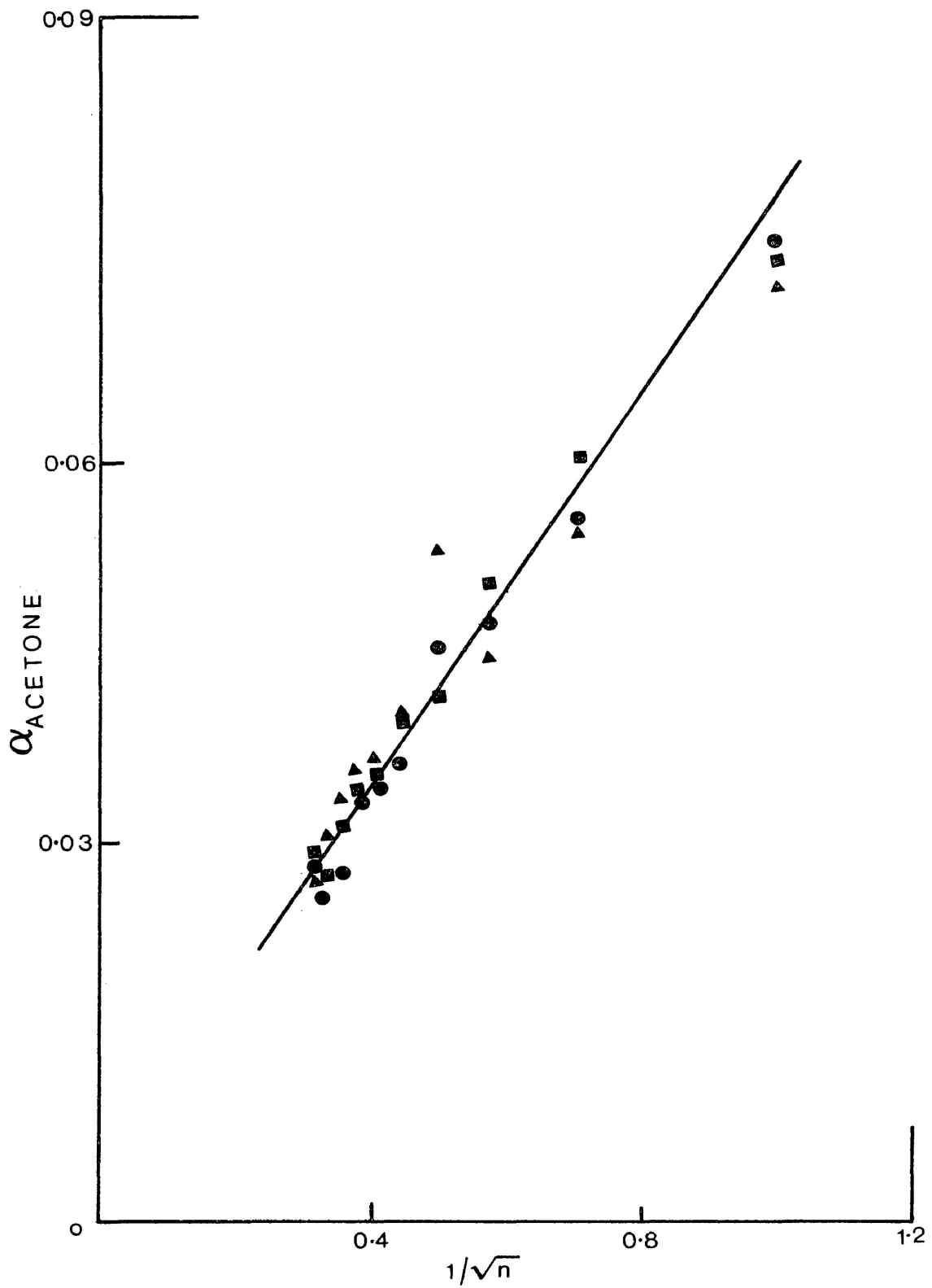


Figure 4.6: Plot of fractional dehydrogenation, α , versus $1/\sqrt{n}$ as a function of injection (2nm^3 inj. size) interval on NiO at 523 K; ●, 17 min; ■, 30 min; ▲, 45 min.

are anomalous because of low recovery of products and reactants, it would appear that A is independent of time interval between injections. The effects of pulse size are shown in Figure 4.7. Plots of α versus $1/\sqrt{n}$ give slopes of 0.076 and 0.069 for 2 and 4 nm³(μ l) injection size respectively on nickel oxide and similar slopes of 0.192 and 0.188 are obtained for 1 and 2 nm³(μ l) injection size respectively on the sample containing 0.5 mol percent Al₂O₃.

The effect of reactant-catalyst contact time has been examined by changing both the catalyst size and the flow rate. Figure 4.8 shows the effects of changing catalyst weight, in this case a sample containing 14.29 mol percent Al₂O₃, on the production of acetone and the poisoning of the catalyst. These results are summarized in Table 4.1.

Table 4.1 The effect of changing catalyst weight on self-poisoning

Wt. of Catalyst (g)	Ratio of Weight	Ratio of A (equation 4.2)			
		Flow rate (cm ³ min ⁻¹) 75	60	40	30
0.0989	1	1	1	1	1
0.1600	1.60	2.07	1.65	1.42	1.52
0.2828	2.86	2.87	2.57	2.61	2.43

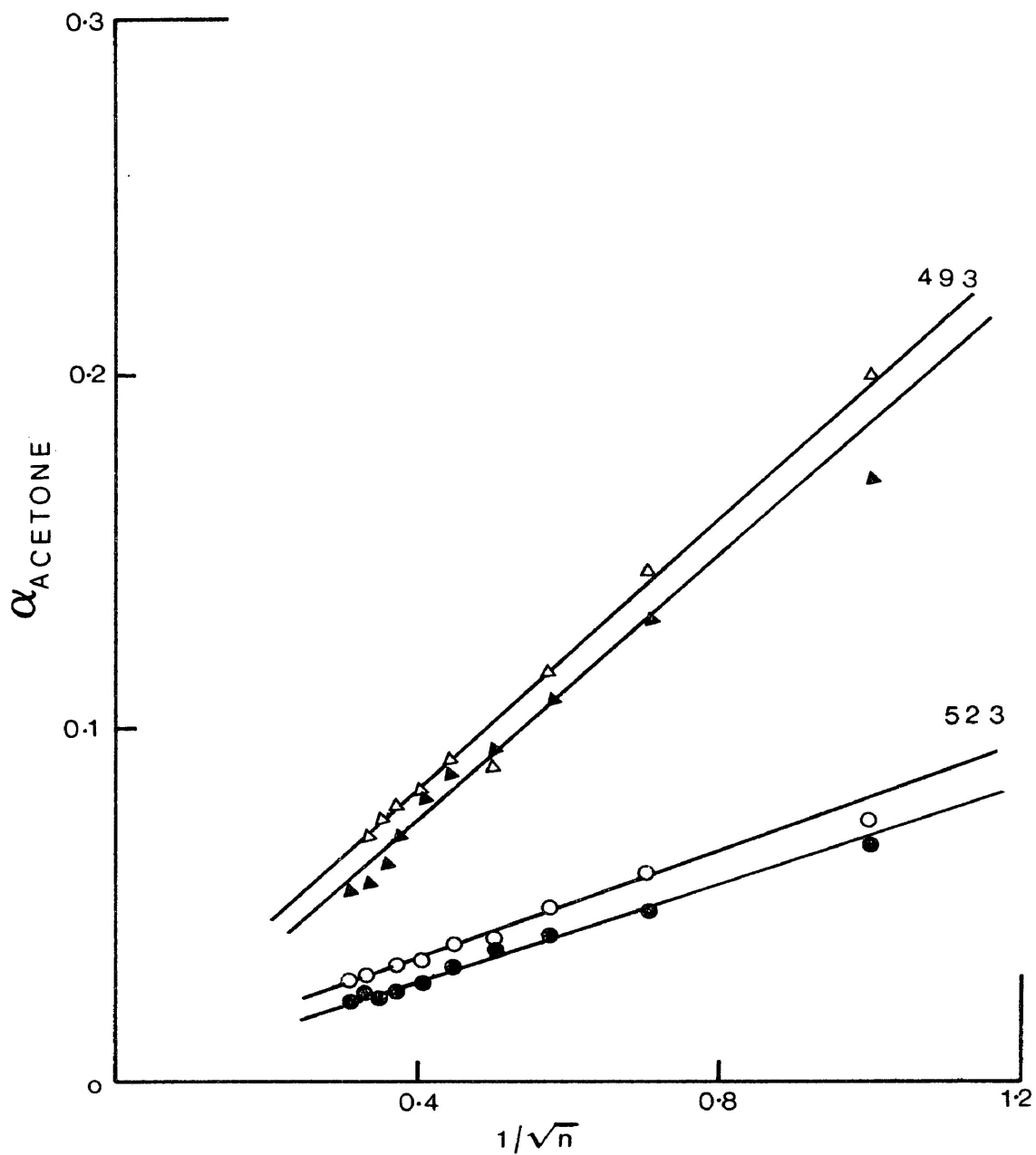


Figure 4.7: Plot of fractional dehydrogenation, α , versus $1/\sqrt{n}$ as a function of injection size.

NiO: \circ , 2nm^3 ($2\mu\text{l}$); \bullet , 4nm^3 ($4\mu\text{l}$);

$0.5\text{ mol \% Al}_2\text{O}_3$: Δ , 1nm^3 ($1\mu\text{l}$); \blacktriangle , 2nm^3 ($2\mu\text{l}$);

Reaction temperatures (K) are indicated in Figure.

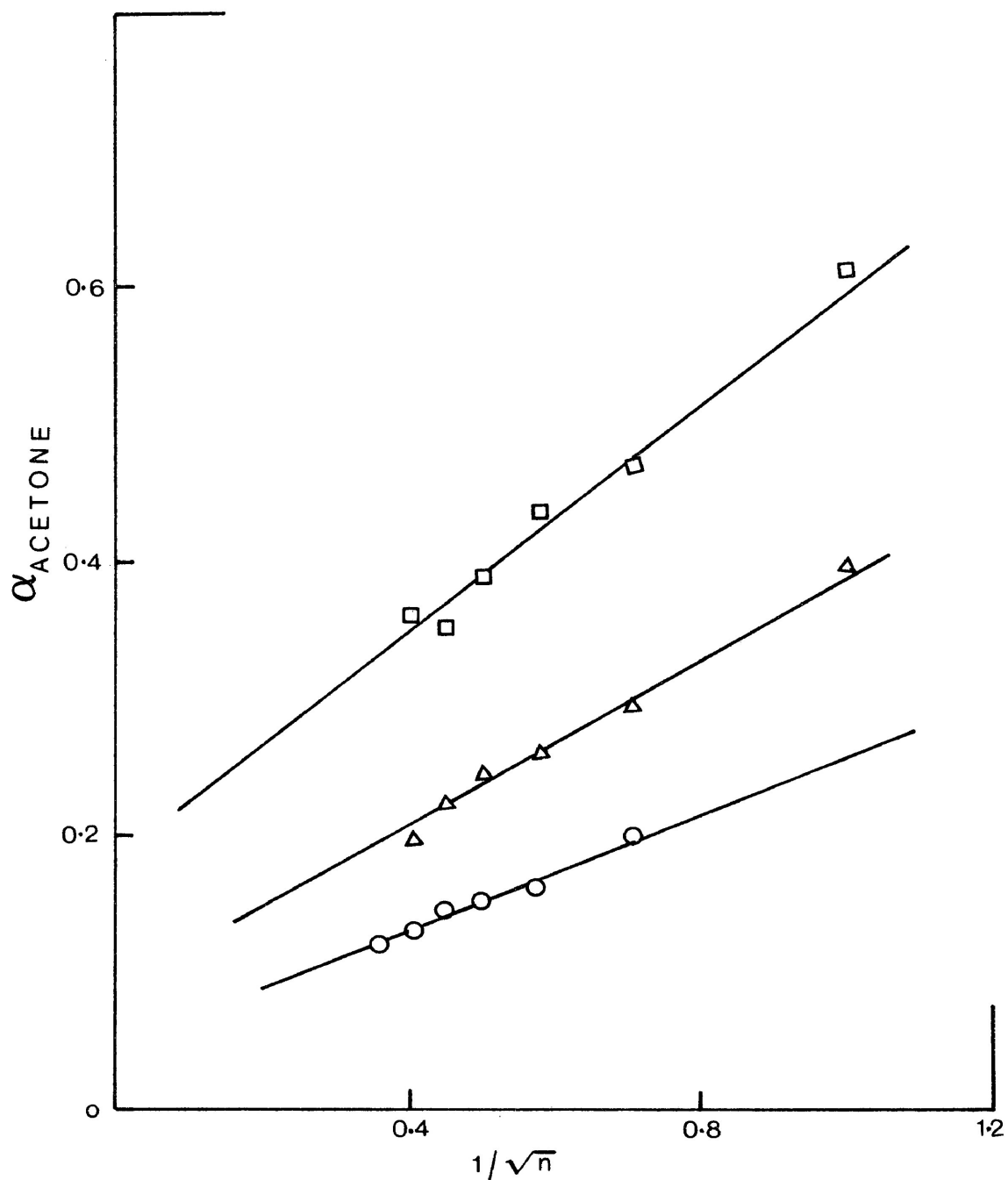


Figure 4.8: Plot of fractional dehydrogenation, α , versus $1/\sqrt{n}$ (2nm^3 inj. size) as a function of catalyst weight on sample containing 14.29 mol % Al_2O_3 at 523 K; \circ , 0.0989 g; Δ , 0.1600 g; \square , 0.2828 g.

The effect of flow rate on the dehydrogenation reaction is shown in Figure 4.9 for a catalyst containing 14.29 mol percent Al_2O_3 . The inverse ratio of the flow rates used in this experiment is 1.87, and the ratio of A (equation 4.2) obtained from the α versus $1/\sqrt{n}$ plot is 1.83. The results shown in Figures 4.8 and 4.9 and Table 4.1 indicate that the fraction dehydrogenation, α , is proportional to the alcohol-catalyst contact time, i.e. W/F , where W is the catalyst weight and F is the flow rate.

By considering all these aspects, the acetone formation can be given by the following equation:

$$\alpha = k'\tau/\sqrt{\Sigma\tau} = k'\tau/\sqrt{T_c} \quad \dots 4.3$$

where T_c is the total alcohol-reactant contact time, τ is the contact time for an individual pulse, and k' is the surface reaction rate constant. If one flow rate and one catalyst weight is considered, equation 4.3 reduces to the form:

$$\begin{aligned} \alpha &= k'\tau/\sqrt{n\tau} \\ &= \frac{k'\tau^{1/2}}{n^{1/2}} = \frac{\text{Constant}}{n^{1/2}} \quad \dots 4.4 \end{aligned}$$

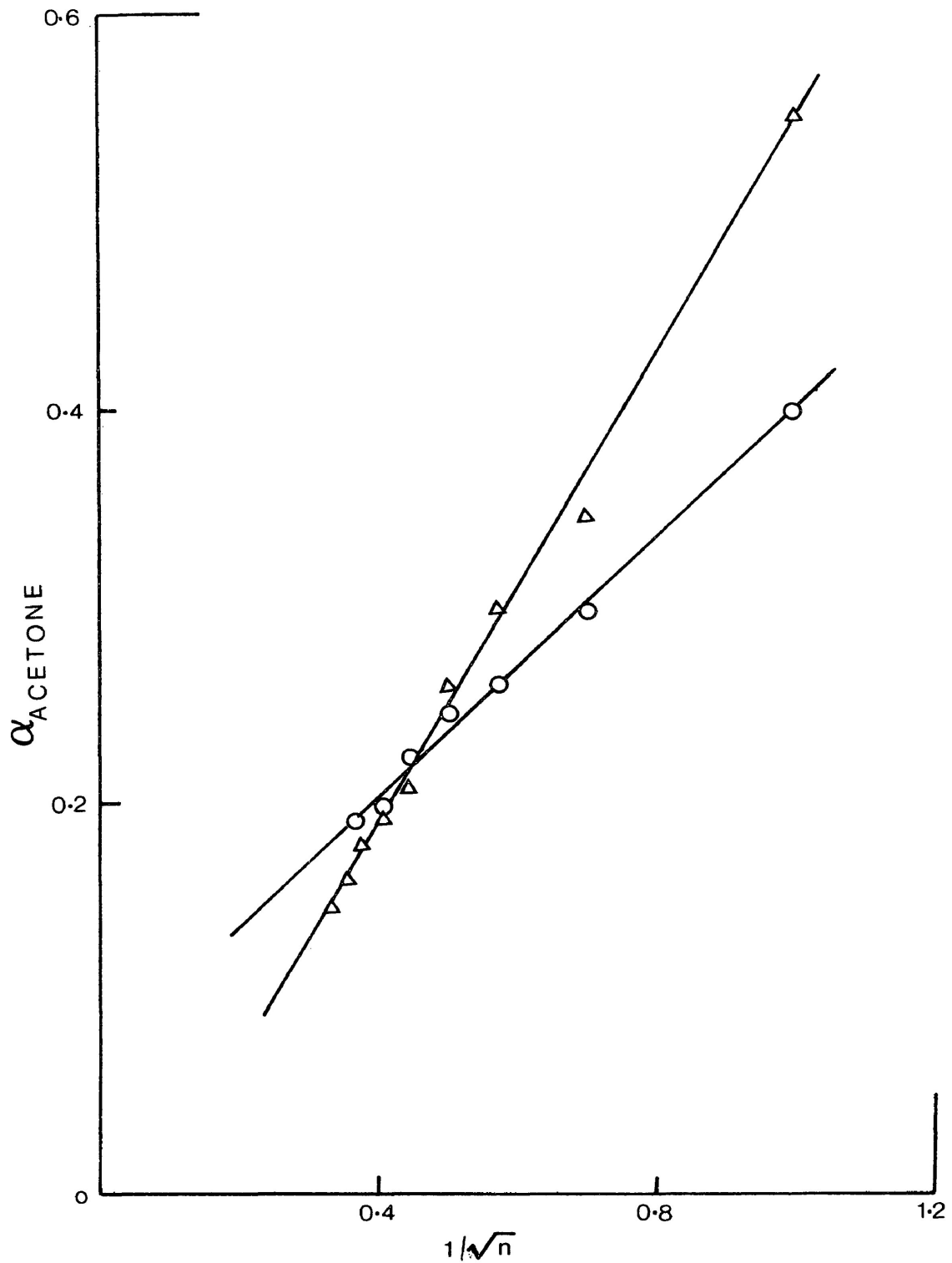


Figure 4.9: Plot of fractional dehydrogenation, α , versus $1/\sqrt{n}$ (2nm^3 inj. size) as a function of flow rate on sample containing 14.29 mol % Al_2O_3 ; Δ , $40\text{cm}^3\text{min}^{-1}$; \circ , $75\text{cm}^3\text{min}^{-1}$.

Equation 4.3 has been tested by studying the dehydrogenation reaction rates on three different catalyst weights and four different flow rates, i.e. twelve different reaction conditions (Table 3.1.6). The results, plotted in the form appropriate to equation 4.3 are shown in Figure 4.10. This is a severe test of equation 4.3 and while the results are reasonably satisfactory for any one catalyst weight at different flow rates, there is a discrepancy between the plots for different catalyst weights. Again, there is marked deviation in the initial injections which is ascribed to the low recovery of reactants and products.

Modification of equation 4.3 to satisfy the results in Figure 4.10 would give:

$$\alpha = \frac{k' \tau}{\sqrt{T_c}} + B \quad \dots 4.5$$

where B appears to be dependent upon the catalyst weight or surface area. In light of the interpretation of the kinetics on stabilized catalysts, identification of B, in equation 4.5, with the irreversibly adsorbed reactant, which undergoes dehydrogenation independent of the

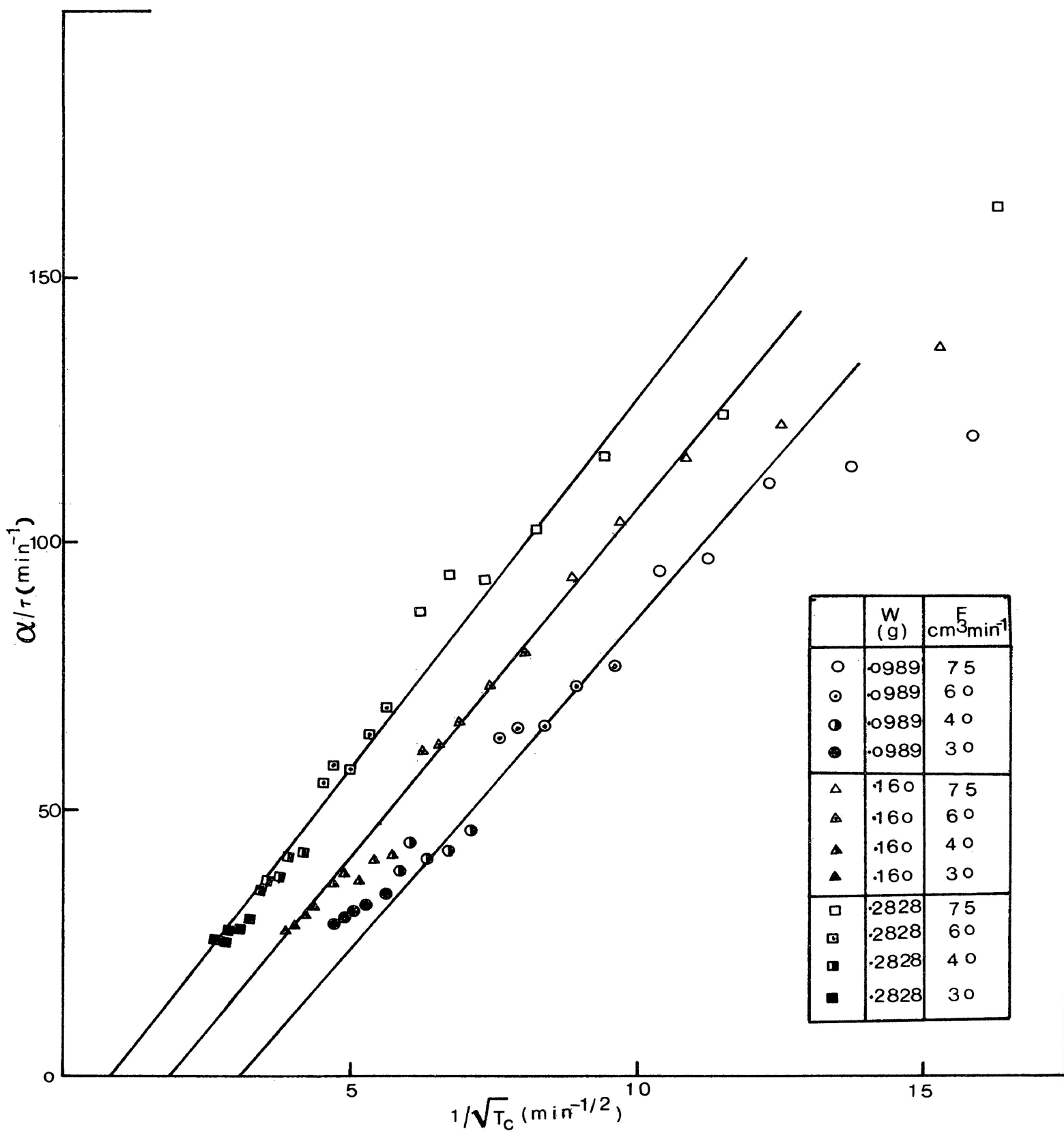


Figure 4.10: Plot of α/τ versus $1/\sqrt{T_c}$ under different reaction conditions (2nm³ inj. size) on sample containing 14.29 mol % Al₂O₃ at 523 K; W is catalyst weight (g), F is carrier gas flow rate (cm³ min⁻¹).

flow rate is reasonable. The larger the surface area, the more would be the amount of the reaction due to the irreversibly adsorbed reactant.

Changes in k' in equation 4.4, as a function of temperature and catalyst composition are shown in Table 4.2.

Table 4.2 Effect of temperature and catalyst composition on k'

Catalyst (Mol % Al_2O_3)	k' ($\text{min}^{-\frac{1}{2}}$)	
	Temperature (K)	
	493	523
0	0.036	0.076
0.5	0.180	0.493
5.26	--	0.284
14.26	0.33	0.575

Table 4.2 indicates that incorporation of Al^{3+} ions in NiO leads to an increase in k' , however, the increase is not uniform with the amount of doping.

Poisoning of catalytic-cracking reactions due to the deposition of coke has frequently been reported. Voorhies (115) and Blanding (116) related the coke content of catalyst to the reaction time. The formation of coke on the catalyst is given by:

$$C = \beta t^{1/2} \quad \dots 4.6$$

where C is the amount of coke and β is a constant. This leads to a relationship for catalytic activity, α , of the type $\alpha = k/\sqrt{T_c}$ which is the same form as equation 4.3. The general interpretation of these reactions is that the rate determining step in the product-forming reaction is the diffusion of the reactant through the coke layer, which is formed in the poisoning reaction. In most cases, it is assumed that the catalysts are porous and coke builds up at the pore mouth.

The interpretation that diffusion is the rate-controlling process is questionable. Froment (117) has reported that for the coking of catalyst, coke is not uniformly deposited in a reactor or inside a catalyst

particle whenever there are gradients in the concentrations of reactants and products. For a consecutive coking mechanism Froment and Bischoff (27,118) obtained a power of 1.0 at short process times and 0.5 at long process times in the Voorhies relationship, equation 4.6. In the present work the most convincing argument against diffusion control is the magnitude of the measured isotope effect. An isotope effect of 1.6 (Table 3.1.8) is significantly larger than would be expected for alcohol diffusion being the rate determining process.

Wojciechowski (30) has derived a theoretical rate expression for catalyst decay assuming a catalyst, free of diffusional limitations, operating in a static bed flow reactor. Considering a catalytic reaction of the type:



where A is the reactant,

s is an active surface site,

n is the number of active sites involved in a reaction event,

B is the product,

the rate expression can be represented by

$$\frac{-dC_A}{d\tau} = k\theta^n C_A \quad \dots 4.8$$

where θ is the fraction of active sites remaining unpoisoned,

C_A is the concentration of the species A in the gas phase,

τ is the contact time between catalyst and reactant A.

If the catalyst ages simply as a result of being on stream, the rate of poisoning is given by:

$$\frac{-d\theta}{dt} = k\theta^m \quad \dots 4.9$$

where θ is the fraction of active sites remaining,

m is the number of sites removed per deactivating event,

t is the catalyst time on stream,

k is a constant containing all other pertinent proportionality factors and in some cases parameters such as the concentration of the poisons in the gas phase.

Solution of equations 4.8 and 4.9 gives:

$$\frac{C_A}{C_A^0} = \exp\left\{-k\tau(1+(m-1)KT_c)^{-n/(m-1)}\right\} \quad \dots 4.10$$

where C_A is the concentration left, and C_A^0 is the initial concentration. The Wojciechowski treatment is for continuous reactant flow and so equation 4.10 must be integrated. However, with a pulse reactor system, equation 4.10 is adequate.

Since for the dehydrogenation reaction,

$$\alpha_{\text{acetone}} = 1 - \frac{C_A}{C_A^0} \quad \dots 4.11$$

equation 4.10 can be written as:

$$1-\alpha = \exp\left\{-\frac{k\tau}{[1+(m-1)KT_c]^{n/(m-1)}}\right\} \quad \dots 4.12$$

On the assumption that the exponential term is small and that $(m-1)kT_c \gg 1$, which will be particularly true for a large number of injections, equation 4.12 reduces to:

$$\alpha = \frac{k\tau}{[(m-1)kT_c]^{n/m-1}} \quad \dots 4.13$$

which is the same form as equation 4.3 if $\frac{n}{m-1} = \frac{1}{2}$.

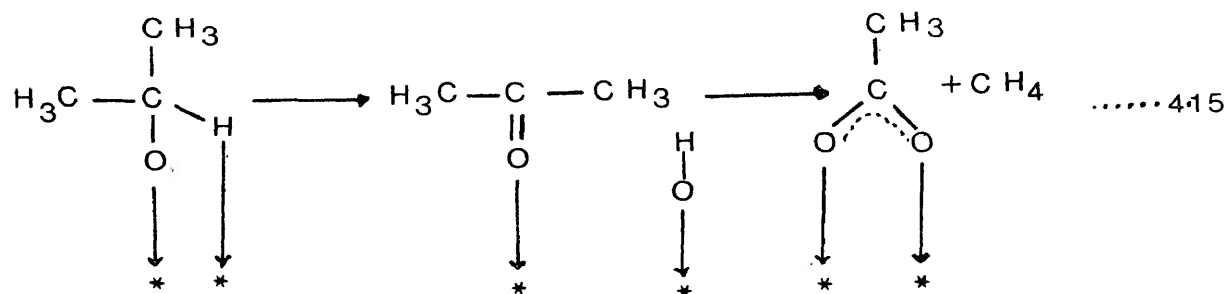
In terms of the model proposed by Wojeichowski the simplest interpretation of equation 4.3 would be that n , the number of sites used in the dehydrogenation reaction, is one, and m , the number of sites poisoned per deactivating event, is three. It may be noted that using the approach of Levenspiel (33), since $\alpha = k'\tau/T_c^{1/2}$

$$\frac{-d\alpha}{dT_c} = \frac{\alpha^3}{2(k'\tau)^2} \quad \dots 4.14$$

which again suggests that the deactivation is a third-order process in terms of acetone.

It is generally proposed that acetone, or products formed from acetone, are responsible for poisoning of dehydrogenation activity. Preadsorption of acetone (Table 3.17). produces a significant reduction in dehydrogenation activity and the decrease in electrical conductivity

with acetone injections follow a similar pattern to that observed with 2-propanol injections (Figure 3.19). Previous reports about how acetone poisons active catalytic sites are contradictory. For example, the work of Deo et al (82) suggests that a carboxy species can be formed by acetone on the surface, viz.,



Strong chemisorption of acetone without further reaction on the surface is preferred by Szabo et al (20). In the present work formation of significant amounts of a carboxy-species seems unlikely. The carboxy-species incorporates surface oxygen of the catalyst in its formation and in its decomposition to carbon dioxide, the catalyst surface would be reduced. There is no evidence of catalyst reduction in the X-ray powder diffraction patterns of used catalyst (Table 3.3) while conductivity studies show that on catalyst

reactivation the initial conductivity is restored (Figure 3.21). Moreover, removal of trace amounts of oxygen from the carrier gas does not appear to affect the acetone yield (Appendix IV). Miyata et al (119) have reported that the presence of oxygen can significantly affect the carboxylate formation and the production of acetone. The conductivity results shown in Figure 3.22 are more indicative of an activated desorption process being responsible for catalyst reactivation.

It has been mentioned earlier in this section that self-poisoning of the dehydrogenation reaction causes the elimination of three sites per deactivating event. The strong chemisorption of acetone itself, in the form shown in Figure 4.11, would effectively block more than one active site.

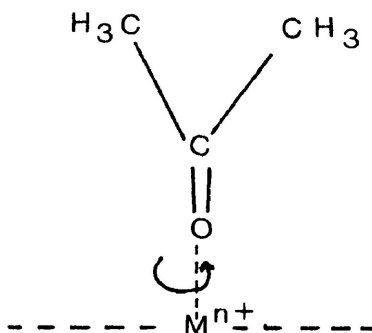


Figure 4.11

On the assumption that the acetone molecule is free to rotate, the chemisorption could exclude an area of approximately 20 \AA^2 of the surface from other reactant molecules. Considering the simplest situation, the (100) plane in nickel oxide, there is one Ni^{2+} ion in every 8.7 \AA^2 of the surface. The possibility of a chemisorbed acetone excluding three Ni^{2+} sites is not unreasonable.

4.2.3 Effects of added poisons

Potential poisons such as acetic acid, phenol, acetone, aniline and n-butyl amine reduce the dehydrogenation activity significantly (Table 3.17). A characteristic feature of these poisons is that they have lone pairs of electrons available for donation to the catalyst and, as shown by conductivity studies (Figures 3.17 and 3.18) the reaction of 2-propanol also involves electron donation to the catalyst.

The results indicate that positive holes, i.e. Ni^{3+} sites, are used in the dehydrogenation reaction and the poisons essentially reduce the number of these sites by adsorption via their lone pairs of electrons. The

conclusion is in agreement with the earlier proposal, section 4.1(b), in which reduction in dehydrogenation activity is associated with a decrease in the concentration of positive holes by replacement of some of Ni^{3+} ions by Al^{3+} ions.

4.2.4 Isotope effects

Kinetic isotope effects are observed in the production of acetone when there is a deuterium substitution at the α -hydrogen of 2-propanol. The observed isotope effect rules out desorption of acetone as being the rate-controlling step in the reaction. The magnitude of the isotope effect is 1.7 at the reaction temperature of 486 K and decreases to a value of 1.5 at 530 K, which is low in comparison with other reported results (59,60) and is substantially less than the theoretical values, Table 4.3. This could indicate a cyclic or strained transition state. However, the kinetic isotope effect clearly shows the rupture of $\text{C}_{\alpha}\text{-H}$ bond as the rate controlling step.

Table 4.3 Comparison of theoretical and observed isotope effect on the catalyst sample containing 5.26 mol percent Al_2O_3

<u>Temperature (K)</u>	<u>Theoretical Isotope Effect*</u>	<u>Observed Isotope Effect</u>
486	3.05	1.70
506	2.90	1.68
530	2.79	1.50
547	2.67	1.35

*Based on a linear transition state, (128).

4.2.5 The dehydrogenation mechanism

In terms of a dehydrogenation reaction mechanism the results and previous discussion in the earlier sections point to the following general conclusions:

- a) the α -carbon-hydrogen bond fission is involved in the rate determining step in the reaction (kinetic isotope effect studies)

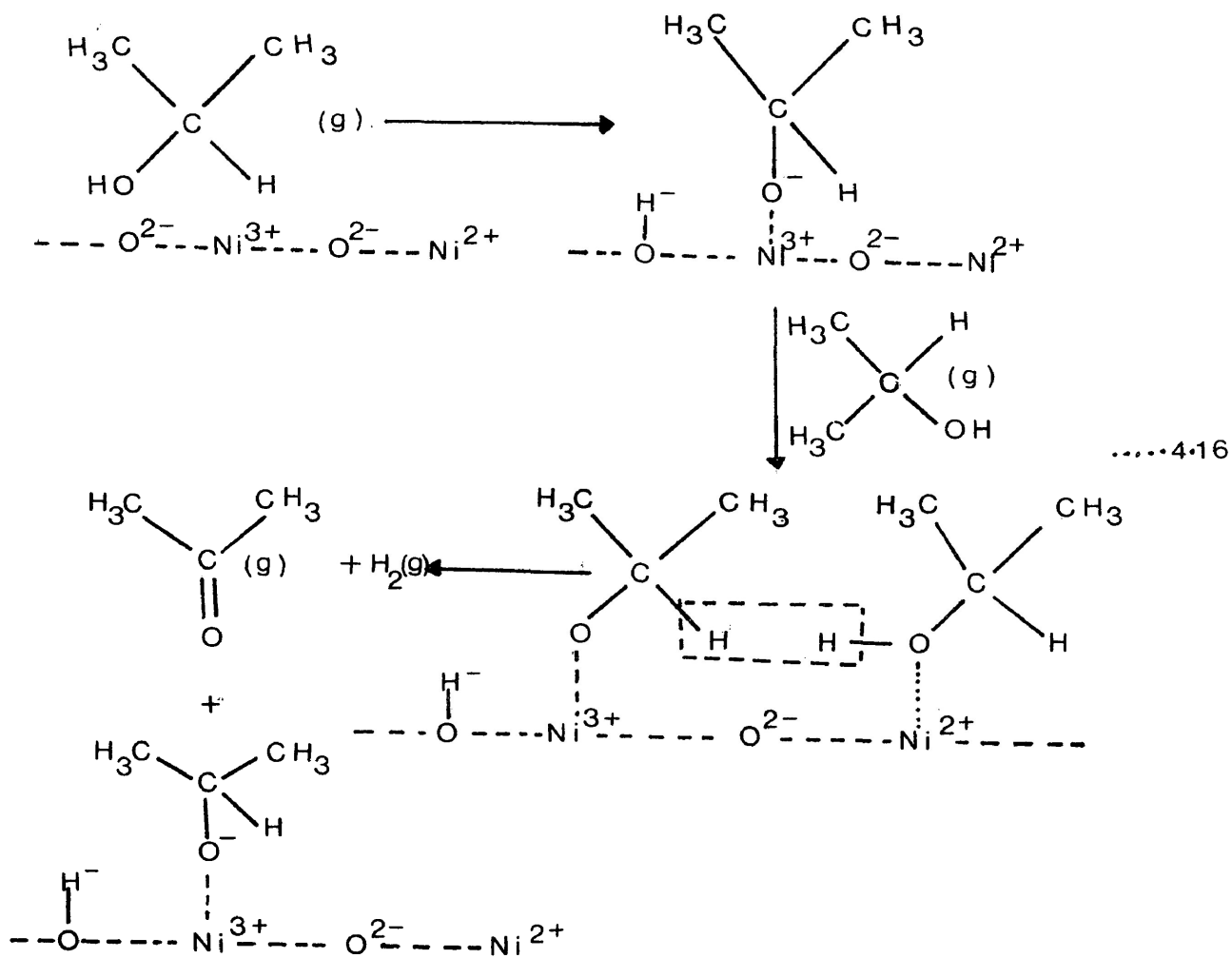
- b) positive holes, i.e. Ni^{3+} are associated with the active surface sites for dehydrogenation reaction (dopant effects on catalytic activity and conductivity studies).

- c) each alcohol molecule uses one active catalyst site in the reaction, while three active sites are used in the self-poisoning, (self-poisoning studies).

Although the isotope effect results clearly rule out the mechanisms in which desorption of product is the rate limiting step (57), the present studies do not present unambiguous evidence for anyone of the mechanisms outlined in the introduction. The basic character of nickel oxide might be expected to favour an ionic mechanism, i.e. a mechanism involving formation of alkoxide and subsequent transfer of hydride ion. If this is the case the alkoxide would be adsorbed on the electron acceptor sites on the catalyst surface. The observations that the dehydrogenation reaction is poisoned by molecules with lone pair of electrons is consistent with this view. Thus, the mechanisms (57,62) involving only the oxide ions of the catalyst appear not to be applicable to the present system. Additionally, the application of the Wojciechowski model (30) to the self-poisoning results indicates that one active

site per alcohol molecule is required in the dehydrogenation reaction. The mechanisms of Szabo et al (20) and Nondek et al (59) require two metal ion sites per alcohol molecule.

Because of polarizability differences between the cation and anion, the catalyst surface will be preferentially terminated by oxide ions. It is therefore suggested that the availability of oxide ions will not be a limiting factor in the catalytic reaction and the conclusions from the self-poisoning studies refer only to the metal ion sites. The effects of small amounts of the dopants on the dehydrogenation activity suggest that these active sites are either Ni^{3+} sites or Ni^{2+} sites near a Ni^{3+} ion in order to permit ready electron transfer. Since only one metal ion is involved in the reaction, transfer of hydride ions could be visualized by interaction with other physically or chemisorbed alcohol molecules. On this basis the mechanism of 2-propanol dehydrogenation could be represented in the following way:

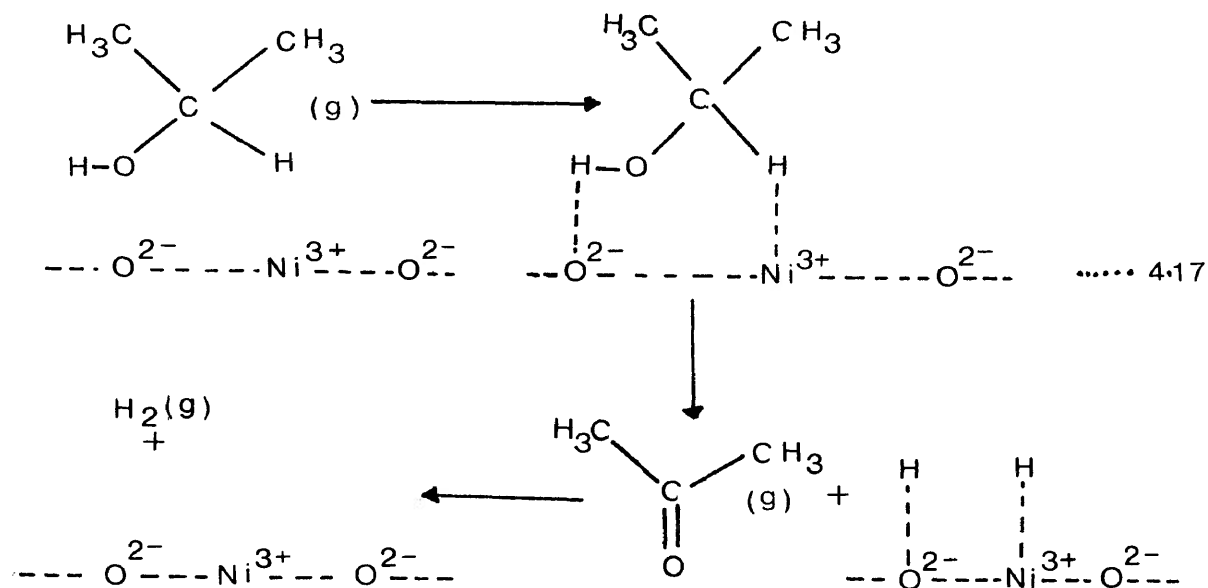


MECHANISM I

The above scheme has certain similarities to the proposal of Kibby and Hall (63) in that the hydride ion transfer to

another molecule of alcohol is required and to the proposal of Tamaru (67) in that the acetone is effectively displaced from the catalyst surface by another alcohol molecule, or more correctly in the present scheme by an alkoxide ion.

An alternative mechanism, not involving alkoxide ion, is one in which adsorption of the alcohol occurs by hydrogen bonding to the surface. Gale et al (120) report a heat of adsorption of 70 kJ mol^{-1} for this type of adsorption of 2-propanol on nickel oxide. In this scheme the metal ion would act as the hydride ion acceptor; viz.



MECHANISM II

Although the dehydrogenation mechanisms I and II have used the Ni^{3+} ions as the active sites, the major requirement, as mentioned earlier, is that a Ni^{3+} ion must be in the region of an active site. Thus, Ni^{2+} ions could be the active sites provided a Ni^{3+} ion is nearby to facilitate electron transfer.

4.2.6 Activation energies and catalyst selectivity

Because of the self-poisoning reaction, the activation energy for the dehydrogenation reaction could only be determined for catalysts which were reactivated between injections. Some results of $\log \alpha$ (the fractional conversion to acetone) as a function of reciprocal temperature are shown in Figure 4.12, from which an apparent activation energy of 47 kJ mol^{-1} has been determined for the dehydrogenation reaction.

Previous studies of the dehydrogenation of secondary alcohols (20,63,121) have reported activation energies in the range 92 to 150 kJ mol^{-1} , although Pepe et al (122) have also obtained a very low value of activation energy for 2-propanol decomposition on CoO-MgO solid solutions. In the latter work, the authors point

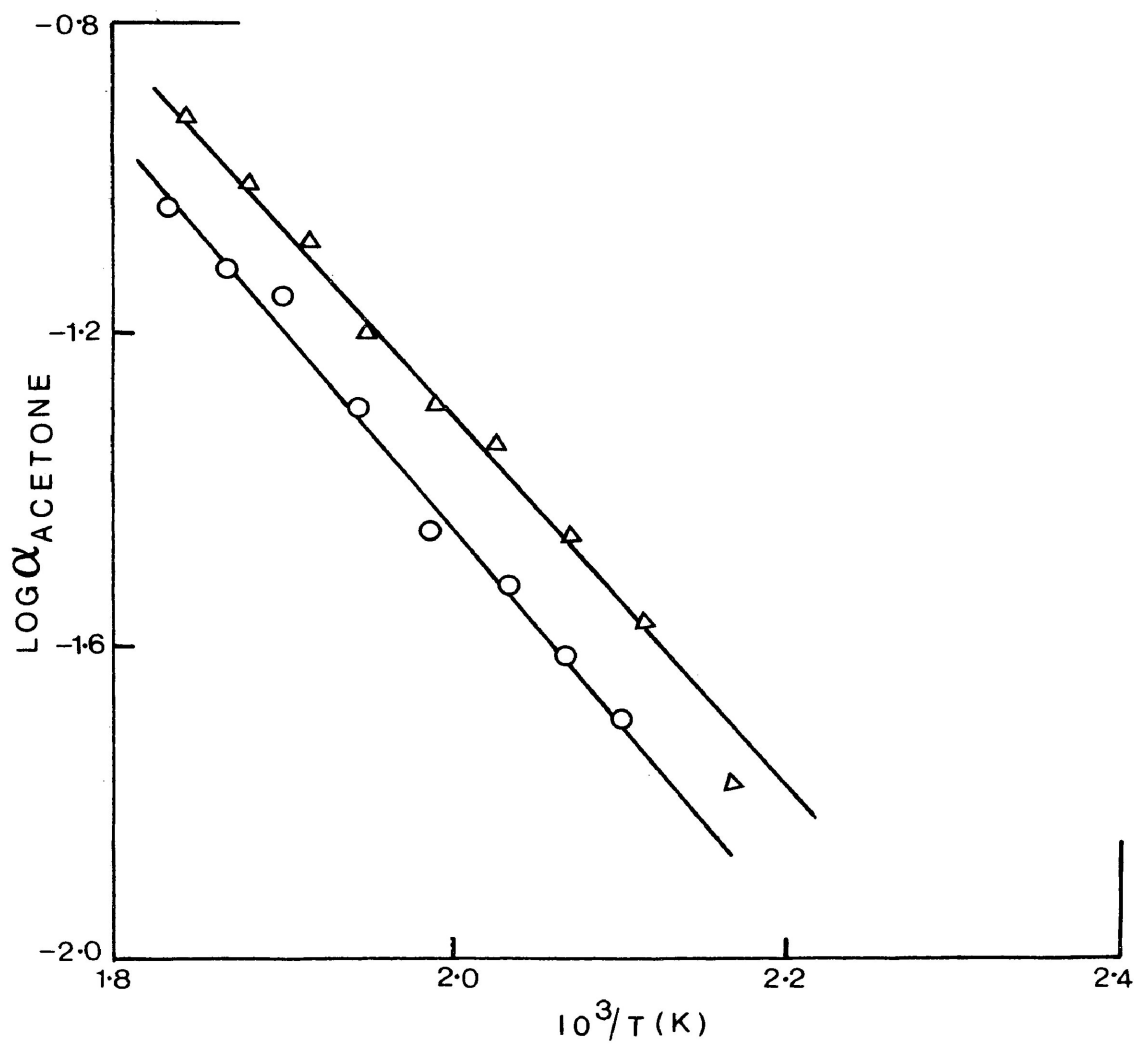


Figure 4.12: Plot of log fractinal dehydrogenation, α , versus reciprocal temperatures (2nm^3 inj. size); O , 5.26 mol % Al_2O_3 ; Δ , 14.29 mol % Al_2O_3 (catalyst reactivated between each injection).

that, if the amounts of reactant produce less than a monolayer coverage, the apparent activation energy will be lower than the true activation energy by an amount corresponding to the heat of adsorption of 2-propanol, which has been reported as 70 kJ mol^{-1} for adsorption on nickel oxide (120). In the present study a typical reactant pulse (2nm^3) contains 1.57×10^{19} molecules while for a typical catalyst surface (5m^2), there will be 5×10^{19} to 5×10^{20} sites available.

The studies on the reactivated catalysts also point out the problems of discussing catalyst selectivity in systems where surface poisoning is possible. Figure 4.13 illustrates the dehydrogenation selectivity for used (stabilized) catalysts and for catalysts reactivated between injections as a function of temperature. A decrease in selectivity with increase in temperature is observed for used catalysts. It should be noted that because of the extent of reaction it was not possible to carry out measurements at temperatures higher than 547 K but, on the basis of the earlier discussion, it would be anticipated that the dehydrogenation selectivity of used catalysts would increase again at higher temperature because of the commencement of

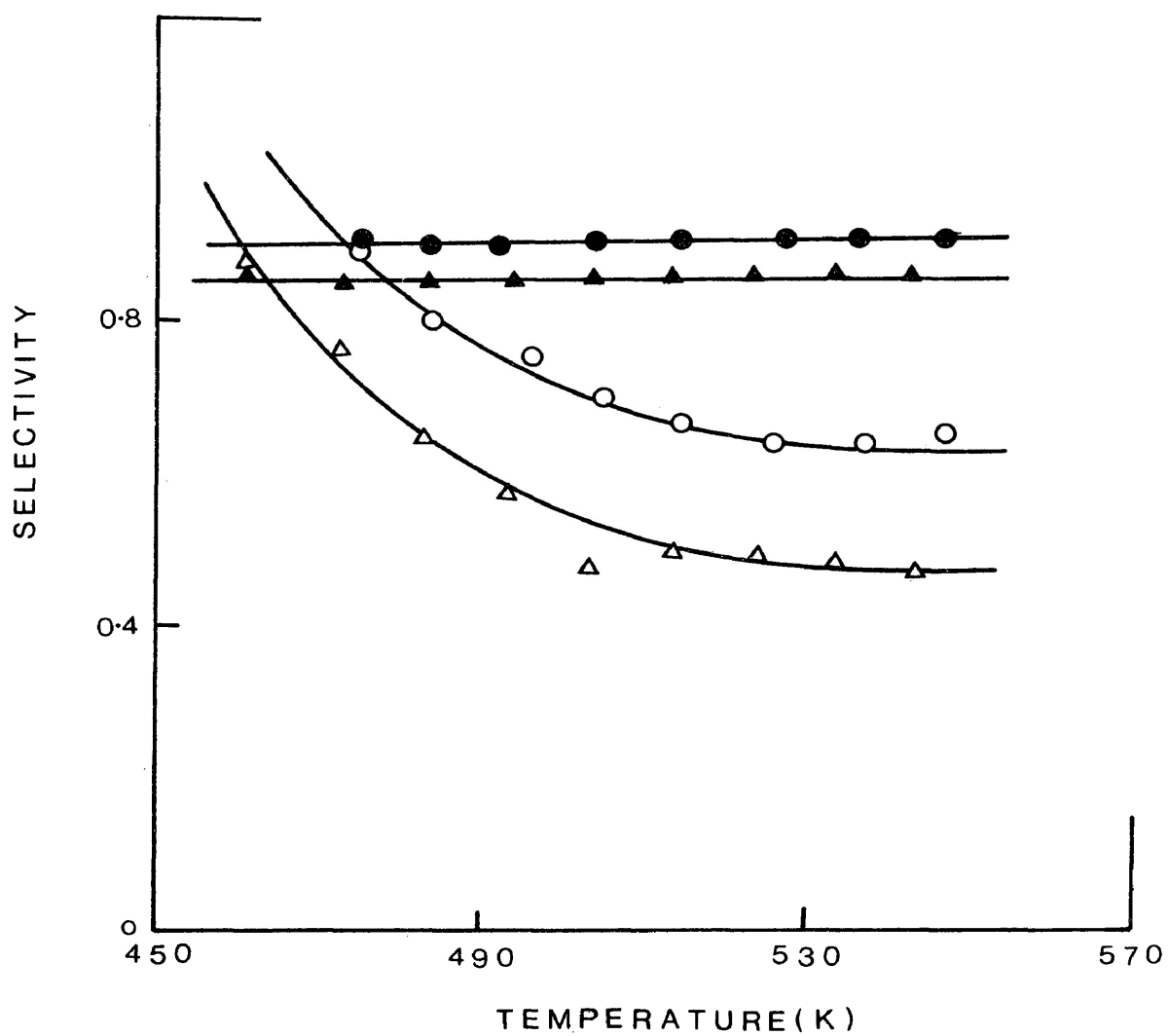


Figure 4.13: Dehydrogenation selectivity as a function of temperatures (2nm³ inj. size); O, ●, 5.26 mol % Al₂O₃; Δ, ▲, 14.29 mol % Al₂O₃; open symbols for usual runs, solid symbols for 'reactivated' catalysts.

catalyst reactivation processes. The interesting feature of the results for the reactivated catalysts is that the selectivity appears to be independent of temperature (Figure 4.13). One possible conclusion from this is that on a 'clean' surface the same intermediate is involved in the dehydration and dehydrogenation reactions. From a geometric point of view the formation of an alkoxide-type species on the surface could lead to both dehydration and dehydrogenation since either the α -hydrogen or a β -hydrogen could interact with the surface.

4.3 The Dehydration Reaction

4.3.1 Kinetics and activation energies

The plots of α (for propene formation) against reciprocal space velocity (Figure 3.8) indicate zero order kinetics. A finite intercept at infinite flow rate ($1/F=0$) is obtained in the plots for the higher temperatures. The finite intercept can be interpreted in the same way as for the dehydrogenation kinetics, section 4.2.1.

Plots of $\log \alpha$ (for propene formation) versus reciprocal temperatures for different catalyst samples are

shown in Figures 4.14 and 4.15. A characteristic feature is the deviation from linearity in the plots at higher temperatures. Since the degree of conversion α is small, the apparent activation energy for the dehydration reaction has been determined from the linear region of the plots and the results are reported in Table 4.4.

Table 4.4 Break temperature and apparent activation energy for dehydration of 2-propanol on different catalyst samples

Catalyst Mol % Al ₂ O ₃	Break temperature (K)	Activation Energy (kJ mol ⁻¹)
0.1	494	97.35
0.5	485	100.23
2.56	503	130.12
5.26	498	93.96
14.29	485	122.39
25.0	446	138.77
50.0	434	169.16

The activation energy for dehydration of 2-propanol to propene on alumina catalysts in the temperature range 446-497 K has been reported by Knozinger et al (123) as 113.02 kJ mol⁻¹. The activation energies determined in

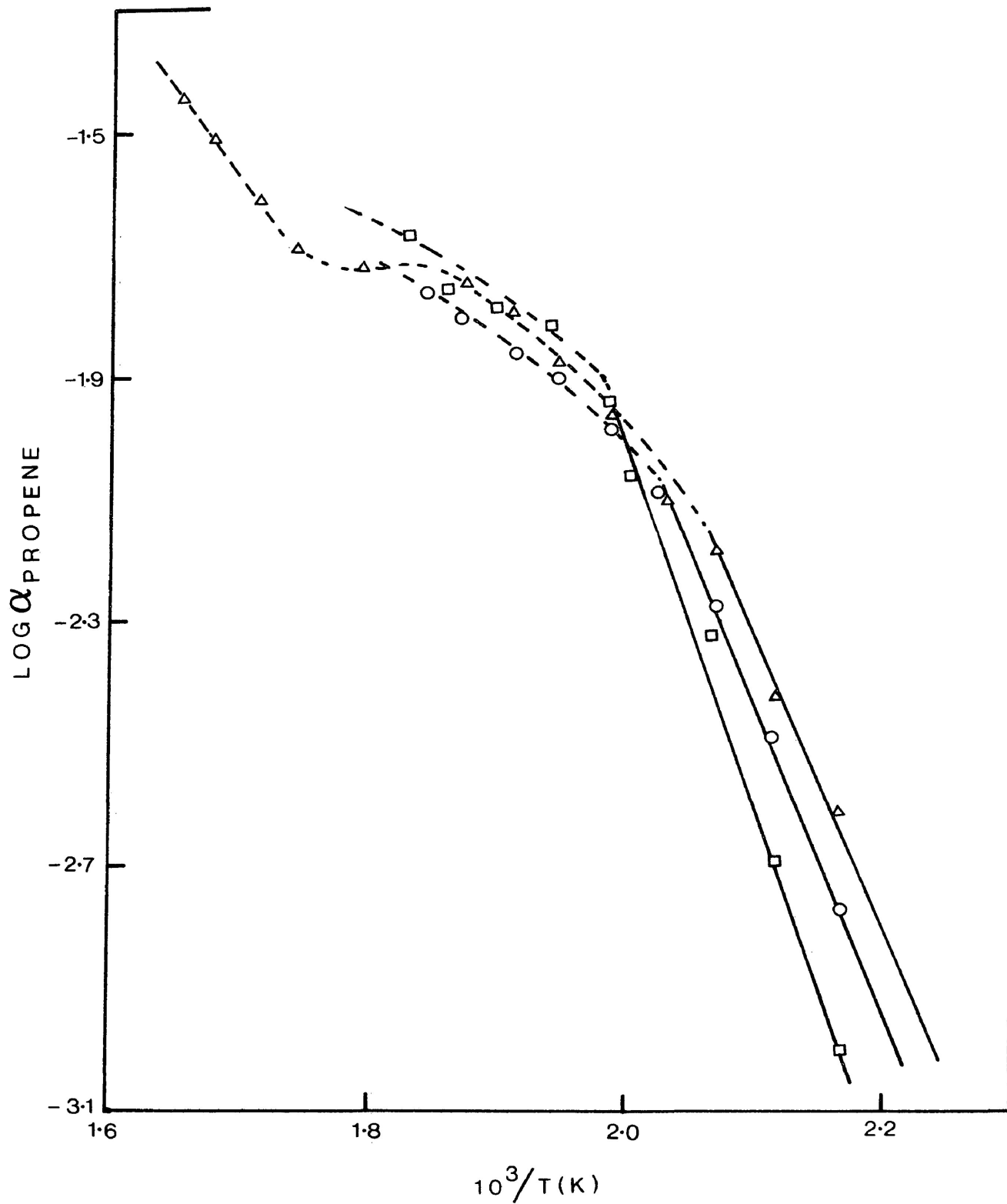


Figure 4.14: Plot of log fractional dehydration, α , versus reciprocal temperatures for different catalyst samples (2nm^3 inj. size); O, 0.1 mol % Al_2O_3 ; Δ , 0.5 mol % Al_2O_3 ; \square , 2.56 mol % Al_2O_3 .

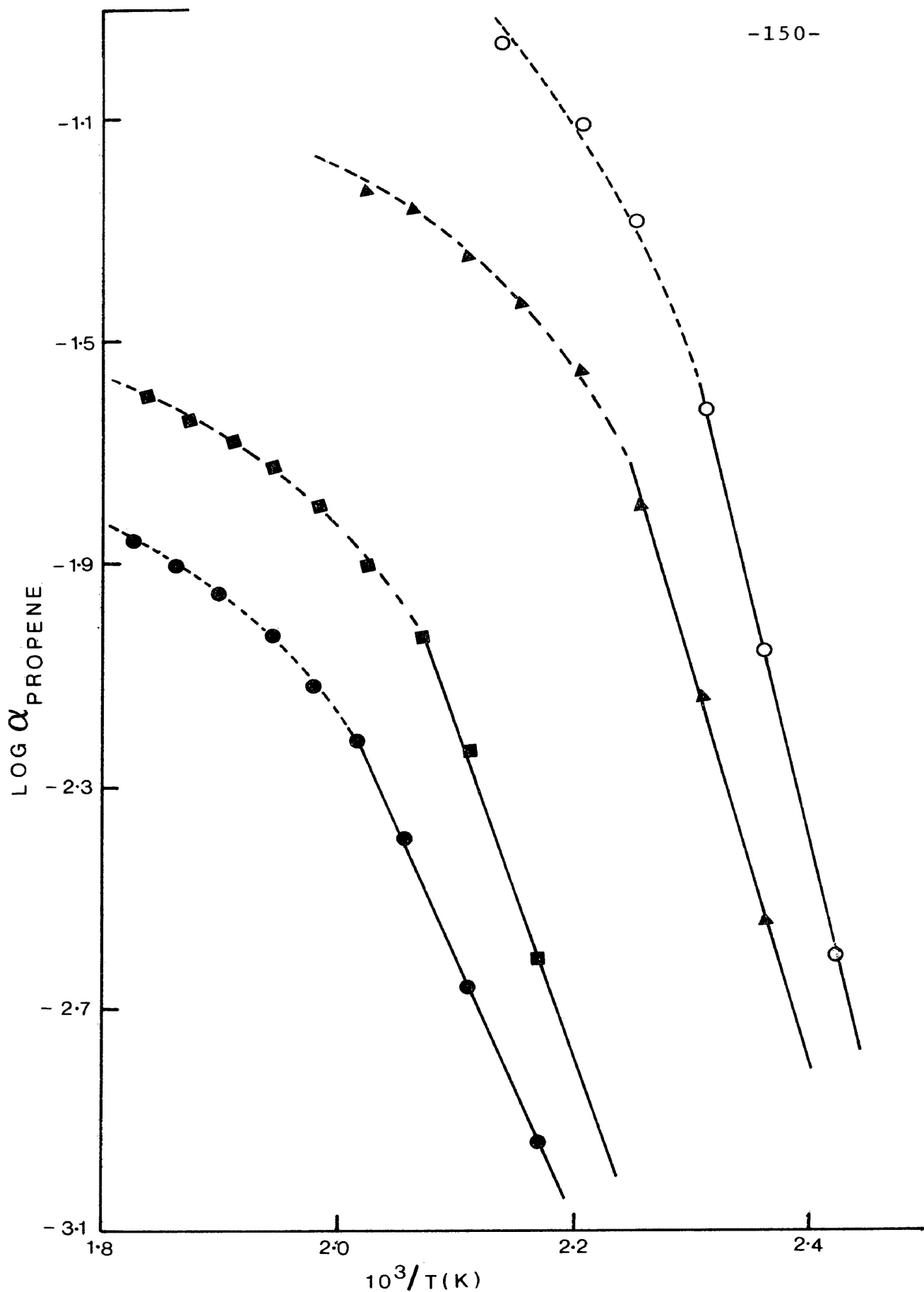


Figure 4.15: Plot of log fractional dehydration, α , versus reciprocal temperatures for different catalyst samples (2nm^3 inj. size);
 ●, 5.26 mol % Al_2O_3 ; ■, 14.29 mol % Al_2O_3 ; ▲, 25 mol % Al_2O_3 ; ○, 50 mol % Al_2O_3 .

the present investigation are in the range of 96-125 kJ mol⁻¹ for samples containing from 0.1 - 14.29 mol percent Al₂O₃ in the temperature range 461-493 K, which appears to be in good agreement with the reported values. However, samples containing 25 and 50 mol percent Al₂O₃ show a higher activation energy, 138.77 and 169.16 kJ mol⁻¹ respectively.

The deviation from linearity in the log α versus 1/T plots implying a process of lower activation energy is frequently interpreted as the on-set of a diffusion-controlled reaction. As with the dehydrogenation reaction, the present results do not support this view. The following points may be noted:

- (a) an isotope effect of 1.5 (Table 3.18), which is not consistent with diffusion-control, is obtained in this region,
- (b) there is a marked variation in the activity (per square metre of catalyst) at which the deviation occurs for the various samples,
- (c) in the decomposition of 2-hexanol on the catalyst containing 5.26 mol percent Al₂O₃ (Appendix V), the deviation occurs at the same temperature but at a very different value of α than that for 2-propanol decomposition on the same sample.

The same type of behaviour has been observed by Butt and coworkers (124) for the dehydration of ethanol on alumina. A deviation from linearity in the Arrhenius-type plot occurs and is considered to be associated with surface dehydration or dehydroxylation. It is interesting that, in the present results, the 'break' temperature appears to decrease with increasing Al^{3+} content, particularly with the more heavily doped samples. A similar observation has been discussed earlier in reference to the dehydroxylation studies, section 4.1.

It is proposed that the deviation from linearity in the $\log \alpha$ versus $1/T$ plot is not due to diffusion-control behaviour but rather to the decomposition of some surface species. While surface hydroxyl is the most likely species in this respect, it may be noted that recovery of reactants and products from the first injection on to a catalyst is anomalously low (Table 3.8) and so additional species may be retained on the catalyst surface. Previous workers have proposed that the formation of a carboxylate species (125) and the deposition of carbon (126) on the catalyst surface occurs during alcohol dehydration. These species are thought to be responsible for deactivation

of the dehydration activity of the catalyst. However, in the present investigation no deactivation is observed in dehydration activity, rather a slight increase in activity is obtained with successive injections. This observation is not in accord with the idea of either a carboxylate species or carbon deposition on the surface. Although existence of these species on the surface is not completely ruled out, it appears that they do not affect the dehydration reaction. Hence it is reasonable to assume that the break in the Arrhenius plot is probably associated with the decomposition of hydroxyl on the surface.

There is also evidence to indicate that the hydroxyl, or another unidentified surface species, is involved in the dehydration reaction at the lower temperatures. In experiments, in which the catalyst is reactivated between injections, no deviation from linearity is observed in the $\log \alpha$ versus $1/T$ plots, Figure 4.16, and the apparent activation energy for the dehydration reaction is markedly lower (40 kJ mol^{-1}) than previously observed. In the catalyst sample with 0.5 mol percent Al_2O_3 which was not activated between injections, there is some indi-

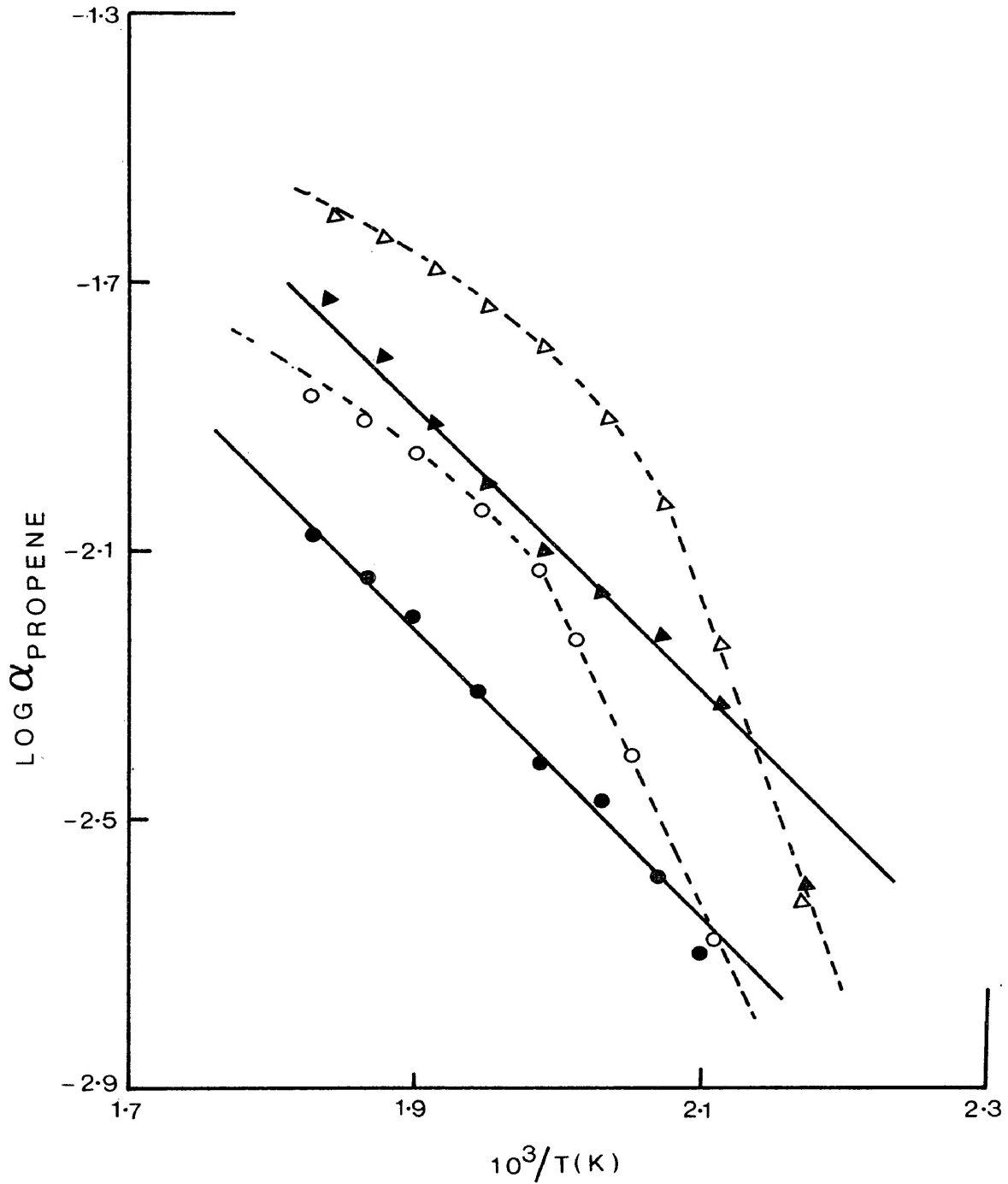


Figure 4.16: Plot of fractional dehydration, α , versus reciprocal temperatures (2nm^3 inj. size); \circ , \bullet , 5.26 mol % Al_2O_3 ; Δ , \blacktriangle , 14.29 mol % Al_2O_3 ; open symbols for usual runs, solid symbols for reactivated catalysts.

cation that a similar activation energy is obtained at higher temperatures, Figure 4.14. Presumably, in the samples reactivated between injections, the surface species, believed to be involved in the low temperature dehydration reaction, is removed or decomposed by the reactivation process.

4.3.2 Effect of added poisons on the dehydration reaction

Both acidic and basic substances poison dehydration activity (Table 3.17) which indicates that dehydration is associated with acidic and basic sites. At lower temperatures any base, weak or strong, reduces the dehydration capacity, while at higher temperatures, significant poisoning is observed only with strong bases like n-butyl amine. Weak bases such as benzene or aniline do not produce any significant effect.

The question arises as to what types of surface sites on the catalyst are active for the dehydration reaction. Since pure nickel oxide is completely a dehydrogenation catalyst, the dehydration activity is probably due to aluminum ions or to the nickel aluminate.

Some consideration of the more thoroughly studied alumina catalysts is useful. Peri (127) and later Spannheimer and Knozinger (24) point out that the alumina surface is partially hydroxylated under catalytic conditions and the existence of three kinds of surface sites, namely oxygen ions, hydroxyl groups and incompletely co-ordinated aluminium ions have been proposed. Hydroxyl groups of at least three chemically distinct types remain on the surface of alumina after it has been dried under vacuum above 923 K and some of these hydroxyl groups of the alumina are considered to have weak proton or Bronsted acidity (24, 37). Participation of basic sites in the dehydration reaction has been proved by poisoning experiments with tetracyanoethylene (80) and on this basis, Dautzenberg and Knozinger (81) suggest that the alcohol is adsorbed by interaction with a surface hydroxyl and an oxide ion. The results of poisoning experiments in conjunction with the properties of alumina, discussed so far, lead to the suggestion that dehydration reaction at lower temperatures proceeds on the nickel aluminate or the doped nickel oxide through basic sites (O^{2-}) and weakly acidic, surface hydroxyls. The latter would be poisoned by weak bases which is in agreement with the observed results.

With increase in temperature, partial dehydroxylation of the surface is expected. Removal of hydroxyl groups from the surface would give rise to O^{2-} and exposed Al^{3+} ions. If dehydration is also considered to proceed by adsorption of the alcohol, through the oxygen of the alcoholic hydroxyl group on an incompletely co-ordinated surface Al^{3+} ion, then poisoning would be expected only with strong bases. The significant poisoning only with n-butyl amine justifies the above position.

4.3.3 Kinetic isotope effects

A kinetic isotope effect in propene formation is observed when there is deuterium substitution at the β -hydrogens of the alcohol. A maximum isotope effect of 1.75 is observed at the reaction temperature of 486 K and the value decreases to 1.21 with the increase in the reaction temperature, Table 3.18.

A simple model (128) for the calculation of isotope effects gives:

$$\frac{k_H}{k_D} = \left(\frac{M_D}{M_H}\right)^{1/2} \frac{h\nu_D}{h\nu_H} \times e^{(h\nu_H - h\nu_D)/2RT} \frac{1 - e^{-h\nu_H/RT}}{1 - e^{-h\nu_D/RT}} \quad \dots 4.18$$

where k_H/k_D is the kinetic isotope effect, M_H and M_D are the reduced masses of the normal and deuterated substrates and ν_H and ν_D are the frequencies of the stretching vibration of C-H and C-D bonds. In this model, it is assumed that the C-H and C-D bonds are completely broken in the transition state. At moderate temperatures, equation 4.18 can be approximated to:

$$k_H/k_D = e^{h(\nu_H - \nu_D)/2RT} \quad \dots 4.19$$

Infrared spectra of 2-propanol and 2-propanol-d₆ (60) indicate that insertion of deuterium in the methyl group reduces its C-H stretching frequencies by 738 cm⁻¹. Substitution of this value in equation 4.19 gives an isotope effect of 2.98 at a reaction temperature of 486 K, a value which is relatively high in comparison with the experimentally observed result. The theoretically calculated isotope effect diminishes slightly with increasing temperature (Figure 4.17) but a more pronounced temperature dependence is observed with the experimental results (Figure 4.17). A low value of the isotope effect could be attributed to incompletely broken bonds in the transition state and may be indicative of an E-2 type mechanism for dehydration. However, the stronger than expected temperature

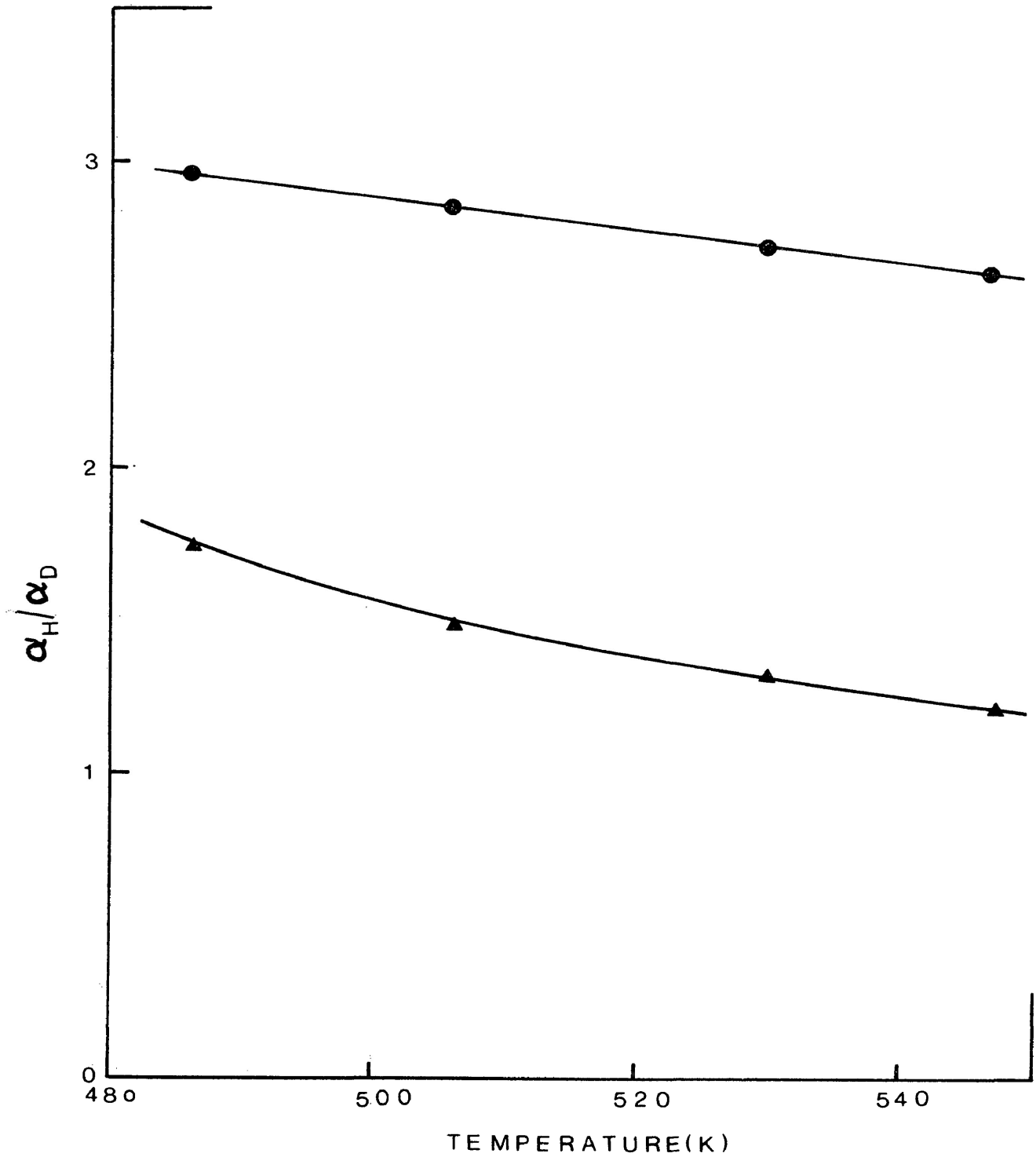
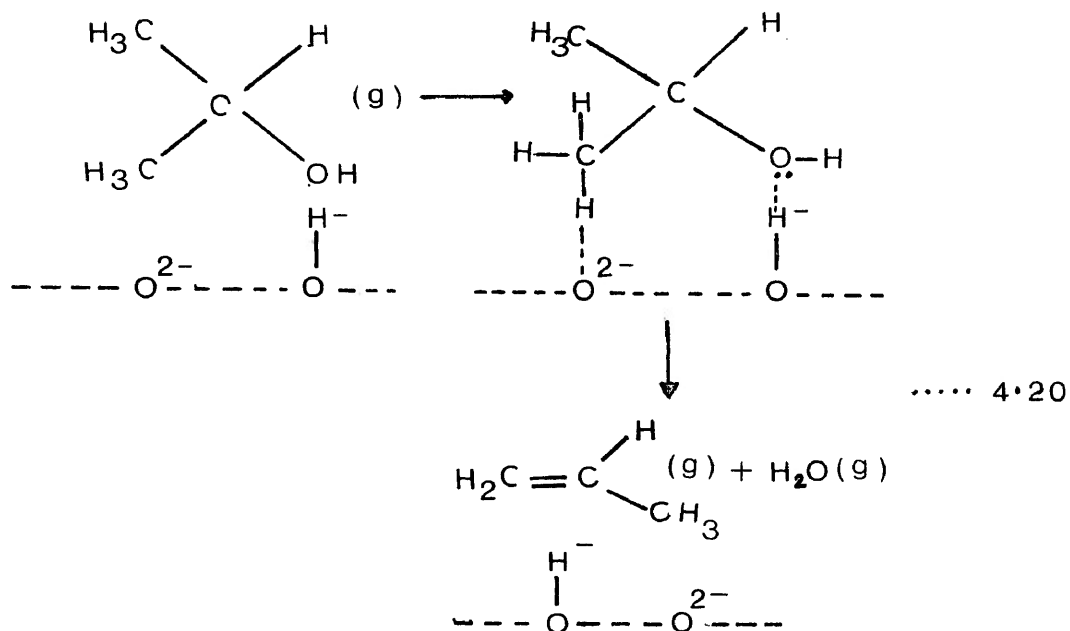


Figure 4.17: Dependence of theoretical and observed isotope effect with temperature for dehydration of 2-propanol; ●, theoretical isotope effect, ▲, observed isotope effect.

dependence suggests that the E-1 character of the transition state becomes more pronounced as the temperature is increased. This type of variation of the isotope effect with temperature has also been observed by Knozinger et al (68). They suggest that below 473 K primary, secondary and tertiary alcohols are dehydrated via E-2-like reaction intermediates, and at elevated temperatures, depending upon substrate structure, the reaction may proceed through an E-1-type mechanism.

4.3.4 Dehydration reaction mechanisms

The previous sections dealing with the activation energy, poisoning and kinetic isotope effects indicate that there is a change in the reaction mechanism and in the nature of the catalytic sites with increasing reaction temperature. At lower temperatures one of the active sites has been tentatively identified as a hydroxyl group and the results of the present work are consistent with the type of mechanism proposed by Knozinger et al (81) and Deo et al (82), namely:

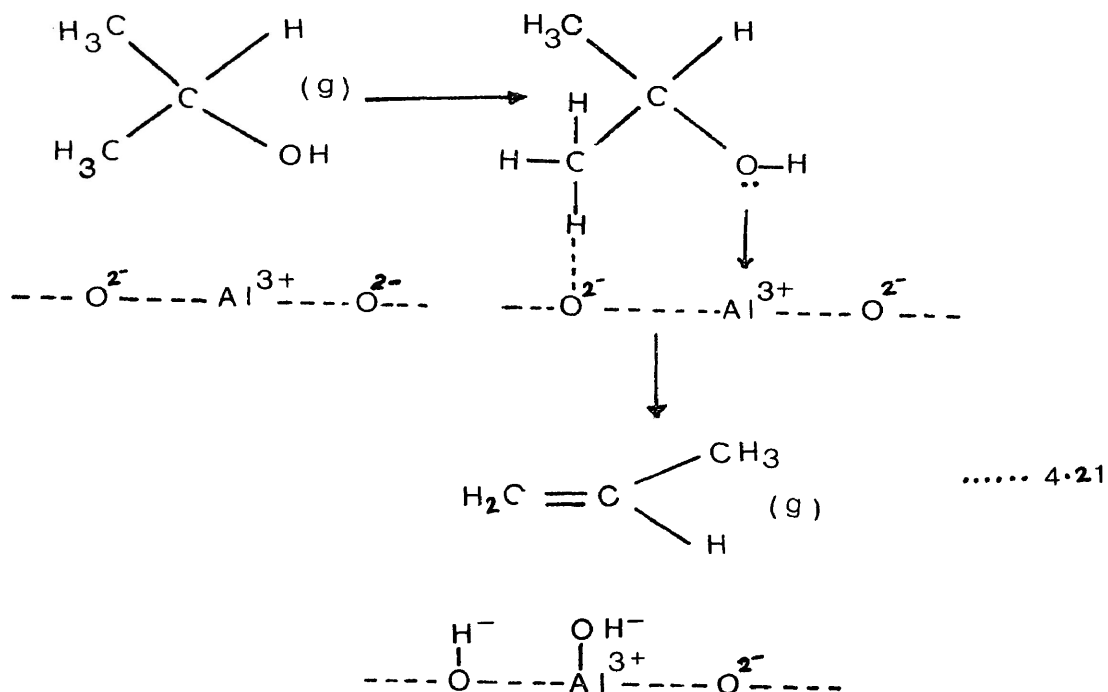


MECHANISM I

The water formed in the reaction could readsorb on the surface forming more hydroxyl groups and thus accounting for the slight increase in dehydration activity with successive injections, which is observed particularly with fresh or reactivated catalysts.

At higher temperatures, the on-set of surface dehydroxylation will expose more co-ordinatively unsaturated cations at the surface and a reaction involving Lewis acid

sites may become more important. The type of mechanism suggested by Krylov (71), Pines and Haag (72) and Jain and Pillai (73) is in accord with this view, viz.



MECHANISM II

Dehydroxylation of the surface would then reform the catalytically active sites. It should be noted that isotope

effect results indicate that an E-1-type transition state is more fully developed in the second mechanism.

The mechanism involving the Lewis acid centres would be expected for a 'clean' catalyst surface and so is likely to be the predominant mechanism for samples which are reactivated between injections. Consequently, the apparent activation energy for mechanism II is believed to be 40 kJ mol^{-1} , (Figure 4.16). This compares favourably with a reported value of 46 kJ mol^{-1} for decomposition of ethanol on alumina at higher temperatures where again an E-1 mechanism is proposed (126). Even assuming mechanisms I and II are correct, it is unlikely that one will act exclusively in any temperature region, both mechanisms will be operative with one predominating in a particular temperature range. The low dehydration activity of catalysts containing less than 25 mol percent Al_2O_3 can be rationalised with the dehydroxylation model proposed in section 4.1. Only low concentrations of Al^{3+} are envisaged in the surface zones in regions I and II.

4.4 CONCLUSION

It has been shown that nickel oxide is purely a dehydrogenation catalyst for the decomposition of 2-propanol, but the incorporation of Al^{3+} ions in the host matrix leads to the development of some dehydration activity. Formation of nickel aluminate at the higher dopant concentrations is evident from X-ray diffraction patterns, and nickel aluminate is found to be purely a dehydration catalyst yielding propene. The significant change in catalyst activity and selectivity with very small concentrations of Al^{3+} ions in region I is believed to be associated with electronic changes in the nickel oxide brought about by the substitutional incorporation of Al^{3+} ions, while the marked increase in activity and dehydration selectivity in region III is ascribed to increasing amounts of nickel aluminate in the surface zones of the catalyst samples.

Self-poisoning in dehydrogenation reaction is considered to be due to strong chemisorption of acetone on the catalyst surface. It is proposed that in the dehydrogenation reaction each alcohol molecule uses one active site on the catalyst, while three active sites are involved in the self-poisoning.

Isotope effect measurements indicate that the deviation from linearity in the Arrhenius plots at higher reaction temperatures for the dehydration reaction is not due to a diffusion-controlled reaction. It is suggested that the deviation is associated with the decomposition of hydroxyl groups on the catalyst surface.

It appears that electron acceptor sites on the catalyst surface are the active sites for the dehydrogenation reaction, while for the dehydration reaction, an E-2-type mechanism is suggested for the lower temperature reaction and with increasing temperature there is a trend towards an E-1-type mechanism.

4.5 Suggestions for Further Work

The present study could be extended to investigate in more detail the variations of catalyst activity and selectivity with the catalyst compositions. For example, the variations in activity and selectivity in region I are believed to be due to changes in the p-type character of the catalyst. This could also be examined by doping the oxide with monovalent ions like Li^+ . The surface in region II is considered to be essentially nickel oxide deposited on nickel aluminate; by choosing a higher firing temperature and a prolonged time of firing for the catalyst preparation, the increased amount of diffusion could lead to a more homogeneous mixture of the phases and more significant variations in catalyst selectivity may be observed. Additionally, more dopant concentrations in region III should be investigated.

The sample containing 2.56 mol percent Al_2O_3 has shown anomalous behaviour both with respect to the dehydroxylation activation energy and to self-poisoning. Whether this is due to the particular sample preparation or due to the formation of new compound at this dopant concentration is not clear. Further studies of the catalyst

structure and activity in this range are required.

In order to establish the proposed reaction and self-poisoning mechanisms, it would be advantageous to undertake in-situ infrared studies of the catalyst under reaction conditions. Also, the use of carbon-14 labelled 2-propanol could provide evidence of the stability of the 'surface retained' species and whether, in the dehydrogenation reaction, the formation of acetone in the gas phase is due to its displacement from the surface.

REFERENCES

1. A.A. Balandin, "Multiplet Theory of Catalysis", Chapter 1, Pub. M.G.U., 1963; ch. 2, 1966, (in Russian) also Adv. Catal., 19(1969)1.
2. O.V. Krylov, "Catalysis by Non-Metals", Academic Press, New York, (1970)115-34.
3. K. Hauffe, "Reactions on Solids and Their Surfaces", IL. 1962 (in Russian).
4. G.M. Schwab, Adv. Catal., 2(1952)229.
5. W.E. Garner, D.A. Dowden and J.F. Garcia de la Banda, Anales Real. Soc. Espan. Fis. Quim., 50B(1954)35.
6. F.F. Wolkenshtein, Probl. Kinetika i Kataliz, 3(1962)509.
7. S.Z. Rogiskii, Zh. Fiz. Khim., 6(1935)334.
8. S.Z. Rogiskii, Dokl. Akad. Nauk SSSR, 67(1949)97.
9. E.F. McCaffrey, T.A. Micka and R.A. Ross, J. Phys. Chem., 76(1971)3778.
10. G.K. Boreskov, "Catalysis in Sulphuric Acid Production", Russian State Press for Chemical Literature (1954).
11. D.A. Dowden and D. Wells, Actes du Deuxieme Congres International de Catalyse, Paris, 1960, Editions, Technip, 2(1961)1489.
12. J. Harber and F.S. Stone, Trans. Faraday Soc., 59(1963)192.
13. R.L. Burwell, G.L. Haller, K.C. Taylor and J.F. Read, Adv. Catal., 20(1969)2.
14. J. Deren and E. Fryt, Bull. Acad. Polon. Sci. Ser. Sci. Chim., 14(1966)407.

15. F. Pepe and F.S. Stone, Proc. 5th Internat. Congress Catalysis, Palm Beach, 1972, ed. J.W. Hightower, North-Holland, Pub. Co., Amsterdam, 1(1973)137.
16. E.J. Odumah, M.Sc. Dissertation, UMIST, 1973.
17. J.C. Vickerman, Catalysis, Specialist Periodical Report, Chem. Soc., 2(1977)107.
18. H.S. Taylor, Proc. Roy. Soc., A108(1925)105.
19. W.F.N.M. De Vleeschauwer, in "Physical and Chemical Aspects of Adsorbents and Catalysts", (B.G. Linsen, Ed.), Academic Press, London, (1970)265-314.
20. Z.G. Zabo, B. Jover and R. Omacht, J. Catal, 39(1975)225.
21. B.H. Davis, J.C. S. Faraday I, 76(1980)92.
22. F. Freund and V. Sperling, Mater. Res. Bull., 11(1976)621.
23. H. Knozinger and P. Ratnasamy, Catal. Rev. Sci. Eng., 17(1)(1978)52.
24. H. Spannerheimer and H. Knozinger, Ber. Bunsenges, Phys. Chem., 70(1966)570,575.
25. C.N. Satterfield, "Heterogeneous Catalysis in Practice", McGraw-Hill Book Company, New York, (1980)14.
26. E.E. Wolf and E.E. Petersen, J. Catal., 47(1977)28.
27. G.F. Froment and K.B. Bischoff, Chem. Eng. Sci., 16(1961)189.
28. S. Masamune and J.M. Smith, AIChE. J., 12(1966)384.
29. Y. Murakami, T. Kobayashi, T. Hattori and M. Masuda, Ind. Eng. Chem. Fundam., 7(1968)599.

30. B.W. Wojciechowski, *Cand. J. Chem. Eng.*,
46(1968)48.
31. S.J. Khang and O. Levenspiel, *Ind. Eng. Chem. Fund.*, 42(1973)185.
32. L.L. Hegedus and E.E. Petersen, *Ind. Eng. Chem.*, 11(1972)579.
33. O. Levenspiel, *J. Catal.*, 25(1972)265.
34. J. Corella, J.M. Asua and J. Bilbao, *Cand. J. Chem. Eng.*, 59(1981)647.
35. G.F. Froment, "Catalyst deactivation", *Proceedings of the International Symposium, Antwerp, 1980, Elsevier Scientific Pub. Co., Amsterdam-Oxford-New York, Chapter 1, (1980).*
36. C. Kembell, in "Catalysis-Progress in Research", (F. Basolo and R.L. Burwell, Jr. Eds.) Plenum, New York, (1973)85.
37. H. Pines and W.O. Haag, *J. Amer. Chem. Soc.*,
82(1960)2471.
38. K. Beranek, M. Kraus, K. Kochloefl and V. Bazant, *Actes. Congr. Int. Catal. 2nd Paris, 1960;*
1(1961)749.
39. H. Knozineger, *Adv. Catal.*, 25(1976)184.
40. R.H. Clark, W.E. Grahm and A.G. Winter,
J. Amer. Chem. Soc., 47(1925)2748.
41. C.N. Hinshelwood, "The Kinetics of Chemical Change"
Oxford University Press (1949).
42. P.B. Weisz and C.D. Prater, *Adv. Catal.*, 6(1954)
144.
43. A.A. Balandin, *Lzv. Aka. Nauk. SSSR, Ser. Chim.*,
4(1961)761.
44. A.A. Balandin, *Izv. Akad. Nauk. SSSR., otd. khim. Nauk.*, 3(1961)416.

45. J.B. Galeski and J.W. Hightower, *Cand. J. Chem. Eng.*, 48(1970)151.
46. R.J. Kokes, H. Tobin and P.H. Emmett, *J. Amer. Chem. Soc.*, 17(1955)5860.
47. D.W. Bassett and H.W. Habgood, *J. Phys. Chem.*, 64(1960)769.
48. G.A. Gaziev, V. Yu. Filinovskii and M.I. Yanovskii, *Kinet. Katal.*, 4(1963)688.
49. G.M. Schwab and A.M. Watson, *J. Catal.*, 24(1965)570.
50. J.A.S. Bett and W.K. Hall, *J. Catal.* 10(1968)105.
51. T. Hattori and Y. Murakami, *J. Catal.*, 10(1968)114.
52. T. Hattori and Y. Murakami, *J. Catal.*, 12(1968)166.
53. T. Hattori and Y. Murakami, *J. Catal.*, 31(1973)127.
54. T. Hattori and Y. Murakami, *J. Catal.*, 33(1974)365.
55. W.A. Blanton, Jr., C.H. Byers and R.P. Merrill, *Ind. Eng. Chem. Fund.*, 7(1968)611.
56. K. Makar and R.P. Merrill, *J. Catal.*, 24(1972)546.
57. O.V. Krylov, *Zh. Fiz. Khim.*, 39(1965)2911.
58. A. Bielanski, J. Deren, J. Haber and J. Sloezynaki, *Actes du deuxieme Congr. Intern. de Catalyse, Paris (1960)*1653, *Tech. Paris (1961)*.
59. L. Nondek and J. Sedlacek, *J. Catal.*, 40(1975)34.
60. I.M. Hoodless, *Cand. J. Chem.*, 55(1977)153.

61. Y. Dechatre and S.J. Teichner, Bull. Soc. Chim., France, (1967)2804.
62. F. Pepe and F.S. Stone, J. Catal., 56(1979)160.
63. C.L. Kibby and W. Keith Hall, J. Catal., 31(1973)65.
64. A. Eucken, Naturwisseuschaften, 36(1949)48.
65. A. Eucken and K. Heur, Z.Physik. Chem. (Leipzig), 196(1950)40.
66. E. Wicke, Z. Elektrochem., 53(1949)279.
67. O. Koga, T. Onishi and K. Tamaru, J.C.S. Faraday 1, 76(1980)19.
68. H. Knozinger, and A. Scheglila, J. Catal., 17(1970)252.
69. K. Kochioefl and H. Knozinger, Proc. 5th Inter. Congr. Catal. North-Holland Publ. Co., Amsterdam, 2(1972)1171.
70. H. Knozinger and A. Schegelila, Z. Phys. Chem. Frankfurt, 63(1969)197.
71. O.V. Krylov, Zh. Fiz. Khim., 39(1965)2656.
72. H. Pines and W.O. Haag, J. Amer. Chem. Soc., 83(1961)2847.
73. J.R. Jain and C.N. Pillai, J. Catal., 9(1967)322.
74. J.B. Senderns, Bull. Soc. Chim. France, 1(1907)692.
75. V.N. Ipatieff, "Catalytic Reactions at High Pressures and Temperatures, MacMillan Co., New York, 1936.
76. K.V. Topchieva, K. Yun-Pin and I.V. Smirnova, Adv. Catal., 9(1957)799.

77. H. Knozinger, E. Ress and H. Buhl, *Naturwissenschaften*, 54(1967)516.
78. H. Knozinger and E. Ress, *Z. Physik. Chem. (Frankfurt)*, 54(1967)136.
79. H. Knozinger, E. Ress and H. Stolz, *Ber. Bunsenges, Phys. Chem.*, 74(1970)1056.
80. F. Figueras Roca, A. Nohl, L. De Mourges and Y. Trambouze, *C.R. Acad. Sc., Ser.*, C2,66(1968)1123.
81. D. Dautzenberg and H. Knozinger, *J. Catal.*, 33(1974)142.
82. A.V. Deo, T. T. Chuang and I.G. Dalla Lana, *J. Phys. Chem.*, 75(1971)234.
83. B. Crzybowska and J. Deren, *Bull. Acad. Polon. Sci., Ser. Chim.*, 12(8)(1964)575-9.
84. W. Milligan and L. Merten, *J. Phys. Chem.*, 50(1946)465.
85. V.V. Levina, V. Ya. Danyshevskii, E.A. Koevskaya, G.I. Kapustind, and V.I. Yakerson, *Izv. Akad. Nauk., SSSR, Ser. Khim.* 12(1975)2646-52. (Russ).
86. L.G. Simonova, V.A. Dzisko, M.S. Borisova, L.G. Karakchiev, and I.P. Olen'kova, *Kinet. Catal.*, 14(1973)1380.
87. C.S. Narasimhan, C.S. Swamy, *Current Science*, 45(21)(1976)759.
88. R. Uma, R. Venkatachalam and J.C. Kuriacose, *Proc. 5th Internat. Congress Catalysis, Palm Beach, 1972*, ed. J.W. Hightower, North-Holland, Pub. Co., Amsterdam, 1(1973)245.
89. I.M. Hoodless, Unpublished work.
90. S. Brunauer, P.H. Emmett and E. Teller, *J. Amer. Chem. Soc.*, 60(1938)309.

91. S. Brunauer, L.E. Copeland and D. L. Kantro, "The Solid-gas Interface", Vol. 1, ed. E.A. Flood, Marcel Dekker Inc., New York, (1967).
92. S.J. Gress and K.S. Sing, "Adsorption, Surface Area and Porosity", Academic Press, New York and London (1967).
93. American Society for Testing Material Index (1972).
94. X-ray Powder Data File, 4-0835, American Soc. for Testing and Materials. (1960)582.
95. Powder Diffraction File, 10-39, American Soc. for testing and Materials. (1967)659.
96. A.W. Coats and J.P. Redfern, Nature, (1964)69.
97. R.B. Fahim and A.I. Abu-Shady, J. Catal., 17(1970)10.
98. K.M. ABD.El-Salaam and E.A. Hassan, Surface Technology, 11(1980)55.
99. J.H. Sharp, Trans. J. Brit. Ceram. Soc., 72(1973)21.
100. C.D. West, Amer. Min., 17(1932)316; 19(1934)281.
101. M.C. Ball and H.F.W. Taylor, Min. Mag., 32(1961)754.
102. W. Van Gool, "Principles of Defect Chemistry of Crystalline Solids", Academic Press, New York, (1966)134.
103. S.P. Mitoff, J. Chem. Phys., 35(1961)882.
104. H.G. Sockel and H. Schmalzried, Ber. Bunsenges, Physik, Chemie, 72(1968)745.
105. Y.D. Trtiyakov and R.A. Rapp, Trans. AIME, 245(1965)1235.
106. V.V. Levina, V. Ya. Danyshvskii, E.A. Koevskaya, G.I. Kapustin, and V.I. Yakerson, Izv. Akad. Nauk, SSSR, Ser. Khim., 12(1975)2646. (Russ).

107. C.R. Barrett, W.D. Nix, A.S. Tetelman, "The Principles of Engineering Materials", Prentice-Hall, Chapter 5, 1973.
108. F.A. Kroger, "The Chemistry of Imperfect Crystals", North-Holland Pub. Co., Amsterdam, (1964)730.
109. M. Schiavello, M. Lo Jacono and A. Cimino, J. Phys. Chem., 75(1971)1051.
110. W. Milligan and L. Merten, J. Phys. Chem., 50(1946)465.
111. A.M. Rubinshtein, A.A. Slinkin and N.A. Pribytkova, Izv. Akad. Nauk. SSSR, otd. khim. N., (1958)874.
112. V.M. Akimov, A.A. Slinkin, L.D. Kretalova, and A.M. Rubinshtein, *ibid.*, (1960)624.
113. L.G. Simonova, V.A. Dzis'ko, M.S. Bonsova, L.G. Karakchiev, and I.P. Olen'kova, Kin. and Catal. 14(1973)1380.
114. J.A.S. Bett and W.K. Hall, J. Catal., 10(1968) 105.
115. A. Voorhies, Jr., Ind. Eng. Chem., 37(1945)318.
116. F.H. Blanding, Ind. Eng. Chem., 45(1953)1186.
117. G.F. Froment, Proc. Sixth Inter. Congress on Catalysis, (1976)10. (The Chemical Society, London).
118. G.F. Froment and K.B. Bischoff, Chem. Eng. Sci., 17(1962)105.
119. H. Miyata, M. Nakamiya and Y. Kubokawa, J. Catal., 34(1974)117.
120. R.L. Gale, J. Haber and F.S. Stone, J. Catal., 1(1962)32.
121. A.A. Silinkin, V.I. Yakerson and A.M. Rubinstein, Izv. Akad. Nauk. SSSR, 3(1960)435.
122. F. Pepe and F.S. Stone, J. Catal., 56(1979)160.

123. H. Knozinger, H. Buhl and K. Kochloefl, J. Catal., 24(1972)57.
124. J.E. Dabrowski, J.B. Butt and H. Bliss, J. Catal., 18(1970)297.
125. R. Leaute and I.G. Dalla Lana, J. Catal., 60(1979)460.
126. D.E.R. Bennett and R.A. Ross, J. Chem. Soc., (1968)1524.
127. J.B. Peri, J. Phys. Chem., 69(1965)211,220.
128. K.B. Wiberg, Chem. Rev., 55(1955)713.
129. Powder Diffraction File, 15-87, (1972)837, Joint Committee on Powder Diffraction Standards.
130. Inorganic Index to Powder Diffraction File, Joint Committee on Powder Diffraction Standards (1972).

APPENDIX I

APL COMPUTER PROGRAMS WERE USED IN THE
ANALYSIS OF DATA FOR THIS THESIS. KRBET
WAS USED IN SURFACE AREA CALCULATIONS.

APPENDIX II

Fractional conversions of 2-propanol and deuterio-2-propanol on stabilized catalyst sample containing 5.26 mol percent Al_2O_3

Reactant	Reaction temp. (K)	* α propene	* α acetone
2-propanol	486	0.0181	0.0380
	506	0.0485	0.0941
	530	0.0920	0.1286
	547	0.1261	0.1459
2-propanol- d_6 (CH_3) $_2$ CDOH	486	0.0109	0.0335
	506	0.0321	0.0784
	530	0.0689	0.1129
	547	0.1029	0.1389
2-propanol	486	0.0176	0.0336
	506	0.0463	0.0771
	530	0.0895	0.1078
	547	0.1240	0.1352
2-propanol- 2d_1 (CH_3) $_2$ CDOH	486	0.0162	0.0197
	506	0.0431	0.0437
	530	0.1006	0.0725
	547	0.1315	0.0896

α -values are not corrected to m^2 of the catalyst surface

APPENDIX III

X-Ray Diffraction Pattern of 5.26 mol percent Al_2O_3 Doped
Nickel Hydroxide

Prepared Sample		Nickel aluminium hydroxide (129)		*Hydrated Nickel hydroxide (130)	
dÅ	Intensity	dÅ	I/I ₁	dÅ	I/I ₁
7.52	vs	7.57	100	7.60	100
3.65	ms	3.77	90		
2.65	ms	2.603	40	2.66	80
		2.552	90	2.55	80
		2.375	50		
		2.264	80		
		2.031	20		
		1.917	90		
		1.708	70		
		1.613	60		
1.54	ms	1.510	80		
		1.481	80		
		1.401	30		
		1.373	60		
		1.256	50		
		1.241	10		
		1.183	40		

*Only the major lines are available

APPENDIX IV

EFFECT OF OXYGEN REMOVAL FROM CARRIER GAS

on

ACETONE PRODUCTION

* α Acetone

No. of Injections	Carrier gas containing trace quantities of oxygen	Oxygen free Carrier gas
----------------------	---	----------------------------

1	0.3297	0.3190
2	0.2036	0.1998
3	0.1686	0.1562
4	0.1424	0.1342
5	0.1365	0.1248
6	0.1226	0.1140
7	0.1140	0.1086

* α -values are not corrected to per m^2 of the catalyst surface.

APPENDIX V

FRACTIONAL CONVERSION OF 2-HEXANOL TO HEXENE AS
A FUNCTION OF TEMPERATURE FOR CATALYST CONTAINING
5.26 MOL PERCENT Al_2O_3

Temperature (K)	α Hexene	(per m^2 of catalyst surface)
453		0.0027
463		0.0042
475		0.0069
485		0.0114
495		0.0170
506		0.0229
516		0.0282
527		0.0385
538		0.0437
547		0.0614